

19th Asian Pacific Corrosion Control Conference

第19届亚太腐蚀控制会议

ABSTRACTS 摘要集

2023.11.16-18

Guangzhou, China

中国·广州

Content

1.A new strategy for lithium salt sealing of porous anodic aluminum oxide film	1
2.Hexafluoroisopropanol based silk fibroin coatings on magnesium alloy with enhanced adhesion, corrosion resistance and biocompatibility	2
3.Evading the Efficiency-Voltage Trade-off in Magnesium-Air Batteries	4
4. Exceptionally high corrosion resistance of Mg enabled by Ca micro-alloying.	5
5. Designing of the high corrosion-resistant magnesium alloy.....	6
6.Bridge for the thermodynamics and kinetics of electrochemical corrosion: Designing a corrosion-resistant HP-13Cr stainless steel by Cu micro-alloying for use in an H ₂ S-containing geothermal environment	7
7.Constructing an In-Situ Self-Repairing film on magnesium for restricting corrosion	8
8. Sputtering, a bottom-up approach for developing protective coatings	10
9.The different secondary phase particle effects on the high-temperature oxidation of Mg-RE alloys.....	11
10.Evaluating the Dissolution Corrosion Resistance of Hastelloy Exposed to Liquid Bismuth Eutectic at 500°C	12
11.Investigation of Oxide Nano-porosity in Zirconium Alloys using Machine-learning and 3D Reconstruction	13
12.Study on the influence of magnetic induction heating parameters on the temperature gradient of thermal-mechanical fatigue	14
13.Corrosion thermodynamics diagram of aluminum alloy in the semiconductor manufacturing industry	15
14.Hexafluoroisopropanol based silk fibroin coatings on magnesium alloy with enhanced adhesion, corrosion resistance and biocompatibility	18
15.An ionic liquid-assisted strategy for enhanced anticorrosion of low-energy PEO coatings on magnesium–lithium alloy.....	20

16. Corrosion behaviors of hot-dip galvanized and Zinc-Aluminum-Magnesium coated steels	21
17. Fretting crevice corrosion of high-speed rail steel U75V with PA66 liner.....	24
18. Improved corrosion resistance of laser melting deposited CoCrFeNi-series high-entropy alloys by Al addition	26
19. Data-Driven Identification and Experimental Verification of Optimal Sn Microalloying Composition for Corrosion Resistance in Low-Alloy Steel	27
20. Innovative Surface Modification for Enabling CVD Graphene Coating on Steels for Remarkable Corrosion Resistance	28
21. From Inhibitor Mobility in Active Protective Coatings to Local Inhibitor-Metal Microstructure Interactions	29
22. Conversion coatings and their role in the protection of different alloys.....	31
23. Surface Treatment of Recycled Aluminium and its Effect on Filiform Corrosion.....	33
24. Advanced electrochemical and spectroscopic monitoring & modelling of transport of water and ions in organic coatings of metal	35
25. Corrosion behaviors of multilayer C/Cr/SS bipolar plates for proton exchange membrane fuel cells under dynamic potential polarization based on New European Driving Cycle	36
26. Environmental Protection Coating System for Refractory Metal Alloys in extreme environments	38
27. Gradient Cu^{2+} Releasing Rate Enhanced the Antibacterial, Cytocompatibility, and Degradation Resistance of Cu-containing PEO coated Pure Mg.....	39
28. Advancing Concrete Durability with Graphene Oxide-Based Coatings against Rebar Corrosion	40
29. Passive Film and Its Influence on Surface Properties of Titanium Alloy	41
30. Preparation and corrosion protection mechanism of MXene-based composite coatings on metals	42
31. Green surface protection programme for marine microbiologically influenced corrosion and biofouling	44

32. Inhibition of Duplex Steel in Acidizing of Sour Wells	45
33. Active learning approach towards discovery of new efficient corrosion modulators Mikhail Zheludkevich.....	47
34. Photoelectrochemical effect of Cu ₂ O on the corrosion behavior of Cu.....	47
35. Exploring the potential of transfer learning in extrapolating accelerated corrosion test data for long-term atmospheric corrosion forecasting	49
36. International standardization of corrosion of metals and alloys	50
37. Unveiling the Phase Transformation at Nano Scale	51
38. Preliminary Exploration of the Integration of Generative Artificial Intelligence with Corrosion Data Processing.....	52
39. Detection of the Durability of Epoxy-coated Reinforcement under Marine environment in South China for 25 years	53
40. Understanding into properties controlling durability of pre-painted steel sheets.....	54
41. Corrosion behavior of Laser Powder Bed Fusion Al-Mn-Mg-Sc-Zr Alloy...	55
42. Initial localized corrosion induced by multiscale precipitates in the new generation high-strength Al-Zn-Mg-Cu alloy	56
43. Initial Corrosion Behavior and Mechanism of Bogie Steel with Different Heat Treatment Structures in Industrial Polluted Environment Containing S.....	58
44. Corrosion resistance of 12Cr1MoV and welded Inconel 625 coating on heat exchange surfaces with increasing steam parameters in waste incinerators.....	61
45. Title Ablation resistance of Ir/HfO ₂ ultra-high temperature thermal protection coating.....	62
46. High temperature corrosion resistance of enamel coating on 316L stainless steel in the environment of NaCl + water vapor + air	63
47. (Fe,Co,Ni) ₃ O ₄ Spinel Coating on Solid Oxide Fuel Cell Interconnect Steel	65
48.Environmentally Assisted Cracking of Stainless Steels – From 3D/4D Time-lapse Imaging, Bipolar Electrochemistry, to Simulated Marine Environments	66
49.Results Using a New Methodology to Test the Fatigue of Materials in	

Corrosive Media at High Pressures.....	67
50. Atomic-scale analysis of hydrogen embrittlement in high-strength Al alloys	68
51. Correlating oxidation, localized oxidation and stress corrosion cracking of austenitic alloys and weldments in pressurized water reactor primary coolants .	69
52. Corrosion challenges of the supercritical CO ₂ transportation pipeline.....	71
53. Corrosion test result on Rotating Cage Autoclave (RCA) and comparison of some configuration of cage to wall shear stress of corrosion test sample to achieve the better accuracy	72
54. Defeating hydrogen-induced grain-boundary embrittlement via triggering unusual interfacial segregation in FeCrCoNi-type high-entropy alloys	74
55. Effect of cold work on stress corrosion cracking behavior of 316L and 316NG stainless steels in high temperature water	75
56. Effect of gradient microstructure induced pre-torsion on hydrogen embrittlement of pure iron	76
57. Effect of microstructure and reversed austenite on the hydrogen embrittlement susceptibility of Ni-Cr-Mo-V/Nb high strength steel	77
58. Effect of Nb alloying on resistance to hydrogen embrittlement in multiphase stainless steel.....	81
59. Enhancing Effect of High-Temperature Water on Crack Growth of 316LN Stainless Steel Under Various Loading Frequencies	82
60. New insights and experimental/modeling confirmations of the HELP+HEDE model for the synergistic action of hydrogen embrittlement in metallic materials	83
61. Microscopic criteria for stress corrosion crack initiation of Monel 400 alloy in hydrofluoric acid vapor.....	87
62. Non-steady electrochemical mechanism of stress corrosion cracking and its protection techniques	89
63. Progress in Design of Hydrogen Embrittlement-Resistance High Strength Steel and Prospects	92

64. Rendering a predictive and protecting mechanism on stress corrosion cracking: Cleavage dissolution model	93
65. Hydrogen embrittlement susceptibility of X80 pipeline steel in hydrogen-blended natural gas environments	94
66. Superwetting Coatings inside Capillary Tubes for in-vitro Diagnosis Lidong Sun	95
67. The role of Mg/MgO interfaces in the accelerated corrosion of additive manufactured Mg alloys	96
68. Corrosion in low carbon energy technologies Gareth Hinds	97
69. Insight into physical interpretation of electrochemical impedance spectra of Mg.....	98
70. Interpretation on the fast corrosion process of Mg-alloys using electrochemical impedance spectroscopy	100
71. on Corrosion Behavior of Fe-Ga Alloy in Simulated Marine Environment	101
72. Sequential dual-passivation of Cr and Mn in stainless steel and its applications at high potentials.....	102
73. Spatially Resolved Local Electrochemical <i>In Operando</i> Techniques Visualize the Interface of biodegradable Metals.....	104
74. Chloride Susceptibility Index (CSI): an <i>ab initio</i> based corrosion resistance indicator	106
75. Effect of Heat Flow on the Corrosion Behavior of Carbon Steel H ₂ SO ₄ Solution Interface.....	108
76. Effects of temperature and acetic acid on electrochemical corrosion behavior of X80 steel	109
77. Cellular automaton simulation of electrochemical behavior of B30 copper-nickel alloy in seawater environment	110
78. Effect of Er addition on the microstructure and corrosion performance of zinc aluminum magnesium coating	112
79. Deterioration corrosion of steel affected by <i>Shewanella algae</i> under degradation and transformation of oil in marine rust layer.....	114

80. Electrochemical behaviour of corrosion products and their effect on structural alloy in molten fluoride salt	116
81. How to estimate the stable pitting transition according to the electrochemical noise transient	118
82. Corrosion behavior of pure metals (Ni and Ti) and alloys (316H SS and GH3535) in liquid GaInSn.....	120
83. Preparation and performance study of environmentally responsive microencapsulated self-healing coatings	126
84. 6061 galvanic corrosion behavior in simulated seawater	128
85. Anisotropic Corrosion and Discharge behavior of Mg-Y Binary Alloys with High Rare Earth Content in Natural Seawater	129
86. Mitigation of stress corrosion cracking of X80 steel induced by sulfate reducing <i>Desulfovibrio vulgaris</i> biofilm using THPS	131
87. Study on hydrogen compatibility and influencing factors of hydrogen transport pipe	132
88. Evading the Efficiency-Voltage Trade-off in Magnesium-Air Batteries	133
89. Study on the influence of magnetic induction heating parameters on the temperature gradient of thermal-mechanical fatigue	135
90. Study on hydrogen compatibility and influencing factors of hydrogen transport pipe	136
91. A Modified Polyurea Platform with Nano Titanium Dioxide for Antibacterial and Drag-Reducing Applications in Marine Structures	137
92. Advanced surface analytical methods for corrosion research Philippe Marcus	139
93. A case study on a failed superheater used in a biomass thermal power plant: Metallurgical investigation	139
94. All-In-One passive, active and self-healing properties control of epoxy coating by microenvironment regulation for long-term anticorrosion	140
95. Transformational Discovery Methods for Corrosion Protection in a Circular Economy	141

96. Corrosion behavior of monophasic and multiphasic Al ₅₀ Au ₅₀ ribbons in AlCl ₃ + HCl solution.....	144
97. Effect of the impurities in LiF-NaF-KF molten salt on the corrosion behavior of GH3535 alloy	144
98. Effects of temperature and acetic acid on electrochemical corrosion behavior of X80 steel.....	145
99. Experimental study on dew point corrosion coupled with ash deposition in simulated MSW incineration environment	146
100. Corrosion behavior of mild steel in acid solutions with presence of triazole derivatives	147
101. Preparation of CeO ₂ /ZnO resistive thin film and its corrosion behavior in 3.5wt% NaCl solution.....	149
102. Remarkably Corrosion Resistant Graphene Coating on Steel Enabled Through Metallurgical Tailoring.....	150
103. Research on fatigue properties of Q690 high strength steel in marine corrosive environment	151
104. Self-Healing Enhancement of Diphenylmethane Diisocyanate (MDI) Polyurea Coating via Polytetramethyleneoxide-di-p-Aminobenzoate for Corrosion Protection in Marine Structures	152
105. Surface Morphology, Microstructure and Emissivity of Rhenium Electrodeposited from Molten Salts.....	154
106. Bridge for the thermodynamics and kinetics of electrochemical corrosion: designing of the high corrosion-resistant copper-nickel alloy.....	155
107. 油气钻采装备工具耐蚀合金修复层腐蚀磨损行为及机制研究.....	158
108. 海洋菌藻共生对金属腐蚀与污损的影响机制	158
109. 油气钻采装备/工具耐蚀合金修复层腐蚀磨损行为及机制研究	159
110. 氮化碳薄膜用于光阴极防腐蚀.....	160
111. 超临界二氧化碳中 AlCrFeNi 系高熵合金的腐蚀行为研究.....	161
112. 二回路水化学条件下溶解氧对流动加速区 CRUD 的影响.....	162

113.钛基表面涂层的催化反应活性调控和结构相转变规律研究.....	164
114.表面组织调制对降低 AlMg 变形铝合金板晶间腐蚀速率的关键作用 .	167
115.Er 的添加对锌铝镁镀层组织和腐蚀性能的影响	169

1. A new strategy for lithium salt sealing of porous anodic aluminum oxide film

A new strategy for lithium salt sealing of porous anodic aluminum oxide film

Yanlong Ma¹, Mengting Zou¹, Jiangrong Yan¹, Haisheng Wu², Liang Wu³

¹*College of Materials Science and Engineering, Chongqing University of
Technology, Chongqing, 400054, China*

²*Beijing Satellite Manufacturing Factory Co., Ltd, Beijing 100094*

³*College of Materials Science and Engineering, Chongqing University, Chongqing
400044, China*

myl@cqu.edu.cn

Abstract Anodizing treatment has been widely used to improve corrosion resistance of aluminum alloys. Apart from the alloy substrate and anodizing process, post-sealing of the anodized alloy in a specific medium is deemed the key factor affecting the anti-corrosion performance of the coating system. Previously, we have developed a new sealing process that involves post-treatment of the anodized aluminum alloy in a dilute lithium salt solution, at a temperature ranging from room temperature to 90 °C, within 30 min. In this work, we propose a new strategy for the lithium salt sealing technology by considering the different sealing behavior occurring at different temperatures. Specifically, an anodized 7075-T6 alloy was first treated in a lithium salt solution at relatively low temperature for 10~15 min and then in the same solution but at elevated temperature for 10~15 min. Compared with the sealing processes carried out at constant temperature, the multi-step sealing processes turn out to be more effective. This work provides not only a new approach for further improving the corrosion resistance of aluminum alloys but also new insight on the mechanism of lithium salt sealing.

Keywords Anodizing; Post-treatment; Lithium salt sealing; Hydroxides; Multi-step

Reference

[1] D. Mata, M. Serdechnova, M. Mohedano, C.L. Mendis, S.V. Lamaka, J. Tedim, T.

Hack, S. Nixon, M.L. Zheludkevich, Hierarchically organized Li-Al-LDH nano-flakes: a low-temperature approach to seal porous anodic oxide on aluminum alloys, *Rsc. Adv.* 7 (2017) 35357-35367.

[2] B. Yang, Y. Ma, H. Wu, Z. Liang, Y. Li, L. Wu, L. Sun, Improving corrosion resistance of anodized AA2099-T83 Al-Cu-Li alloy through post-treatment in a lithium nitrate-based solution, *Surf. Coat. Technol.* 441 (2022), 128501.

[3] P. Zhu, Y. Ma, W. Huang, M. Zou, B. Yang, Y. Liao, Z. Liang, Post-treatment of anodized AA2099-T83 alloy in lithium carbonate solutions of different temperature-concentration combinations, *T. Nonferr. Metal. Soc.*, accepted, 2023.8

2. Hexafluoroisopropanol based silk fibroin coatings on magnesium alloy with enhanced adhesion, corrosion resistance and biocompatibility

Hexafluoroisopropanol based silk fibroin coatings on magnesium alloy with enhanced adhesion, corrosion resistance and biocompatibility

Kang Yang¹, Haotong Li¹, Xinru Cao¹, Liang Wu²

¹*School of Materials Science and Engineering, Anhui University of Technology,*

Maanshan 243002, China

²*College of Materials Science and Engineering, Chongqing University, Chongqing*

400044, China

Kang Yang's e-mail address: ykang@ahut.edu.cn

Abstract The application of biomacromolecule coatings on biomedical magnesium alloys has garnered significant interest due to their potential to enhance corrosion resistance and biocompatibility. While Silk fibroin (SF) coatings based on aqueous solvents have shown promise for magnesium alloys, a complex pretreatment process is required due to their susceptibility to corrosion in water. In this study, an SF coating using hexafluoroisopropanol (HFIP) solvent was developed to streamline processing and improve adhesion. Additionally, Ethylene glycol diglycidyl ether (EGDE) was

employed to further stabilize the coating through enhanced chemical crosslinking. It was confirmed that the compactness and adhesion strength of HFIP-based SF surpassed those of aqueous-based SF. Electrochemical evaluations and in vitro degradation tests in simulated body fluid demonstrated that the HFIP-based SF coating exhibited significantly heightened corrosion resistance. Furthermore, post-treatment with EGDE led to a substantial enhancement in corrosion resistance (the corrosion current density, I_{cor} , of the SF-HFIP-EGDE samples was measured at $9.93 \times 10^{-10} \text{ A cm}^{-2}$, representing a two-order-of-magnitude reduction compared to pure SF samples). Subsequent work involved multi-ion (Ca, Sr/P) doping of the HFIP-based SF coating to further enhance corrosion resistance and osteogenic activity of the magnesium alloys. The results revealed that the I_{cor} of the multi-ion-doped SF coating was reduced by an additional order of magnitude compared to undoped silk protein coating. Simultaneously, osteogenic activity was significantly enhanced. This study demonstrates that HFIP-based SF coatings can be effectively applied to medical magnesium alloys to simultaneously enhance corrosion resistance and osteogenic activity.

Keywords magnesium alloy; silk fibroin; biomedical application

Reference

- [1] Z. Wenhao, T. Zhang, J.L. Yan, Q.Y. Li, P.P. Xiong, Y.Y. Li, Y. Cheng, Y.F. Zheng, In vitro and in vivo evaluation of structurally-controlled silk fibroin coatings for orthopedic infection and in-situ osteogenesis, *Acta Biomater.* 116 (2020) 223-245.
- [2] P. Xiong, Z.J. Jia, W.H. Zhou, J.L. Yan, P. Wang, W. Yuan, Y.Y. Li, Y. Cheng, Z.P. Guan, Y.F. Zheng, Osteogenic and pH stimuli-responsive self-healing coating on biomedical Mg-1Ca alloy, *Acta Biomater.* 92 (2019) 336-350.
- [3] H. Fang, C.X. Wang, S.C. Zhou, Z. Zheng, T. Lu, G. Li, Y.H. Tian, T. Suga, Enhanced adhesion and anticorrosion of silk fibroin coated biodegradable Mg-Zn-Ca alloy via a two-step plasma activation, *Corros. Sci.* 168 (2020), 108466.
- [4] C.X. Wang, H. Fang, X.Y. Qi, C.J. Hang, Y.R. Sun, Z.B. Peng, W. Wei, Y.S. Wang, Silk fibroin film-coated MgZnCa alloy with enhanced in vitro and in vivo

performance prepared using surface activation, *Acta Biomater.* 91 (2019) 99-111.

3. Evading the Efficiency-Voltage Trade-off in Magnesium-Air Batteries

Evading the Efficiency-Voltage Trade-off in Magnesium-Air Batteries

Hongxing Liang¹, Liang Wu², Wenbo Du¹

¹ *Beijing University of Technology, 100 Pingleyuan, Chaoyang District, Beijing 100124, China.*

² *Chongqing University, No.174, Shapingba Street, Chongqing City, 400044, China.*

Presenter's e-mail address: hongxingliang@bjut.edu.cn

Abstract The magnesium-air (Mg-air) battery, known for its exceptional energy density and cost-effectiveness, holds the potential to revolutionize applications that conventional rechargeable batteries have yet to conquer [1]. This includes serving as range extenders for electric vehicles and powering long-range drones. However, the long-standing barrier of the efficiency-voltage trade-off has hindered its widespread adoption, impeding further advancements in energy density [2]. We surmounted this obstacle by pioneering a novel active learning framework specifically tailored to screen high performance magnesium anodes. The innovative framework integrates the physically interpretable variables, machine learning, Pareto front exploration, experimental feedback, and feedback from generated data. Within an extensive compositional space (~350,000 possibilities), we have pinpointed a novel anode, Mg-1Ga-1Ca-0.5In, with exceptional energy density ($2548 \pm 220 \text{ W h kg}^{-1}$). We have identified that the excellent performance of Mg-1Ga-1Ca-0.5In is attributed to the concept of "grain boundary activation" and "intra-grain inhibition". This concept stands apart from the conventional design concept commonly reported in existing studies, which primarily emphasize the influence of second phases on discharge behavior, with the impact of solute atoms on discharge behavior overlooked. We believe that our findings hold immense promise for the future of energy storage.

Keywords Magnesium anode; Corrosion; Machine learning; Theoretical calculation

Reference

- [1] Y. Li, J. Lu, Metal–air batteries: will they be the future electrochemical energy storage device of choice?, *ACS Energy Letters* 2(6) (2017) 1370-1377.
- [2] Z. Liu, J. Bao, J. Sha, Z. Zhang, Modulation of the discharge and corrosion properties of aqueous Mg-air batteries by alloying from first-principles theory, *The Journal of Physical Chemistry C* 127(21) (2023) 10062-10068.

4. Exceptionally high corrosion resistance of Mg enabled by Ca micro-alloying

Exceptionally high corrosion resistance of Mg enabled by Ca micro-alloying

Min Deng¹, Linqian Wang¹, Daniel Höche², Sviatlana V. Lamaka², Cheng Wang²,

Darya Snihirova², Yiming Jin², Yuhui Zhang^{2,3}, Mikhail L. Zheludkevich²

¹*School of Materials Science and Engineering, Hebei University of Technology,*

300401 Tianjin, China

²*Institute of Surface Science, Helmholtz-Zentrum Hereon, 21502 Geesthacht,*

Germany

³*Powder Metallurgy Research Institute, Central South University, 410083 Changsha,*

China

Presenter's e-mail address: dengmin@hebut.edu.cn

Abstract Severe corrosion of Mg and Mg alloys is a major issue hindering their wider applications in transportation industry, medical implants, and aqueous batteries. Previously, no Mg-based material has been found with a significantly lower corrosion rate than that of ultra-high-purity Mg, i.e. 0.25 mm y⁻¹ in concentrated NaCl solution [1, 2]. In this work for the first time, highly corrosion-resistant Mg is found to be accomplishable by Ca micro-alloying, bringing “stainless Mg” closer. The designed Mg-Ca lean alloys possess incredibly low corrosion rates, less than 0.1 mm y⁻¹ in 3.5 wt% NaCl solution, which are significantly lower than that of ultra-high-purity Mg

and all Mg alloys reported thus far. The outstanding corrosion resistance is attributed to inhibition of cathodic water/oxygen reduction kinetics, impurities stabilizing and a protective surface film induced by Ca micro-alloying. Combined with the environmental benignity and economic viability, Ca micro-alloying renders huge feasibility on developing advanced Mg-based materials for diverse applications.

Keywords Mg corrosion; Micro-alloying; Cathodic kinetics; Oxygen reduction; Impurities stabilizing

Reference

- [1] F. Cao, Z. Shi, J. Hofstetter, P.J. Uggowitzer, G. Song, M. Liu, A. Atrens, Corrosion of ultra-high-purity Mg in 3.5% NaCl solution saturated with Mg(OH)₂, *Corros. Sci.*, 75 (2013) 78-99.
- [2] A. Atrens, Z. Shi, S.U. Mehreen, S. Johnston, G.-L. Song, X. Chen, F. Pan, Review of Mg alloy corrosion rates, *Journal of Magnesium and Alloys*, 8 (2020) 989-998.

5. Designing of the high corrosion-resistant magnesium alloy

Designing of the high corrosion-resistant magnesium alloy

Duo Wang, Peng Zhou, Yi Zhang, Tao Zhang, Fuhui Wang

Shenyang National Laboratory of Material Science, Northeastern University, 3-11

Wenhua Road, Shenyang 110819, China

Presenter's e-mail address: zhangtao@mail.neu.edu.cn

Abstract A new designing idea was proposed for the high corrosion-resistance magnesium (HCR Mg) alloy based on dissolution-ionization-diffusion-deposition (DIDD) model. HCR Mg alloy consists of low-alloying element (LA) and micro-alloying element (MA), characterized as “Mg-LA-MA” alloying system. The downwards-magnifying effect of MA-LA-Mg on the nucleation played a key role in achieving passivation behavior. The designed HCR Mg alloy (Mg-3Nd-1Gd-0.6In)

showed superior corrosion resistance (near AA2024 alloy) and good mechanical performance (UTS, 259.30 ± 0.27 MPa). Overall, a universal way for designing new alloy systems with superior corrosion resistance was proposed, promising for future applications.

Keywords Magnesium alloy; High corrosion resistance; Alloy designing; DIDD model; TEM

Reference

- [1] Y. Zhao, T. Zhang, H. Xiong, F. Wang, Bridge for the thermodynamics and kinetics of electrochemical corrosion: modeling on dissolution, ionization, diffusion and deposition in metal/solution interface, *Corros. Sci.* 191 (2021), 109763
- [2] Y. Zhao, W. Qi, T. Zhang, H. Xiong, F. Wang, Bridge for thermodynamics and kinetics of electrochemical corrosion: cathodic process with a complex equilibrium and deposition competition, *Corros. Sci.* 208 (2022), 110613
- [3] M. Deng, L. Wang, D. Hoche, S.V. Lamaka, C. Wang, D. Snihirova, Y. Jin, Y. Zhang, M.L. Zheludkevich, Approaching "stainless magnesium" by Ca micro-alloying, *Mater. Horiz.* 8 (2021) 589–596

6. Bridge for the thermodynamics and kinetics of electrochemical corrosion: Designing a corrosion-resistant HP-13Cr stainless steel by Cu micro-alloying for use in an H₂S-containing geothermal environment

Bridge for the thermodynamics and kinetics of electrochemical corrosion: Designing a corrosion-resistant HP-13Cr stainless steel by Cu micro-alloying for use in an H₂S-containing geothermal environment

Yang Zhao¹, Wenlong Qi¹, Hao Feng², Jidong Wang¹, Tao Zhang^{1*}, Huabing Li^{2*},
Fuhui Wang¹

¹*Shenyang National Laboratory of Material Science, Northeastern University, 3-11 Wenhua Road, Shenyang, 110819 China.*

²*School of Metallurgy, Northeastern University, 3-11 Wenhua Road, Shenyang 110819*

China.

Presenter's e-mail address: zhangtao@mail.neu.edu.cn

Abstract The dissolution–ionization–diffusion–deposition (DIDD) model was used for developing a corrosion-resistant stainless steel (SS) by means of micro-alloying and the guidelines for the process were proposed. The novel HP-13Cr–Cu SS was designed to resist corrosion in H₂S-containing geothermal environment. The results indicated that HP-13Cr–Cu presented a low corrosion rate and high SSC resistance in a temperature range of 25–200 °C and an H₂S pressure of 0.1–0.5 MPa. The preferential deposition of CuS promoted the heterogeneous nucleation rate of Cr₂O₃, FeCr₂O₃, and FeS, which formed denser corrosion products. As a result, this alloy exhibited a low corrosion rate and a high sulfide stress cracking (SSC) resistance. The results were consistent with the theoretical calculation conducted as per the DIDD model. That novel designing methodology provides a distinct selection principle of the alloying element and quantifies the relationship between alloying element and corrosion resistance in a specific environment.

Keywords DIDD model; Micro-alloying; HP-13Cr–Cu SS; Heterogeneous nucleation; High SSC resistance.

Reference

- [1] Y. Zhao, T. Zhang, H. Xiong, F. Wang, Corros. Sci. 191 (2021) 109763.
- [2] Y. Zhao, W. Qi, T. Zhang, H. Xiong, F. Wang, Corros. Sci. 208 (2022) 110613.
- [3] H. Feng, J. Dai, H. Li, Y. Zhao, S. Zhang, T. Zhang, Corros. Sci. 201 (2022) 110279.

7. Constructing an In-Situ Self-Repairing film on magnesium for restricting corrosion

Constructing an In-Situ Self-Repairing film on magnesium for restricting corrosion

Lifeng Hou, Junli Sun, Qixin Yan, Zhiqiang Gao, Yinghui Wei

*College of Materials Science and Engineering, Taiyuan University of Technology,
Taiyuan, China*

Presenter's e-mail address: houlifeng@tyut.edu.cn

Abstract Magnesium (Mg) and its alloys, being the lightest metal structural materials, possess small specific gravity, high specific strength, good thermal conductivity, and the potential for achieving lightweight products. However, the strong corrosion sensitivity of magnesium alloys restricts their application. And a porous Mg(OH)₂ film will be formed on its surface, which could not provide the protection of Mg alloy. In this study, a Mg-In alloy with excellent corrosion resistance was prepared, and its electrochemical dissolution and self-corrosion process were analyzed.

The real-time monitoring of the anodic dissolution of Mg-In alloy in NaCl solution was conducted using the simultaneous online monitoring system. The characteristics of the electrochemical dissolution of the materials were discussed through potentiodynamic polarization tests, surface morphology analysis, and composition analysis. The results indicate that the passivation film consists of a simple inner layer and a dense corrosion layer composed of Mg(OH)₂ and In(OH)₃. Within the dense corrosion layer, In/In(OH)₃ is alternately or sandwiched. The evaluation of the corrosion resistance of the Mg-In alloy involved weight loss measurements, hydrogen evolution analysis, and electrochemical tests. The results demonstrate the notable protective effect of the double-layer film. Furthermore, the critical value of In content required for the formation of the dense corrosion layer was determined by examining the self-corrosion behavior of the Mg-In alloy in NaCl solution.

Finally, the rationality and conditions of the coexistence of activation and inhibition mechanisms are discussed and defined. The results demonstrate that different charge transfer rates on the alloy surface cause different reaction driving forces, resulting in two mechanisms: activation and inhibition. In this study, during the self-corrosion process of Mg-In alloy, atoms can be accumulated on the surface of the alloy through displacement reaction, thus realizing self-deposition and effectively improving the

corrosion resistance of the material.

Keywords Magnesium alloy; Corrosion resistance; Dissolution behavior; passivation films

8. Sputtering, a bottom-up approach for developing protective coatings

Sputtering, a bottom-up approach for developing protective coatings

Albano Cavaleiro^{1,2*}

¹*University of Coimbra, Portugal*

²*Instituto Pedro Nunes, Portugal*

*Corresponding author e-mail: albano.cavaleiro@dem.uc.pt

Abstract Sputtering is a bottom up processing technique based on the sequential deposition of individual atoms/molecules onto a substrate to produce a thin film or a coating. By playing with the composition of either the materials sources (targets) or the gases environment as well as the deposition conditions, different structural and morphological arrangements can be produced in the thin films. Monolithic, graded and multilayer cross section morphologies can be easily deposited allowing to achieve specific properties required for particular applications. Epitaxial, nanocrystalline, nanocomposite or amorphous structures can be controlled and varied in the same system of chemical elements.

In this talk, several examples of sputtered films will be presented showing the potentiality of sputtering for tailoring the morphology and/or the structure of thin coatings for applications where corrosion resistance and high-temperature oxidation protection are required. The procedure and processing steps behind the tailoring of a coating as a function of the required properties will be presented and discussed.

9. The different secondary phase particle effects on the high-temperature oxidation of Mg-RE alloys

The different secondary phase particle effects on the high-temperature oxidation of
Mg-RE alloys

Zhao Shen, Xiaoqin Zeng

1National Engineering Research Center of Light Alloy Net Forming and State Key

2Laboratory of Metal Matrix Composites, School of Materials Science and
Engineering, Shanghai Jiao Tong University, Shanghai 200240, China

shenzhao081@sjtu.edu.cn

Abstract Although RE elements are believed to improve the high-temperature oxidation resistance of magnesium alloys [1-3], the understanding of their mechanism is still insufficient, especially the effects of RE-rich precipitate particles. The oxidation of Mg-Nd and Mg-Y-Al alloys in Ar-20%O₂ at 500 °C and the different secondary phase particle effects were studied and compared [4]. The results show that the areas initially taken up by Mg-Nd precipitates underwent more severe internal oxidation than the α -Mg matrix in the Mg-Nd alloy. The dissolution of Mg₁₂Nd precipitates could increase the localized preferential oxidation of Nd and resulted in the generation of more internal oxide precipitates with a core-shell structure (Nd₂O₃ core wrapped by MgO shell). The enhanced internal oxidation is believed to be caused by the accelerated inward oxygen diffusion along the interfaces between the internal oxide precipitate and the metal matrix. However, although the network-like LPSO phase in the Mg-Y-Al alloy was decomposed into needle-like LPSO phase and polygonal Mg₂₄Y₅ phase, the oxidation resistance of Mg-Y-Al alloy was not deteriorated. On the contrary, the accelerated in-situ oxidation of the needle-like LPSO phase facilitated the formation of a thicker and continuous Y₂O₃ oxide scale.

Keywords Mg alloy; Precipitates; Rare-earth element; Preferential oxidation; Advanced characterization.

Reference

- [1] Q.Y. Tan, A. Atrens, N. Mo, M.X. Zhang, Oxidation of magnesium alloys at elevated temperatures in air: A review, *Corros. Sci.* 112 (2016) 734-759.
- [2] Y. Cai, H. Yan, M.Y. Zhu, K. Zhang, X.N. Yi, R.S. Chen, High-temperature oxidation behavior and corrosion behavior of high strength Mg- x Gd alloys with high Gd content, *Corros. Sci.* 193 (2021) 109872.
- [3] J.J. Wu, Y. Yuan, L. Yang, T. Chen, D.J. Li, L. Wu, B. Jiang, M. Steinbrück, F.S. Pan, The oxidation behavior of Mg-Er binary alloys at 500 °C, *Corros. Sci.* 195 (2022) 109961.
- [4] Z. Wang, Z. Shen, Y. Zhao, B. Hu, D. Li, X. Zeng, A study on the high-temperature oxidation of ZM6 alloy through advanced characterization, *Corros. Sci.* 111150 (2023).

10. Evaluating the Dissolution Corrosion Resistance of Hastelloy Exposed to Liquid Bismuth Eutectic at 500°C

Evaluating the Dissolution Corrosion Resistance of Hastelloy Exposed to Liquid Bismuth Eutectic at 500°C

Jiajian Shi¹

¹ 中山大学中法核工程与技术学院

Abstract The present study investigated the dissolution and oxidation corrosion behaviors of Hastelloy subjected to static liquid lead bismuth eutectic (LBE) at 500 °C with oxygen concentration of 1×10^{-6} mass%. Hastelloy exhibited better LBE corrosion resistance than the Montel alloy. Both dissolution and oxidation corrosions were present in the Hastelloy, and the maximum LBE penetration depth and spinel layer thickness in the corroded sample with exposure time of 4000 h reach $169 \pm 126 \mu\text{m}$ and $27 \pm 12 \mu\text{m}$, respectively. Microstructural characterization revealed that the spinel layer formed between penetrated LBE contributed to the

slower dissolution rate of Hastelloy. Volumetric change induced by LBE penetration promotes the formation of stacking faults and dislocations, which could provide more channels for interdiffusion between penetrated LBE and base metal, leading to the propagation of dissolution attack.

Keywords Hastelloy; Liquid Lead-bismuth eutectic; Dissolution mechanism; Twin boundary

11. Investigation of Oxide Nano-porosity in Zirconium Alloys using Machine-learning and 3D Reconstruction

Investigation of Oxide Nano-porosity in Zirconium Alloys using Machine-learning and 3D Reconstruction

Hongliang Zhang

¹ 复旦大学

Abstract Understanding the corrosion mechanisms of zirconium (Zr) alloys in aqueous environments is important, as Zr alloys are the most commonly used cladding materials in pressurized and boiling water nuclear reactors. In the corrosion of Zr alloy, the oxide grows at a decreasing rate until reaching critical thickness, followed by the sudden loss of the protective property and a new cycle of oxide growth. The oxidation-induced pores in oxide may provide pathways to oxidizing species. Traditionally, TEM is usually used to determine pore density and size. However, some of the small-sized pores are invisible in TEM at only one angle. Manually counting pores will also bring some artifacts. We precisely quantify the oxide porosity in corroded Zircaloy-4 as function of exposure time and temperatures using our newly developed Machine-learning-based quantification method. The size, spatial distribution, morphology and interconnectivity of the pores are obtained and quantified through the 3D reconstruction. Furthermore, the chemical composition in different regions of the oxide are studied using APT and correlated to pore distribution

to further our understanding of alloying elements effects on corrosion.

Keywords Zr alloys; Corrosion; Nano-porosity; Machine-learning; 3D Reconstruction

12. Study on the influence of magnetic induction heating parameters on the temperature gradient of thermal-mechanical fatigue

Study on the influence of magnetic induction heating parameters on the temperature gradient of thermal-mechanical fatigue

Xie Bing^{1,2}, Hao Xuelong^{1,2}

¹*Guobiao(Beijing) Testing & Certification Co., Ltd, 11 Xingke East Street, Yanqi Economic Development Zone, Huairou District, Beijing 101407, China*

²*National Center of Analysis and Testing for Nonferrous Metals and Electronic Materials, General Research Institute for Nonferrous Metals, Beisanhuanzhong Road, Xicheng District, Beijing 100088, China*

xiebing@cutc.net, haoxuelong@gbtcgroup.com

Abstract The control of temperature gradient determines the accuracy of thermal-mechanical fatigue test results. There are no clear regulations on the types of magnetic induction coils, the distribution of thermocouples, and the definition of temperature gradients in the testing methods for thermal-mechanical fatigue both domestically and internationally. In this study, the individual and hybrid effects of different types of magnetic induction coils and the distribution of thermocouples on the temperature gradient of thermal-mechanical fatigue were investigated. Thermal strain and zero pressure tests are measured under different turns of the induction coil and spacing between thermocouples. The significant finding of this study is the effect law of magnetic induction heating parameters on the temperature gradient of thermomechanical fatigue.

Keywords thermal-mechanical fatigue, temperature gradient

Reference

- [1] Huo Shiyu, Yan Qun, Gao Xiang. The influence of induction heating coil parameters on the temperature field of engine blades [J] Hot working process, 2018, 47 (18): 70-4
- [2] Chen Jingyang, Jing Fulei, Yang Junjie. Thermal-mechanical fatigue behavior and life modeling of nickel-based single crystal superalloys [J]. Journal of Aerodynamics, 2021,36 (05): 897-906
- [3] Sun J, Yuan H, Vormwald M. Thermal gradient mechanical fatigue assessment of a nickel-based superalloy[J]. International Journal of Fatigue, 2020, 135(Jun.):105486.1-105486.14.DOI:10.1016/j.ijfatigue.2020.105486.
- [4] Gao Shengyong, Wang Yiwen, Su Ru, Wu Dayong, Kang Jie, Bao Yanping. Low-Cycle Fatigue Behavior of GH4169 Superalloy. Chinese Journal of Rare Metals. 2022,46(3):289-296.
- [5] Li Jingnan, Dong Ruifeng, Chen Zishuai, Huang Dongnan, Qu Jinglong. Formability of Free Forging GH4720Li Superalloy with Different Gradient Heating Process. Chinese Journal of Rare Metals. 2022,46(2):162-168.

13. Corrosion thermodynamics diagram of aluminum alloy in the semiconductor manufacturing industry

Corrosion thermodynamics diagram of aluminum alloy in the semiconductor manufacturing industry

Xiaohan Wang, Tao Zhang*, Fuhui Wang

¹*Shenyang National Laboratory of Material Science, Northeastern University, Shenyang*

Presenter's e-mail address: Xiaohan Wang (wxh070707@163.com); Tao Zhang (zhangtao@mail.neu.edu.cn)

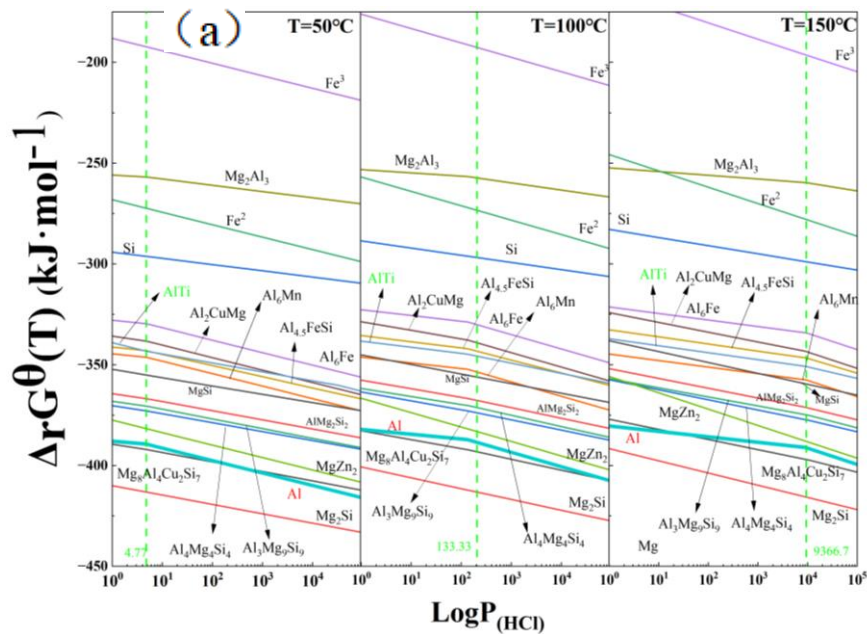
Abstract Aluminum alloys are widely used in the semiconductor manufacturing

industry (SEMI) due to its excellent structural performance, however, when the wafer is etched, parts made of aluminum alloy will be etched too which may release particles to pollute the etching environment. Different from the traditional corrosion, corrosion of SEMI is the result of gas and plasma coupling, many studies have developed the plasma corrosion mechanism of materials, but detailed research on corrosion in SEMI has not yet been conducted. The characteristic of SEMI environment can be grouped into following aspects: high temperature (maximum to 150 °C); aggressive medium are electronic special gases, including O₂, Cl₂, HCl, HF, HBr, CF₄, Ar, NF₃ and so on; the thin gas environment: the partial pressure of special gas is controlled at 100 Torr.[2] Research on the corrosion of aluminum alloys in SEMI is still relatively scarce. At present, research on improving the corrosion resistance of aluminum alloys in SEMI is mostly focused on the development of corrosion resistant coatings, such as Y₂O₃ and YOF, but there is still a lack of research on the aluminum alloy matrix.

In order to study the corrosion resistance of aluminum alloys in different atmospheres, there is an urgent need for a guideline constructed based on the existing knowledge framework, which guides the selection of aluminum alloy. This article refers to the Pourbaix diagram[3] and Ellingham diagram,[4] constructs a partial pressure-free energy corrosion thermodynamic diagram in SEMI. This diagram first fully considered the sublimation of corrosion products in vacuum atmosphere, and calculated the saturated vapor pressure using methods by K-K equation to draw a solid-gas diagram of corrosion products; Secondly, the thermodynamic data of different precipitated phases (such as Al₂Cu, Al₆Fe, AlMg₂Si₂, etc.) are calculated by first principles. Finally, based on the possible thermodynamic reactions of each substance, the free energy calculation results at ambient temperature and pressure were calculated, and extrapolated to other alternative temperatures and normal pressure environment. According to the above calculation results, corrosion thermodynamic diagrams were drawn under different atmospheres, pressures and temperatures. Finally, the aluminum alloy samples were placed in different gas

environments to verify the above diagrams. The experimental results are consistent with the drawn corrosion thermodynamic diagram, proving that using this diagram to guide the material selection of aluminum alloys in SEEI is feasible.

Through diagrams and experimental results, the following conclusions can be drawn, the corrosion of aluminum alloy in SEMI is mainly caused by the corrosion of aluminum alloy matrix, and the corrosion behavior of the precipitated phase is relatively weak. Because of the sublimation of the corrosion products that react with the Al matrix, Fe-containing phases would stay on the surface, fall off and pollute the chamber. So that the 6xxx or 5xxx aluminum alloys should be most suitable aluminum alloy in SEMI; The reaction trend of Fe-containing phases is smaller than that of Mg-Si-Al phases and smaller than that of aluminum matrix; Try to reduce the quantity of Fe-containing phases as much as possible.



Hexafluoroisopropanol based silk fibroin coatings on magnesium alloy with enhanced adhesion, corrosion resistance and biocompatibility

Kang Yang¹, Haotong Li¹, Xinru Cao¹, Liang Wu²

¹*School of Materials Science and Engineering, Anhui University of Technology,
Maanshan 243002, China*

²*College of Materials Science and Engineering, Chongqing University, Chongqing
400044, China*

Presenter's e-mail address: ykang@ahut.edu.cn

Abstract The application of biomacromolecule coatings on biomedical magnesium alloys has garnered significant interest due to their potential to enhance corrosion resistance and biocompatibility. While Silk fibroin (SF) coatings based on aqueous solvents have shown promise for magnesium alloys, a complex pretreatment process is required due to their susceptibility to corrosion in water. In this study, an SF coating using hexafluoroisopropanol (HFIP) solvent was developed to streamline processing and improve adhesion. Additionally, Ethylene glycol diglycidyl ether (EGDE) was employed to further stabilize the coating through enhanced chemical crosslinking. It was confirmed that the compactness and adhesion strength of HFIP-based SF surpassed those of aqueous-based SF. Electrochemical evaluations and in vitro degradation tests in simulated body fluid demonstrated that the HFIP-based SF coating exhibited significantly heightened corrosion resistance. Furthermore, post-treatment with EGDE led to a substantial enhancement in corrosion resistance (the corrosion current density, I_{cor} , of the SF-HFIP-EGDE samples was measured at 9.93×10^{-10} A cm^{-2} , representing a two-order-of-magnitude reduction compared to pure SF samples). Subsequent work involved multi-ion (Ca, Sr/P) doping of the HFIP-based SF coating to further enhance corrosion resistance and osteogenic activity of the magnesium alloys. The results revealed that the I_{cor} of the multi-ion-doped SF coating was reduced by an additional order of magnitude compared to undoped silk protein coating. Simultaneously, osteogenic activity was significantly enhanced. This

study demonstrates that HFIP-based SF coatings can be effectively applied to medical magnesium alloys to simultaneously enhance corrosion resistance and osteogenic activity.

Keywords magnesium alloy; silk fibroin; biomedical application

Reference

- [1] Z. Wenhao, T. Zhang, J.L. Yan, Q.Y. Li, P.P. Xiong, Y.Y. Li, Y. Cheng, Y.F. Zheng, In vitro and in vivo evaluation of structurally-controlled silk fibroin coatings for orthopedic infection and in-situ osteogenesis, *Acta Biomater.* 116 (2020) 223-245.
- [2] P. Xiong, Z.J. Jia, W.H. Zhou, J.L. Yan, P. Wang, W. Yuan, Y.Y. Li, Y. Cheng, Z.P. Guan, Y.F. Zheng, Osteogenic and pH stimuli-responsive self-healing coating on biomedical Mg-1Ca alloy, *Acta Biomater.* 92 (2019) 336-350.
- [3] H. Fang, C.X. Wang, S.C. Zhou, Z. Zheng, T. Lu, G. Li, Y.H. Tian, T. Suga, Enhanced adhesion and anticorrosion of silk fibroin coated biodegradable Mg-Zn-Ca alloy via a two-step plasma activation, *Corros. Sci.* 168 (2020), 108466.
- [4] C.X. Wang, H. Fang, X.Y. Qi, C.J. Hang, Y.R. Sun, Z.B. Peng, W. Wei, Y.S. Wang, Silk fibroin film-coated MgZnCa alloy with enhanced in vitro and in vivo performance prepared using surface activation, *Acta Biomater.* 91 (2019) 99-111.

15. An ionic liquid-assisted strategy for enhanced anticorrosion of low-energy PEO coatings on magnesium–lithium alloy

An ionic liquid-assisted strategy for enhanced anticorrosion of low-energy PEO coatings on magnesium–lithium alloy

You Zhang 1, Chuping Chen 1, Chen Wen 2, Fei Chen 1

1Beijing Institute of Petrochemical Technology, Beijing 102617, China

2Beijing Spacecrafts, China Academy of Space Technology, Beijing 100190, China

Presenter's e-mail address: youzhang@bipt.edu.cn

Abstract A new, energy-efficient technique called Low-Energy Plasma Electrolytic

Oxidation (LePEO) has been developed to address the high energy consumption and limited corrosion resistance associated with traditional PEO processes. In this study, the potential of ionic liquids (ILs), particularly 1-butyl-3-methylimidazole tetrafluoroborate (BmimBF₄), as sustainable corrosion inhibitors was explored within the context of the LePEO process on LA91 magnesium-lithium (Mg-Li) alloy. Different concentrations of ionic liquids were introduced into a concentrated alkaline electrolyte to facilitate the formation of LePEO coatings on the Mg-Li alloy's surface. Among these coatings, the one prepared with 20 ml/L BmimBF₄ demonstrated the highest contact angle and the best long-term corrosion resistance, with low hydrogen evolution rates. To further investigate the corrosion inhibition effects, various imidazolium-based ionic liquids with distinct chemical structures were employed during the PEO of the Mg-Li alloy. This analysis aimed to identify the unique contributions of each ionic liquid in enhancing corrosion resistance. Molecular dynamics simulations were also utilized to understand the mechanism of ILs during the LePEO coating formation process. The results revealed that BmimBF₄ actively participates in the LePEO coating formation, leading to increased coating thickness and improved corrosion resistance. The LePEO technique, with the assistance of ionic liquids, shows great promise in reducing energy consumption and enhancing coating performance.

Keywords Mg-Li alloy; Plasma electrolytic oxidation; Ionic liquid; Corrosion resistance; Molecular dynamics simulation

16. Corrosion behaviors of hot-dip galvanized and Zinc-Aluminum-Magnesium coated steels

Corrosion behaviors of hot-dip galvanized and Zinc-Aluminum-Magnesium coated steels

Shao Rong*, Li Min, Liu Yongzhuang, Cao Jianping, Li Xuetao

Research Institute of Technology of Shougang Group Co., Ltd., Beijing 100041, China

Presenter's e-mail address: shaorong0907@163.com

Abstract In recent years, numerous types of Zinc-based coatings especially Zinc-Aluminium-Magnesium coating have been developed as alternatives to improve the corrosion resistance of the material[1,2]. In this paper, two kinds of hot-dip galvanized (GI) and Zinc-Aluminum-Magnesium (ZM) coated steel plates were selected for atmospheric corrosion tests in Turpan Xinjiang, Jiangjin Chongqing, Qingdao Shandong and Wanning Hainan. By analyzing the morphologies, microstructures and chemical compositions of the corrosion products, the corrosion behaviors of GI coating and ZM coating in different environment were investigated.

The main microstructure of GI coating is pure zinc phase, while in ZM coating, there are evenly distributed primary zinc phase, Zn-MgZn₂ binary eutectic phase and Zn-MgZn₂-Al ternary eutectic phase. The results of atmospheric corrosion resistance show that the corrosion rates vary widely in different regions. For both GI coating and ZM coating, the corrosion rate relationship between these four regions are Wanning > Qingdao > Jiangjin > Turpan. Compared the corrosion rate of GI and ZM in different regions. The corrosion rate ratio of GI to ZM is 4.56 in Wanning, 3.76 in Jiangjin, 2.84 in Qingdao, and 2.42 in Turpan. The results show that ZM coating has better corrosion resistance than GI coating under the same atmospheric environment. While under different atmospheric conditions, the corrosion rates of GI and ZM alloy coatings are lower in dry atmosphere, but higher in humid industrial atmosphere and offshore atmosphere with high chlorine. The corrosion performance of GI and ZM coating are connected to the formation of protective corrosion products. In a high chlorine environment, the anodic dissolution of MgZn₂ in the coating releases Mg²⁺ ions[3]. Mg²⁺ can react with OH⁻ to form magnesium hydroxide (Mg(OH)₂), which buffered the pH at cathodic sites[4]. It hindered the formation of ZnO and inhibiting the oxygen reduction reaction, and makes the corrosion product Zn(CO₃)₂(OH)₆ more stable.

The salt spray results are consistent with the Atmospheric corrosion result. After 30 cycles of salt spray corrosion, the corrosion resistance of ZM coating is 4 times that of

GI coating. This paper provides theoretical support for the promotion and application of ZM materials.

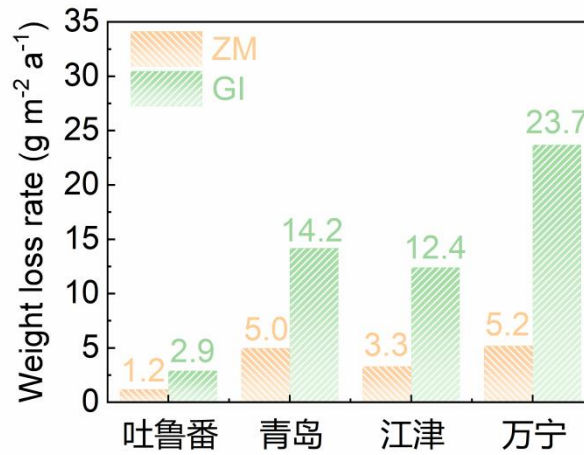


Fig.1 Weight loss rate of GI and ZM coating materials after atmospheric corrosion

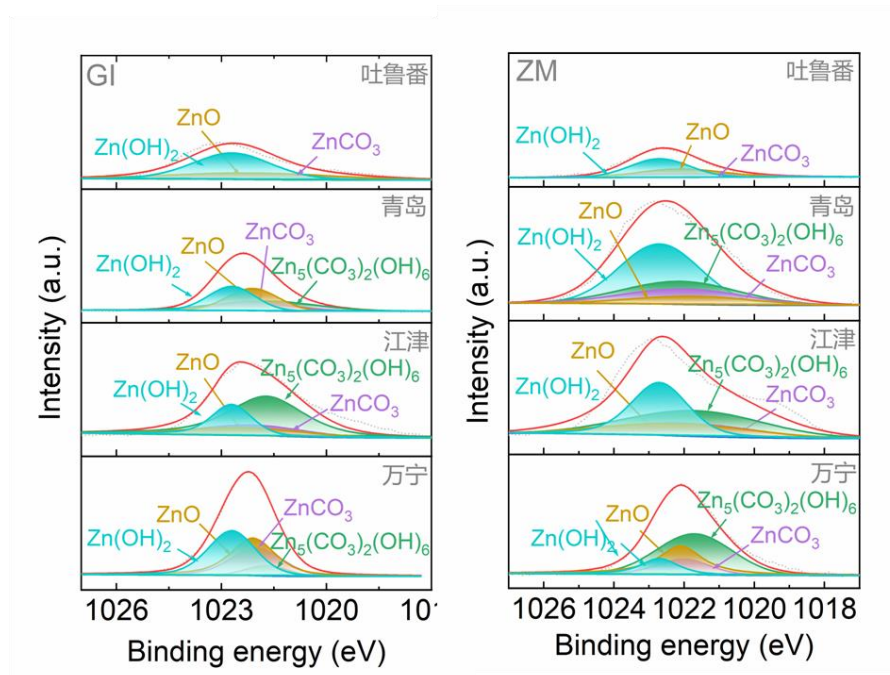


Fig.2 High resolution Zn 2p XPS spectra of (a) GI and (b)ZM coating materials after atmospheric corrosion

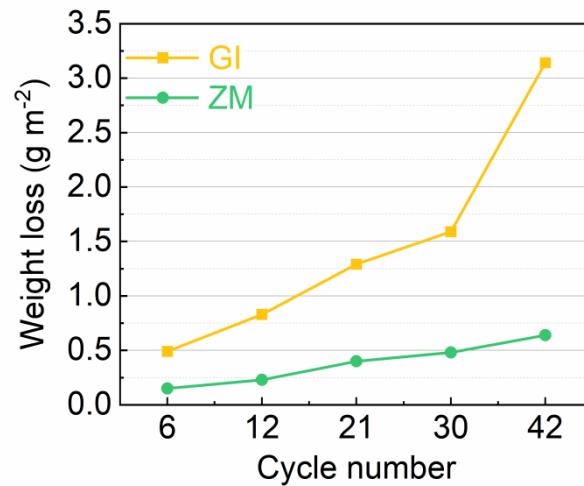


Fig.3 Weight loss rate of GI and ZM coating materials after CCT corrosion

Key words hot-dip galvanized steel ; Zinc-Aluminum-Magnesium; Atmospheric corrosion resistance

Reference

- [1] Yu Z, Hu J, Meng H. A review of recent developments in coating systems for hot-dip galvanized steel[J]. *Frontiers in Materials*, 2020, 7: 74.
- [2] Liu Y, Ooi A, Tada E, et al. Electrochemical monitoring of the degradation of galvanized steel in simulated marine atmosphere[J]. *Corrosion Science*, 2019,147:273-282.
- [3] Prosek T, Persson D, Stouil J, et al. Composition of corrosion products formed on Zn - Mg, Zn - Al and Zn - Al - Mg coatings in model atmospheric conditions[J]. *Corrosion Science*, 2014, 86: 231-238.
- [4] Thierry D, Le Bozec N, Persson D. Corrosion of hot-dip-galvanised steel and zinc alloy-coated steel in ammonia and ammonium chloride[J]. *Materials and Corrosion*, 2020, 71(7): 1118-1124.

17. Fretting crevice corrosion of high-speed rail steel U75V with PA66 liner

Fretting crevice corrosion of high-speed rail steel U75V with PA66 liner

Zexian Wang^{1,2,3}, Weichen Xu^{1,3,*}, Jizhou Duan^{1,3}, Baorong Hou^{1,3}

¹*CAS Key Laboratory of Marine Environmental Corrosion and Bio-fouling, Institute of Oceanology, Chinese Academy of Sciences, Qingdao 266071, People's Republic of China*

²*School of Materials Science and Engineering, Qilu University of Technology, No.3501, Daxue Road, Jinan 250353, People's Republic of China*

³*Laoshan Laboratory Marine Corrosion and Protection Open Studio, Qingdao 266071, People's Republic of China*

Presenter's e-mail address: wangzexian98@163.com

Abstract To investigate the fretting and corrosion morphology on the rail foot surface, a novel testing apparatus was developed to simulate the fretting and corrosion morphology between the rail foot (U75V steel) and the liner (PA66). Electrochemical and surface morphology studies were conducted on the U75V steel of the rail foot surface. It was found in this study that the displacement amplitude set for the experiments predominantly belonged to the partial slip regime. Additionally, the open circuit potential (OCP) and anodic current both increased with the rise in fretting frequency and displacement amplitude. Furthermore, it was observed that the liner, under severe fretting conditions, might inhibit crevice corrosion and reduce surface damage to some extent. Cracks and collapse were evident on the U75V steel surface due to the accumulation of plastic deformation during fretting test, as well as the combined effects of fretting wear, fatigue, and crevice corrosion.

Keywords fretting; crevice corrosion; U75V steel

Reference

- [1] Ren A C, Zhou H, Zhu M, et al. Comparative Study on the Cyclic Corrosion Test of Rail Steel U68CuCr and U75V [J]. *Advanced Materials Research*, 2012, 616-618: 1059-1062.
- [2] Safa M, Sabet A, Ghahremani K, et al. Rail corrosion forensics using 3D imaging and finite element analysis [J]. *International Journal of Rail Transportation*, 2015, 3(3): 164-178.
- [3] Yazici O, Yilmaz S. Investigation of effect of various processing temperatures on

abrasive wear behaviour of high power diode laser treated R260 grade rail steels [J]. Tribology International, 2018, 119: 222-229.

[4] Zhao X H, Fan Y J, Liu Y, et al. Evaluation of fatigue fracture mechanism in a flash butt welding joint of a U75V type steel for railroad applications [J]. Engineering Failure Analysis, 2015, 55: 26-38.

[5] Liu J P, Zhou Q Y, Zhang Y H, et al. The formation of martensite during the propagation of fatigue cracks in pearlitic rail steel [J]. Materials Science and Engineering a-Structural Materials Properties Microstructure and Processing, 2019, 747: 199-205.

18. Improved corrosion resistance of laser melting deposited CoCrFeNi-series high-entropy alloys by Al addition

Improved corrosion resistance of laser melting deposited CoCrFeNi-series
high-entropy alloys by Al addition

Chuanlang Zhang, Jinfeng Li*, Siyuan Lu*

School of Mechanical Engineering and Mechanics, Ningbo University, Ningbo

Institute of Materials, China Academy of Engineering Physics, Mianyang

Abstract The microstructure evolution, pitting performance and passive film status of Al_xCoCrFeNi high entropy alloys (HEAs) via laser melted deposition (LMD) processing are investigated. The results revealed that the Al addition dramatically affects the microstructure of the LMD HEAs by facilitating the precipitation of BCC structured phases, including (Al, Ni)-rich B2 and Cr-rich A2 phases, in the LMD HEAs. Corrosion resistance of the LMD HEAs is improved by adding 10~15 mol. % of Al, which can be ascribed to the modification of passive film chemistry and thickness by Al addition. However, when the passive film on HEAs broke down, pitting in HEAs with Al content larger than 5 mol. % was initiated at B2 phase, due to its lower work function value and depletion in Cr. The current work reveals the Al addition in certain content can successfully improve the corrosion resistance of LMD

CoCrFeNi HEAs, and the regulating of the phase evolution should be the principle for the design of specialized additive manufactured HEAs with high corrosion resistance.

19. Data-Driven Identification and Experimental Verification of Optimal Sn Microalloying Composition for Corrosion Resistance in Low-Alloy Steel

Data-Driven Identification and Experimental Verification of Optimal Sn
Microalloying Composition for Corrosion Resistance in Low-Alloy Steel

Liu Yang¹, Bingqin Wang¹, Xuequn Cheng¹, Xiaogang Li¹

¹ *Institute of Advanced Materials and Technology, University of Science and
Technology Beijing, Beijing 100083, China*

Presenter's e-mail address: d202110693@xs.ustb.edu.cn

Abstract Corrosion resistance is a critical consideration in the selection of materials for various applications. In this study, we employed a data-driven approach using machine learning techniques and a large dataset of corrosion data to design and test four different low-alloy steels with varying amounts of tin (Sn) microalloying (0.1 wt.%, 0.2 wt.%, 0.3 wt.% and Sn-free) for improved corrosion resistance in Beijing outdoor atmosphere. Using experimental methods such as corrosion morphology and rust layer analysis, X-ray diffraction (XRD), X-ray photoelectron spectroscopy (XPS) and potentiodynamic polarization measurements, we verified that the 0.2 wt.% Sn microalloying steel exhibited the best corrosion resistance. Our findings demonstrate the potential of data-driven approaches and machine learning techniques, such as the use of corrosion big data, in the identification and optimization of optimal alloy compositions of corrosion-resistant materials for outdoor environments.

Keywords Corrosion resistance; Data-driven; Machine learning; Sn microalloying

20. Innovative Surface Modification for Enabling CVD Graphene Coating on Steels for Remarkable Corrosion Resistance

Innovative Surface Modification for Enabling CVD Graphene Coating on Steels for
Remarkable Corrosion Resistance

Raman Singh

*Department of Mechanical & Aerospace Engineering, Department of Chemical &
Biological Engineering, Monash University, Vic 3800, Australia*

e-mail: raaman.singh@monash.edu

Abstract Graphene has triggered unprecedented research excitement for its exceptional characteristics. The most relevant properties of graphene as corrosion resistance barrier are its remarkable chemical inertness and impermeability and toughness, i.e., the requirements of an ideal surface barrier coating for corrosion resistance, thus, an interest in graphene coating as a disruptive approach to corrosion mitigation, such as by graphene coating [1-5]. However, the extent of corrosion resistance due to chemical vapour deposition (CVD) graphene coatings has been found to vary considerably in different studies. The author's group demonstrated the ultra-thin graphene coatings developed on copper and nickel by CVD to improve corrosion resistance of the metals by two orders of magnitude in aggressive aqueous chloride environments [3]. In contrast, other reports suggest the graphene coating to actually enhance corrosion rate of copper, particularly during extended exposures. Author's group has investigated the reasons for such contrast in corrosion resistance due to graphene coating as reported by different researchers, and on the basis of the findings, they have succeeded in developing multilayer graphene coatings that conferred durable corrosion resistance to copper and nickel in the aggressive chloride environment [4,5]. However, developing graphene coating on the most common engineering alloy, mild steel by CVD is a non-trivial challenge [1]. The presentation will discuss the challenges, and their successful circumvention that enabled graphene coatings on mild steel, and presents results demonstrating durable and remarkable

corrosion resistance of graphene-coated mild steel [1].

Keywords Graphene Coating, Chemical vapor deposition, Corrosion of mild steel

Reference

[1] R.K. Singh Raman, A. Sanjid, Parama C Banerjee et.al., Remarkably Corrosion Resistant Graphene Coating on Steel Enabled through Metallurgical Tailoring, *Small*, 2023, 2302498.

[2] A. K. Arya, R.K. Singh Raman et.al, Graphene-coated Ni-Cu Alloys for Durable Degradation Resistance of Bi-polar Plates for Proton Exchange Membrane Fuel Cells: Remarkable Role of Alloy Composition, *Small*, 2023, 202305320.

[3] R.K. Singh Raman, P. Chakraborty Banerjee et.al., Protecting Copper from Electrochemical Degradation by Graphene Coating, *Carbon*, 50 (2012) 4040.

[4] M.R. Anisur, P. Chakraborty Banerjee, Christopher D. Easton, R.K. Singh Raman, Controlling Hydrogen Environment and Cooling during CVD Graphene Growth on Nickel for Improved Corrosion Resistance, *Carbon*, 127 (2018) 131.

[5] A. Sanjid, M.R. Anisur, R.K. Singh Raman, Durable Degradation Resistance of Graphene Coated Nickel and Monel-400 as Bi-polar Plates for Proton Exchange Membrane Fuel Cell, *Carbon*, 151 (2019) 68.

21.From Inhibitor Mobility in Active Protective Coatings to Local Inhibitor-Metal Microstructure Interactions

From Inhibitor Mobility in Active Protective Coatings to Local Inhibitor-Metal
Microstructure Interactions

Arjan Mol

*Delft University of Technology, Department of Materials Science and Engineering,
Mekelweg 2, 2628CD Delft, The Netherlands*

J.M.C.Mol@tudelft.nl

Abstract A wide variety of alternative inhibitor types to chromates have been studied for decades as non-toxic candidates for the protection of aerospace aluminium alloys

(AAs) like AA2024-T3. Such alternative inhibitors should provide high intrinsic protection against corrosion in coating defects. Preceding the provision of its protective performance, a complex chain of intricate events ranging from electrolyte ingress in the coating, inhibitor dissolution, inhibitor transport to the coating defect and finally inhibitor-metal substrate interaction should take place. The mechanisms and kinetics of these individual events may also differ and range as a function of inhibitor type, concentration and distribution as well as coating constitution and substrate microstructure.

The vast majority of studies of leaching from inhibited primers focus on release kinetics and use electrochemistry to explore leaching. There are fewer physico-chemical studies which look in detail at the physical and chemical changes in the primer as a result of leaching and fewer still which investigate the role of mechanical degradation resulting from water uptake and inhibitor dissolution on the generation of transport structures in coatings. Furthermore, upon inhibitor release, the complex heterogeneous microstructure of aerospace aluminium alloys has hindered a thorough understanding of the subsequent stages of corrosion protection provided by different classes of inhibitors, such as surface precipitating and surface conversion based inhibitors.

Recent advances in unravelling the subsequent stages of in-coating inhibitor mobility and interaction mechanisms of cerium and lithium based inhibitors with local microstructural features in aerospace aluminium alloys at the micro- and nanoscopic scale will be presented. Several mechanistic and kinetic studies through detailed top-view and cross-sectional electron microscopic investigations along with advanced spectroscopic and electrochemical evaluations shine further light on the complex subsequent mechanisms and kinetics needed to enable the further development of bespoke inhibitor-based active protective coatings.

Keywords Active protective coatings, Corrosion inhibitors, Inhibitor mobility, Inhibitor-metal interactions

22. Conversion coatings and their role in the protection of different alloys

Conversion coatings and their role in the protection of different alloys

Ingrid Milošev

Jožef Stefan Institute, Department of Physical and Organic Chemistry

Jamova c. 39, SI-1000 Ljubljana, Slovenia

Email: ingrid.milosev@ijs.si

Abstract Conversion coatings are formed during simple immersion in an aqueous solution by converting from soluble salt to a slightly soluble or insoluble oxide and/or hydroxide. The coating precipitates either across the metal surface or at intermetallic particles that are electrochemically more noble to the surrounding matrix and where oxygen reduction occurs.¹ Nowadays, two main types of conversion coatings are being explored: rare earth coatings or zirconium and titanium coatings. The inhibitory action of these conversion coatings is based on the retardation of the cathode reaction (i.e. oxygen evolution) on corroding surfaces and the formation of almost insoluble metal (hydr)oxide at the surface. Whilst rare earth coatings are still in the research stage, conversion coatings based on zirconium and titanium are already commercialised.¹ In addition to enhancing corrosion protection, conversion coatings also can provide increased interfacial adhesion to a subsequent organic coating, as most industrial applications use multilayer coating systems consisting of a conversion layer, a main organic layer and a top layer.

In the presentation, mainly zirconium conversion coatings (ZrCCs) will be considered. The formation mechanism of ZrCCs on wrought aluminium alloys is relatively well investigated but less so on cast alloys.¹⁻⁵ First, it will be shown that the composition of the aluminium alloy has a decisive effect on the degree of protection and that surface preparation is a crucial step in preparing well-protective coatings.¹⁻⁵ In addition to aluminium alloys, the protection of other important materials, such as steel and galvanised steel, has to be considered. The selected results on ZrCCs deposited on low-carbon steel and zinc substrates will be presented. The composition, thickness,

and structure of conversion layers were analysed through the top surface and cross-section SEM/EDS, XPS and ToF-SIMS techniques. Basic considerations of the aqueous chemistry of zirconium metal and the general mechanism of coatings formation will also be discussed.⁶

The results show that the deposition mechanism and the resulting ZrCC properties depend strongly on the type of substrate. Besides the substrate itself, the parameters having the most influence on the resulting corrosion resistance are the concentration of hexafluorozirconic acid used in the conversion bath, pH and conversion time. These parameters were optimised to give the highest values of corrosion protection deduced from electrochemical and non-electrochemical measurements. The optimisation was performed using a mathematical model of the system created based on experiments performed according to statistically selected sets of variable combinations. Producing a ZrCC that would be efficient on different substrates is challenging. Using statistical tools when designing experiments seems to allow the determination of critical factors and their effect on a desired output and is thus helpful for optimising coatings for versatile components.

Acknowledgements: The financial support by Slovenian Research Agency is acknowledged (grants No. P2-0393 and P1-0134), and KET4Clean Production Microgrant within the European Union's Horizon 2020 research and innovation programme (grant agreement No. 777441, KET4CP-SME2019-06-NO.05).

References

- [1] I. Milošev, G.S. Frankel, *J. Electrochem. Soc.*, 165 (3) (2018) C127-C144.
- [2] M. Mujdrica Kim, B. Kapun, U. Tiringler, G. Šekularac, I. Milošev, *Coatings*, 9 (2019) 563.
- [3] G. Šekularac, J. Kovač, I. Milošev, *J. Electrochem. Soc.*, 167 (2020) 111506.
- [4] G. Šekularac, J. Kovač, I. Milošev, *Corros. Sci.*, 169 (2020) 108615.
- [5] I. Milošev, B. Kapun, P. Rodič, *J. Electrochem. Soc.*, 169 (2022) 091501.
- [6] A. Kraš, I. Milošev, *J. Electrochem. Soc.*, 170 (2023) 021508.

23. Surface Treatment of Recycled Aluminium and its Effect on Filiform Corrosion

Surface Treatment of Recycled Aluminium and its Effect on Filiform Corrosion

Andreas Erbe, Erlind Mysliu

Department of Materials Science and Engineering, NTNU, Norwegian University of Science and Technology

Abstract Availability and demand of aluminium based on post-consumer scrap is increasing. The ability to produce recycled materials from PCS with the same properties as primary produced materials is a key step for sustainable production. Recycling friendly alloys can be manufactured without mechanical property loss compared to primary based alloys by adjusted composition windows. The role of impurity elements in the adjusted composition windows of the recycling friendly alloys is far from clear, since some trace elements affect electrochemical properties significantly even at the ppm level. Providing a composition-tolerant surface treatment is the biggest challenge towards a wide-scale implementation of recycled aluminium based on PCS. Typical pretreatments before applying organic coatings are (i) anodising and (ii) the sequence of alkaline etching – desmutting – conversion coating. Organic coatings on the final products typically fail by filiform corrosion (FFC). Designing FFC resistant surfaces based on PCS requires a thorough understanding of FFC mechanisms and the different pretreatment, which is the topic of this presentation.

For the mechanism of FFC, recent work by in situ Raman spectroscopy reveals the full complexity of several co-located cathodic processes [1]. In particular, images and spectra reveal gas evolution and the presence of aluminium hydrides in the head of the filaments, pointing to a more prominent role of hydrogen evolution than previously thought [1]. Electrochemically, the pitting potential of an uncoated surface often correlates well with FFC resistance of a coated surface, and dynamic electrochemical impedance spectroscopy is a method which

enables the resource-efficient extraction of major parameters of the system that can be used for ranking of materials [2].

Alkaline etching is frequently used to remove surface layers, e.g., from extrusion. Etching rates overall depend on minor details of the alloy composition [3]. During etching, not only Al, but also significant fractions of the investigated elements Cu, Fe, Mg, Mn, Ni, and Zn dissolve. Surface analysis of samples in different stages of the etching process show (i) an increase in oxide layer thickness with etching time, (ii) an enrichment of important alloy elements and impurities (Cr, Cu, Fe, Mg, Mn, Si) near the metal/oxide interface, and (iii) the deposition of Mg, Fe, Si-containing aluminium hydroxide on the surface. In situ fast electrochemical experiments show that the aluminum dissolution rate during etching is limited by the transport of species through the oxide precursor layer, thus is potential-independent. Characteristic differences in etching rates between different alloy classes, are most likely related to differences in the anodic dissolution mechanisms [3].

Conversion coating is often the last pretreatment step before organic coatings are applied. Combining in situ electrochemistry and surface analysis reveals that for the generation of ZrO₂-based conversion coatings with metal ion additives, co-precipitation of the metal hydroxides of the additives may contribute significantly to the overall FFC-damping effects of conversion coatings [4].

References

- [1]. Mysliu, O. Lunder, A. Erbe: *Phys. Chem. Chem. Phys.* 25, 11845-11857 (2023).
- [2]. Mysliu et al.: *ChemElectroChem*, accepted (2023).
- [3]. Mysliu et al.: *J. Electrochem. Soc.* 170, 011503 (2023).
- [4]. Mysliu et al.: *Deposition mechanism and structure of ZrO₂-based conversion coatings on AA6060 aluminium alloys and their susceptibility to filiform corrosion*, submitted (2023).

24. Advanced electrochemical and spectroscopic monitoring & modelling of transport of water and ions in organic coatings of metal

Advanced electrochemical and spectroscopic monitoring & modelling of transport of water and ions in organic coatings of metal

*Negin Madelat *, Benny Wouters, Zahra Jiryaisharahi, Annick Hubin, Tom Hauffman, Herman Terry*

¹Research Group Electrochemical and Surface Engineering, Vrije Universiteit Brussel, Pleinlaan 2, 1050 Brussels, Belgium, e-mail: herman.terryn@vub.be

Abstract Organic coatings are widely used for corrosion protection of aluminium substrates, forming a hybrid metal oxide/coating system. The durability of these hybrid systems under inevitable environmental influences is governed by a complex interplay among many factors such as barrier properties of the coating and the metal oxide/coating buried interface. Non-destructive in situ investigations of the buried interfaces is challenging since the accessibility is limited by a μm -thick organic overlayer. The stability of this hidden interfacial zone has been thoroughly investigated by model molecules and thin layers. However, scaling up the knowledge to industrial systems is complex and challenging. Therefore, in this work, an in-depth characterization of the coated metals is done using an integrated spectro-electrochemical technique. Odd random phase electrochemical impedance spectroscopy (ORP-EIS) in combination with attenuated total reflection Fourier transform infrared spectroscopy (ATR-FTIR) in Kretschmann geometry is employed to monitor the general electrochemical behaviour of the system, while simultaneously probing the local interfacial dynamics. The time evolution of the ions ingress front across the coating was correlated to the structure/composition of the coating and the delayed arrival of the ions compared to water was confirmed. Moreover, the electrochemical response of the buried interface was characterized with respect to the arrival time of ions at the interface. Different supplementary techniques are used to

verify the proposed insights. A strategy to determine lateral diffusion of water in the organic coating based on dual ORP EIS measurements will be introduced. FEM element modelling will be discussed to model the water transport in the coatings.

Keywords Transport of water and ions in organic coatings, EIS, FEM modelling

Reference

[1] FEM modelling to predict spatiotemporally resolved water uptake in organic coatings: Experimental validation by odd random phase electrochemical impedance spectroscopy measurements Meeusen, M., van dam, J., Madelat, N., Jalilian, E., Wouters, B., Hauffman, T., Van Assche, G., Mol, A. J. M. C., Hubin, A. & Terryn, H., Sep 2023, In: Progress in Organic Coatings. 182, p. 1-11 11 p., 107710.

[2] Monitoring initial contact of UV-cured organic coatings with aqueous solutions using odd random phase multisine electrochemical impedance spectroscopy Wouters, B., Jalilian, E., Claessens, R., Madelat, N., Hauffman, T., Van Assche, G., Terryn, H. & Hubin, A., Sep 2021, In: Corrosion Science. 190, 109713.

25. Corrosion behaviors of multilayer C/Cr/SS bipolar plates for proton exchange membrane fuel cells under dynamic potential polarization based on New European Driving Cycle

Corrosion behaviors of multilayer C/Cr/SS bipolar plates for proton exchange membrane fuel cells under dynamic potential polarization based on New European Driving Cycle

Qian Hu, Xian-Zong Wang*

State Key Laboratory of Solidification Processing, Northwestern Polytechnical University, Xi'an 710072, PR China

Presenter's e-mail address: xianzong.wang@nwpu.edu.cn

Abstract The New European Driving Cycle (NEDC) induces remarkable degradation of proton exchange membrane fuel cells. In this study, the multilayer C/Cr coating prepared on SS316L includes a surface a-C layer, a C/Cr-C alternating layer, and a

C/Cr composite layer. The long-term cyclic dynamic potential polarizations based on NEDC with four different E_{peak} are investigated on the C/Cr/SS bipolar plates.

The C/Cr/SS achieves superior small ICRs and a low corrosion rate with E_{peak} up to 1.12 V, demonstrating great potential for commercial applications. The enhanced corrosion resistance of the C/Cr/SS is mainly attributed to the increased interfaces and the formation of C-Cr compounds, which optimize the potential distribution across the coating. However, During the 50 h of dynamic potential cycles based on NEDC, as a result of Cr dissolution at the heterogeneous interface between the C/Cr-C alternating layer and C/Cr composite layer, mild local corrosion occurs at 1.16 V and accelerates at 1.22 V. Both of them experience stages of pitting initiation, cavity, delamination, and finally collapse. After the dynamic potential cycles, the ICR values are all below 10 mΩ cm². Such a small increase in ICR is attributed to the well reserved surface a-C layer and the high stability of the multilayer C/Cr coating.

The high corrosion resistance and electrical conductivity, especially the well reserved coating structure, are promising features for the potential application of multilayer C/Cr coating with optimized structure and composition on metal bipolar plates to be used in PEMFCs. The present work offers new insights into NEDC-based potential polarization induced degradation on C/Cr/SS.

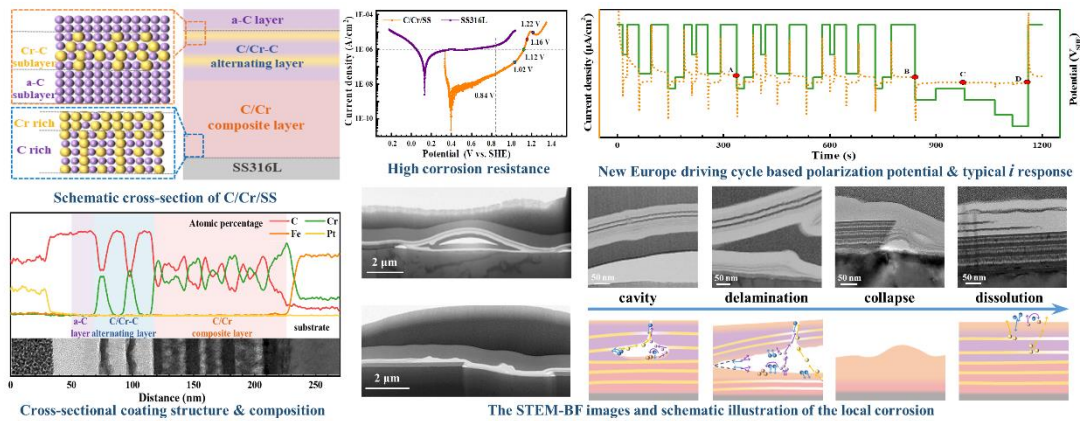


Figure The cross-sectional structure of multilayer C/Cr coating, the dynamic potential cycles based on NEDC, and the schematic illustration of the degradation process of the coating.

Keywords New European Driving Cycle; C/Cr coating; corrosion; metal bipolar plates

Reference

[1] Qian Hu, Jia-Yi Gao, Shi Su, Yu-Xuan Xu, Jing-Li Luo*, Xian-Zong Wang*, Corrosion behaviors of multilayer C/Cr/SS bipolar plates for proton exchange membrane fuel cells under dynamic potential polarization based on New European Driving Cycle, Corrosion Science, 2023, 214:111032. <https://doi.org/10.1016/j.corsci.2023.111032>

26.Environmental Protection Coating System for Refractory Metal Alloys in extreme environments

Environmental Protection Coating System for Refractory Metal Alloys in extreme environments

Ranran Su¹, Hongliang Zhang², John H. Perepezko³

¹*School of Mechanical Engineering, Shanghai Jiao Tong University, Shanghai, China*

²*Institute of Modern Physics, Fudan University, Shanghai, China*

³*Department of Materials Science and Engineering, University of Wisconsin-Madison, WI 53706, USA*

Abstract The refractory multi-principal elements alloys (RMPEAs) are promising structural materials to help increase power efficiency in high-temperature oxidation environments, while the intrinsic poor oxidation resistance of the refractory elements limits their application. The oxidation behavior of a refractory high entropy alloy WMoTaNbV is investigated at 1300 °C. By using an innovative two-step coating strategy with Mo-precoat followed by Si-B pack cementation, a multilayer Mo-Si-B coating with strong oxidation resistance and compatibility as well as a diffusion barrier is developed. The coating can protect the substrate at 1300°C for more than 750 h of thermal cycles. An RMPEA boride phase develops at the alloy/coating interface after longtime service and acts as an additional diffusion barrier to maintain the coating integrity. The oxidation test results demonstrated that this two-step coating system provides robust oxidation protection at high temperatures and can be widely

applied in RMPEAs.

Keywords refractory alloy, coating, thermal cycling, oxidation, high temperature

Reference

- [1] R. Su, H. Zhang, L. Liu, J.H. Perepezko, Boron capture stabilizing the diffusion barriers in a two-step Mo-Si-B coated refractory multi-principal element alloy, *Corrosion Science*. 221 (2023) 111365.
- [2] R. Su, L. Liu, J.H. Perepezko, Alloy designs for high temperature Mo-base systems, *International Journal of Refractory Metals and Hard Materials*. 113 (2023) 106199.
- [3] R. Su, H. Zhang, G. Ouyang, L. Liu, W. Nachlas, J. Cui, D.D. Johnson, J.H. Perepezko, Enhanced oxidation resistance of (Mo₉₅W₅)₈₅Ta₁₀(TiZr)₅ refractory multi-principal element alloy up to 1300°C, *Acta Materialia*. 215 (2021) 117114.

27.Gradient Cu²⁺ Releasing Rate Enhanced the Antibacterial, Cytocompatibility, and Degradation Resistance of Cu-containing PEO coated Pure Mg

Gradient Cu²⁺ Releasing Rate Enhanced the Antibacterial, Cytocompatibility, and Degradation Resistance of Cu-containing PEO coated Pure Mg

Kun Qian^{a,b,c}, Feng Xue^{a,b,c}, Jing Bai^{a,b,c}

¹*School of Materials Science and Engineering, Southeast University, Jiangning, Nanjing 211189, Jiangsu, China*

²*Jiangsu Key Laboratory for Advanced Metallic Materials, Jiangning, Nanjing 211189, Jiangsu, China*

³*Institute of Medical Devices (Suzhou), Southeast University, Suzhou 215163, China*

Abstract Magnesium has become promising orthopedic appliances materials due to its degradability and biocompatibility. However, its application is restricted by the inability of obtaining antibacterial and corrosion resistance properties simultaneously. Nowadays adding antibacterial elements into PEO coated Mg have been researched to solve such problem. Nevertheless, such methods has also been doubted due to the

cytotoxicity of antibacterial elements. In this research, a series of composite coatings with different amounts of Cu compositions were fabricated on pure Mg surface through plasma electrolytic oxidation (PEO) and hydrothermal deposition. The analysis results showed that Cu-containing composite coating mainly composed of PEO coating and particle-deposited layer constitute of CuHPO_4 and $\text{Cu}_3(\text{PO}_4)_2$. The Cu-containing deposition layer effectively seal the micropores on the surface of the PEO coating and improve its corrosion resistance. In addition, the Cu^{2+} generated by the degradation also promotes the deposition of $\text{Ca}_{19}\text{Cu}_2(\text{PO}_4)_{14}$ composed layer on the coatings' surface, which further decreases its degradation rate. When co-cultured for 24 h, the antibacterial rate of Cu-containing composite coatings reached 99.89% to E.coli and 97.14% to S.aureus. Cytotoxicity test showed that Cu-containing composite coating had better biocompatibility than PEO coating after co-cultured for 120 h. It can be explained by the fact that Cu^{2+} ion releasing rate of Cu-containing composite coating exhibited gradient changing phenomenon. Therefore, at early stage of implantation, high content of releasing Cu^{2+} ion can kill bacterial to avoid infection. Then at later implantation stage Cu^{2+} ion releasing rate decreased to an appropriate value for promoting growth and reproduction of cell.

28. Advancing Concrete Durability with Graphene Oxide-Based Coatings against Rebar Corrosion

Advancing Concrete Durability with Graphene Oxide-Based Coatings against Rebar
Corrosion

M. Shariatmadar, M. Mahdavian*, B. Ramezanzadeh*

*Surface Coatings and Corrosion Department, Institute for Color Science and
Technology, Tehran, Iran.*

* Presenting author: M. Mahdavian (mahdavian-m@icrc.ac.ir)

Abstract Concrete structures are reinforced with rebar to provide tensile strength and resistance to loads. However, the construction industry faces a significant challenge

due to the corrosion of rebar induced by chloride ions, which can compromise the safety and integrity of concrete structures. To address this challenge, a new coating system was developed based on the modified graphene oxide. A hydrophobic thin layer was created using epoxy-silicone functionalized graphene oxide (GO-EP) through covalent grafting with (3-aminopropyl)triethoxysilane (APTES) bridges. Characterization by Fourier transform infrared spectroscopy (FTIR), thermal gravimetric analysis (TGA), X-ray photoelectron spectroscopy (XPS), and Raman revealed that APTES and epoxy-silicone modified polyacrylate was successfully grafted on GO.

The GO-EP dispersion in butyl acetate was applied to the concrete surface, resulting in a significant increase in the water contact angle of GO from 40° to 120°, indicating improved hydrophobicity of the concrete surface. The GO-EP thin layer demonstrated excellent waterproofing performance with a capillary water absorption rate of 60.4 g.cm⁻².h^{-1/2}, compared to GO's 684.8 g.cm⁻².h^{-1/2}. Also, the negative zeta potential of GO-EP (10 eV) can reduce the penetration of chloride ions, which was confirmed by the Rapid Chloride Permeability Test (RCPT), according to ASTM C 1202. The results indicated the penetration of 800 Coulomb after 6 h of immersion. Electrochemical impedance spectroscopy (EIS) and open circuit potential (OCP) were used to evaluate the effectiveness of the GO-EP thin layer in preventing chloride-induced corrosion of rebar. Results showed a significant decrease in chloride and water penetration into the concrete, indicating that the GO-EP thin layer was effective in reducing the risk of corrosion.

Keywords Concrete; Rebar Corrosion; Thin layer; Graphene.

29.Passive Film and It's Influence on Surface Properties of Titanium Alloy

Passive Film and It's Influence on Surface Properties of Titanium Alloy

Mei Yu, Zhong Yang, Xinran Zhang, Chao Han, Mingyu Zhao, Songmei Li, Jianhua

Liu

School of Materials Science and Engineering, Beihang University, Beijing 100191

Presenter's e-mail address: yumei@buaa.edu.cn

Abstract Titanium alloys have received widespread attention because of their high specific strength, excellent fatigue performance, and especially excellent corrosion resistance to seawater and marine atmosphere, etc. Commonly, a compact passive film would be spontaneously formed on the surface of titanium alloy, which could effectively isolate the titanium matrix from the corrosion medium and provide a good protection performance for the alloys. Once the passive film is destroyed, it will immediately recover to enhance the corrosion resistance of titanium alloys. And even under the condition of anodic polarization, it will display a passive behavior in a wide potential range. However, this will affect the alloy surface activity, which in turn affects the adhesion of other coatings on the alloy surface, and pretreatment is required to increase the adhesion when preparing other coatings. Therefore, investigating the passive film growth of titanium alloys and their protective behavior for titanium alloys is of great significance.

In the present work, the growth of passive film on the surface of titanium alloys and its effect on the surface behavior of titanium alloys in two kinds of environments, air and simulated seawater, were investigated. Based on the potentiodynamic polarization curve, characteristic potentials were selected as the polarization potentials for potentiostatic polarization of TC18 titanium alloy, and the corrosion resistance of the passive film obtained from different polarization potentials was investigated, and the schematic diagram of the potential dependence of characteristics of the passive film was proposed.

Keywords Titanium alloy, Passive film, Surface property, Corrosion resistance

30.Preparation and corrosion protection mechanism of MXene-based composite coatings on metals

Preparation and corrosion protection mechanism of MXene-based composite coatings

on metals

Huaijie Cao

Shanghai Key Laboratory of Materials Protection and Advanced Materials in Electric Power, Shanghai University of Electric Power, Shanghai 200090, China

E-mail: hjcao0510@shiep.edu.cn

Abstract MXene has large aspect ratio and excellent physical barrier performance, which is expected to be used to improve the anti-corrosion property of coating in harsh environments. Based on the rich functional groups on the surface and strong barrier ability, MXene nanosheet can be uniformly dispersed in other matrix, while improving the anti-corrosion performance of the composite coating. $Ti_3C_2T_x$ /silane composite coating, $Ti_3C_2T_x$ /LDH composite coating, and $Ti_3C_2T_x$ MXene composite coating were prepared by dip-coating method and electrodeposition. Surface microstructure analysis indicates that the incorporation of MXene can reduce the structural defects of the coating. The results of electrochemical tests show that the corrosion current density of MXene composite coating is significantly reduced compared to the bare sample counterpart. The $Ti_3C_2T_x$ MXene can significantly improve the corrosion resistance of the coating. It exhibits excellent anti-corrosion performance in NaCl solution, acidic, and alkaline environments. Long-term immersion test and surface analysis demonstrate that MXene can effectively extend the penetration path of corrosive media and improve the stability of the coating. The corrosion protection mechanisms for MXene composite coatings were proposed according to the surface morphology, composition, and electrochemical analysis.

Keywords: *MXene; composite coating; corrosion protection; metal;*

Reference

- [1] Wang, T.; Cao, H.* *Progress in Organic Coatings*. 2023, 182: 107715.
[2] Jia, W.; Cao, H.*; Wang, T.; et al. *Surface and Coatings Technology*. 2023, 463: 129551. [3] Cao, H.*; Fang, M.; Jia, W.; et al. *Composites Part B: Engineering*. 2022, 228: 109427. [4] Zeng, Y.; Cao, H.*; Jia, W.; et al. *Surface and Coatings*

Technology. 2022, 445: 128709.

[5] He, Z.; Cao, H.*; Zhou, M.; et al. *Surface and Coatings Technology*. 2022, 449: 128952.

[6] Cao, H*. *Colloids and Surfaces A: Physicochemical and Engineering Aspects*. 2022, 652: 129893.

[7] Cao, H.*; Xiong, D.-B. * *Diamond and Related Materials*. 2021, 118: 108504.

31.Green surface protection programme for marine microbiologically influenced corrosion and biofouling

Green surface protection programme for marine microbiologically influenced
corrosion and biofouling

Jinlong Zhao^{1,#}, Chunguang Yang^{1,#}, Tongyu Lian¹, Ke Yang¹, Da Sun², Xinrui Zhang¹

¹ *Institute of Metal Research, Chinese Academy of Sciences, Shenyang 110016, China*

² *Institute of Life Sciences & Biomedical Collaborative Innovation Center of Zhejiang Province, Wenzhou University, Wenzhou 325035, China*

Presenter's e-mail address: jlzhao@imr.ac.cn

Abstract Microbiologically influenced corrosion (MIC) and biofouling are of frequent co-occurrence on the surface of marine engineering equipment. Therefore, a green protection programme was proposed in view of such hazard. It included an integrated functional Cu-bearing antibacterial stainless steel (SS), anodic polarization treatment and metal-based surface coating which could be used to solve the above problems and achieve multi-sea area adaptability. Anodic polarization treatment was used to investigate MIC behavior of 316L-Cu SS against marine *Pseudomonas aeruginosa* using electrochemical tests and morphology observation techniques [1]. The results indicated that anodic polarization treatment endowed 316 L-Cu SS with a decreased corrosion current and increased pitting potential in comparison with conventional 316L SS and 316L-Cu SS incubated in a biotic medium. The surface morphology observations combined with XPS analysis found that 316L-Cu SS

effectively inhibited bacterial reproduction and promoted the formation of a dense protective extracellular polymeric substance (EPS)-Fe membrane, leading to less susceptibility to pitting corrosion than 316L SS. Furthermore, an environment-friendly antifouling coating using pre-alloyed Cu-bearing SS powder as raw material was developed by cold spraying [2]. The experimental results showed that pre-alloyed powder coating effectively inhibits the adhesion of marine fouling organism *Pseudomonas aeruginosa*. Due to the even distribution of Cu, it had better corrosion resistance and lower release rate of Cu ions compared with mixed powder coating, which made it appear protective of the marine environment. In addition, the coating has better wear resistance than commercial self-polishing copolymer coatings, which has the potential to become a new long-life marine antifouling coating.

Keywords Microbiologically influenced corrosion, Extracellular polymeric substances, Anodic polarization, Stainless steel, Environmental-friendly coating

Reference

- [1] J. Zhao*, D. Sun, M. Arroussi, T. Lian, X. Zhang, C. Yang, K. Yang, Effect of anodic polarization treatment on microbiologically influenced corrosion resistance of Cu-bearing stainless steel against marine *Pseudomonas aeruginosa*, *Corrosion Science*, 207 (2022) 110592.
- [2] T. Lian, J. Zhao*, C. Yang, K. Yang, Environment-friendly antifouling coating of Cu-bearing stainless steel prepared by pre-alloyed powder, *Materials Letters*, 344 (2023) 134439.

32. Inhibition of Duplex Steel in Acidizing of Sour Wells

Inhibition of Duplex Steel in Acidizing of Sour Wells

Günter Schmitt¹, Ulf Borgerding¹, Tim Gommlich¹, Stefan Losacker²

¹*IFINKOR-Institute for Maintenance and Corrosion Protection Technologies gGmbH, Iserlohn, Kalkofen 4, 58634 Iserlohn, Germany (gue.schmitt@t-online.de)*

²*ExxonMobil Production Deutschland GmbH, Vahrenwalderstr. 238, 30179*

Hannver

gue.schmitt@t-online.de

Abstract Treatment with acids (acidizing) is widely used to improve (stimulate) the productivity of oil and gas wells. Due to the extreme corrosiveness of the acidizing fluids the use of effective corrosion inhibitors is crucial. Since many decades inhibitors are available that protect satisfactorily carbon steels, ferritic and austenitic steels as well as Ni-based alloys in sweet wells at temperatures up to 150°C. However, these inhibitors fail to protect austenitic-ferritic (duplex) steels in sweet systems above 80° C and fail completely in sour systems, specifically at higher temperatures [1]. The paper reports on an inhibited acidizing fluid that keep the corrosion rate even at duplex steel below 6 µm/h at temperatures up to 150°C in the presence of 14 bar H₂S. The results were obtained in an experimental study testing the corrosion performance of coupons from L80 steel, 22Cr5Ni duplex steel and 28Cr32Ni austenitic steel at 100 °C and 150°C in three different acidizing fluids pressurized with up to 16 bar H₂S. The best inhibited acidizing fluid yielded corrosion rates at L80 of 6 µm/h at 150°C under 19 bar H₂S. Under the same conditions the 28Cr32Ni austenitic steel lost only 0.01 µm/h. It appeared that the efficiency of the same inhibitor at the same concentration acts extremely different in hydrochloric based acids than in strong organic acids.

Keywords carbon steel, duplex steel, super-austenitic steel, acidizing, sour gas wells, hydrochloric acid, strong organic acid, high hydrogen sulfide pressure, high temperature

Reference

[1] G. Schmitt, E. Strobel-Effertz, W. Bruckhoff, "Performance of inhibitors in hydrochloric acid at temperatures up to 150°C in the presence of hydrogen sulfide", *Academia Chimica Hungarica - Models in Chemistry* 133(3) (1996) 267

33. Active learning approach towards discovery of new efficient corrosion modulators Mikhail Zheludkevich

Active learning approach towards discovery of new efficient corrosion modulators

Mikhail Zheludkevich

Institute of Surface Science, Helmholtz-Zentrum Hereon and University of Kiel

mikhail.zheludkevich@hereon.de

Abstract Selecting effective corrosion inhibitors from the vast chemical space is not a trivial task, as it is essentially infinite. Fortunately, machine learning techniques have shown great potential in generating shortlists of inhibitor candidates prior to deeper experimental testing. This work showcases the promise of computer-assisted methods for rapidly and efficiently screen large numbers of organic compounds as potential corrosion modulators for light Mg and Al alloys. Two data-driven quantitative structure-property relationship (QSPR) machine learning models were trained and used for in silico searches. Statistical methods were applied to select the most relevant features to the target property for support vector regression and kernel ridge regression models, respectively, to predict the behavior of untested compounds. The performance of the two supervised learning approaches were compared and the robustness of the data-driven models were assessed by experimental blind testing. The active learning approach was implemented in order to improve the quality of prediction via inclusion of the experimental results of the newly predicted modulators into extended training data sets. The applicability of the suggested models for both selection of corrosion inhibitors and electrolyte additives for primary Mg-batteries has been demonstrated.

34. Photoelectrochemical effect of Cu₂O on the corrosion behavior of Cu

Photoelectrochemical effect of Cu₂O on the corrosion behavior of Cu

Jiarun Li¹, Feng Qian¹, Chongqing Guo¹, Ning Wang^{2, *}, Zhuoyuan Chen^{3, *}, Lei

Wang¹

¹*School of Environment and Safety Engineering, Qingdao University of Science and Technology, 53 Zhengzhou Road, Qingdao 266042, Shandong, China;*

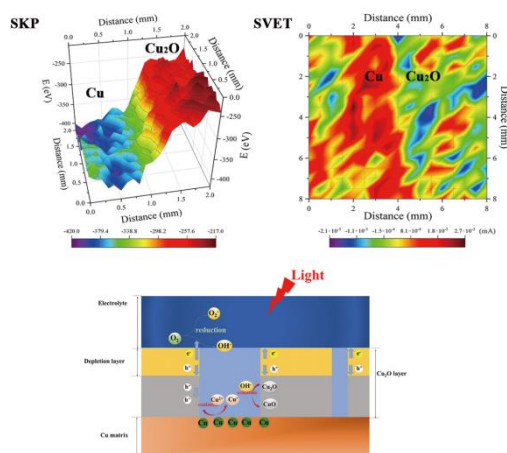
²*Key Laboratory of Marine Environmental Corrosion and Bio-fouling, Institute of Oceanology, Chinese Academy of Sciences, 7 Nanhai Road, Qingdao 266071, Shandong, China*

³*School of Materials Science and Hydrogen Energy, Foshan University, 18 Jiangwanyi Road, Foshan 528000, Guangdong, China*

Presenter's e-mail address: lijiarun@qust.edu.cn

Abstract The electrochemical associated with photoelectrochemical (PEC) behaviors of Cu electrodeposited with Cu₂O layer were investigated in this work. The corrosion of Cu was promoted due to enhanced anodic and cathodic processes under AM 1.5 illumination compared with that in the darkness, especially for the anodic process. The photoinduced corrosion of Cu by Cu₂O was detected by Scanning Vibrating Electro Technique (SVET). The effect of Cu₂O on the promotion of Cu corrosion under illumination can be ascribed to the narrowed depletion layer in Cu₂O under illumination, which facilitates the separation of hole-electron pairs. The resultant holes give rise to the oxidation of Cu matrix and lead to a promoted corrosion consequently. Besides, a method for in-situ determining the photoinduced current of a semiconductor material is proposed.

Keywords photoinduced corrosion, Cu₂O, copper, SVET, p-type semiconductor



35. Exploring the potential of transfer learning in extrapolating accelerated corrosion test data for long-term atmospheric corrosion forecasting

Exploring the potential of transfer learning in extrapolating accelerated corrosion test data for long-term atmospheric corrosion forecasting¹

Vincent Vangrunderbeek^{1}, Leonardo Bertolucci Coelho^{1,2}, Dawei Zhang³, Yiran Li³,
Yves Van Ingelgem¹, Herman Terry¹*

¹*Research Group Electrochemical and Surface Engineering (SURF), Vrije Universiteit
Brussel, Brussels, Belgium*

²*ChemSIN – Chemistry of Surfaces, Interfaces and Nanomaterials, Université libre de
Bruxelles (ULB), Brussels, Belgium*

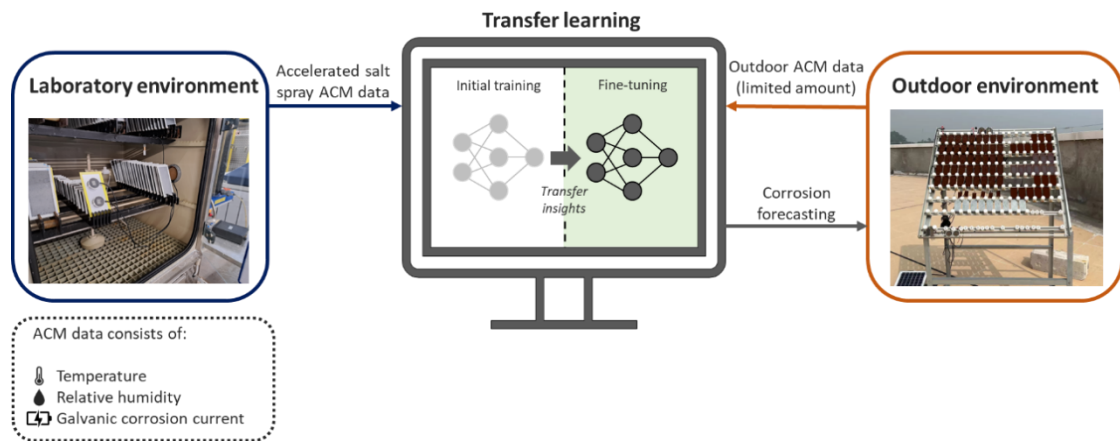
³*Beijing Advanced Innovation Center for Materials Genome Engineering, Institute for
Advanced Materials and Technology, Uni. of Science and Technology Beijing, China*

Presenter's e-mail address: vincent.vangrunderbeek@vub.be

Abstract Atmospheric corrosion sensors (ACM sensors), based on the principle of measuring galvanic corrosion between two electrodes with different electrochemical potentials, have proven to be an efficient way of assessing the corrosiveness of the environment from which the expected corrosion performance of a metal can be derived. Nonetheless, the data generated by ACM sensors is complex, and it is challenging to determine interpretable correlations between the different variables measured using only analytical corrosion expertise. Recently, studies^{2,3} have shown that machine learning models are able to unravel unexplored patterns between the environment and the current output, thereby unlocking the potential to develop predictive atmospheric corrosion models. However, one limiting factor is the large amount of data from long testing times required to make proper predictions in the environment where the sensor was placed.

Our research argues that the specific subdomain of machine learning called transfer learning (TL) can solve this issue. In essence, TL attempts to transfer knowledge from a previously developed machine learning model (the source) to another similar task

(the target). As such, it provides a way to improve the modeling performance in domains where data is scarce. When predicting the sensor's output for a year, fine-tuning of previously trained source model is required. This source model can be trained on data derived from a sensor installed in a controlled lab environment or a different geographical setting. The TL approach proved to be particularly useful during cases when limited target training data was available, outperforming the benchmark models¹.



Reference

- [1] Vangrunderbeek, V. et al. Exploring the potential of transfer learning in extrapolating accelerated corrosion test data for long-term atmospheric corrosion forecasting. *Corrosion Science*. Volume 225 (2023). <https://doi.org/10.1016/j.corsci.2023.111619>.
- [2] Coelho, L.B. et al. Reviewing machine learning of corrosion prediction in a data-oriented perspective. *npj Mater. Degrad.* 6, 8(2022).doi:10.1038/s41529-022-00218-4
- [3] Pei, Z. et al. Towards understanding and prediction of atmospheric corrosion of an Fe/Cu corrosion sensor via machine learning. *Corrosion Science* 170 (2020).doi: 10.1016/j.corsci.2020.108697

36. International standardization of corrosion of metals and alloys

International standardization of corrosion of metals and alloys

Qian Li

China Metallurgical Information and Standardization Institute

Abstract ISO (International Organization for Standardization) is an independent, non-governmental international organization. ISO and its members bring together a network of experts to share knowledge and develop International Standards. ISO/TC 156 Corrosion of metals and alloys is responsible for the standardization in the field of corrosion of metals and alloys including corrosion test methods, corrosion prevention methods and corrosion control engineering life cycle. General coordination of activities in these fields within ISO. Currently, it has published 115 international standards and 31 standards are under development

37. Unveiling the Phase Transformation at Nano Scale

Unveiling the Phase Transformation at Nano Scale

Huang Yizhong

School of Materials Science and Engineering

Abstract Phase transformation is a common event in the research of materials science. It involves either crystalline structured or compositional conversion when materials are subjected to external environments. Understanding the phase changes is of importance in tailoring the design and synthesis of a specified material that is selective for the desirable performance. X-rays and electron beams are powerful sources enabling the determination of the variation of phases.

In this talk, unveiling the transformation of amorphous GeO₂ into crystalline GeO₂ in the presence of water is covered. The dynamic process of the phase transformation is observed by an *in-situ* TEM liquid cell which is sealed and permits the water flow inside TEM during electron beam imaging. We demonstrated that the phase conversion starts with the hydrolysis of amorphous GeO₂ followed by the formation of clusters and the nucleation of crystals. Moreover, the development and evolution of dense liquid clusters during the process of nucleation are directly observed. All the results not only indicate the clusters behave as the basic building units for

crystallization but also suggest that the development of the dense liquid clusters provides a favorable prenucleation position and becomes a necessary step for nucleation from solution, which strongly enriches the understanding of crystallization from solutions.

38. Preliminary Exploration of the Integration of Generative Artificial Intelligence with Corrosion Data Processing

Preliminary Exploration of the Integration of Generative Artificial Intelligence with
Corrosion Data Processing

LU Xinpeng

Towngas Smart Energy Company Limited

Abstract Generative Artificial Intelligence (GAI), a groundbreaking direction in the field of technology, has demonstrated exceptional capabilities in data generation and processing across multiple domains. This study explores the potential of GAI, particularly large language models (LLMs) based on the GPT-4V architecture, in the analysis and simulation of corrosion data within the realm of metal material protection. The application of GAI not only learns from existing corrosion patterns but also predicts future corrosion trends and effects by simulating the data generation process of corrosion phenomena.

The developed GAI model in this research has been trained to identify and generate complex corrosion data that takes into account environmental factors, material properties, and protective measures. Validated by processing real-world corrosion datasets, the model has proven effective in understanding intricate corrosion mechanisms and predicting material lifespan. The incorporation of the GPT-4V architecture has enabled the GAI model to engage in multimodal learning, further enhancing its capability to process imagery and sensor data.

Moreover, the study has established a GAI benchmark specifically for corrosion data processing to assess the model's cognitive and generative abilities across various

corrosion scenarios. A comprehensive set of tests was conducted on the model, evaluating its data processing speed, accuracy, predictive power, and its innovative capacity in generating corrosion protection solutions.

The findings indicate significant efficiency and precision improvements in corrosion data handling and simulation provided by GAI, offering vital technical support for the future monitoring and strategizing of metal corrosion protection. This exploratory study lays the groundwork for the application of GAI in the field of corrosion data processing and forecasts a broad spectrum of potential applications of GAI technology in this sector.

Keywords generative Artificial Intelligence, corrosion data processing, GPT-4V, multimodal learning, data simulation

39. Detection of the Durability of Epoxy-coated Reinforcement under Marine environment in South China for 25 years

Detection of the Durability of Epoxy-coated Reinforcement under Marine
environment in South China for 25 years

Dongfang Zhang

CCCC Fourth Harbor Engineering Institute Co., Ltd

Abstract Epoxy coated-rebar as a useful alternative method to improve the durability of marine infrastructure has been studied for decades. However, the controversial performance of epoxy coated-rebar exhibited in North American forced to the prohibition of further application. The first attempt to apply the epoxy coated-rebar in marine infrastructure in South China can be traced to 1998. In order to evaluate the long-term service condition of epoxy coated-rebar, both corrosion media penetration in concrete and corrosion behaviour of rebar were detected in engineering site and laboratory. The results indicated that the surface image of infrastructure was intact, without any cracks or corrosion products were observed. The in-situ corrosion potential test data revealed that most of the epoxy coated-rebars were kept a positive

potential of above -100 mV vs. CSE, which showed a low corrosion probability of 10%. The positive corrosion potential of -85 mV and low corrosion current density of 0.052 μAcm^{-2} resulted from laboratory were further confirmed the high durability of epoxy coated-rebar in marine environment. The contrary detection of epoxy coated-rebar in marine infrastructure between North American and South China could be attributed to the different concrete material and construction quality. The detection result of epoxy coated-rebar in South China could contribute to their further application in marine infrastructures.

Keywords epoxy coated-rebar, durability, marine environment, corrosion

40. Understanding into properties controlling durability of pre-painted steel sheets

Understanding into properties controlling durability of pre-painted steel sheets

Mehrdad Zia Hoseinpoor

Technopark Kralupy of the University of Chemistry and Technology Prague, Czech Republic

Abstract Corrosion degradation of a wide range of coil-coated steel sheets was studied in the marine and inland climate and in the laboratory to describe critical factors affecting their long-term performance. A new approach was developed to assess surface conditions during field exposure of metallic sheets based on surface time of wetness. For a better understanding of degradation mechanisms in areas of overlap and deformed areas, several innovative techniques have been developed to monitor the presence of water locally. A significant prolongation of wetness periods inside overlaps was confirmed. Together with accumulation of corrosive species, it explains acceleration of corrosion in overlaps of pre-painted steel sheets. Localised water uptake measurements were able to assess the extent of damage to the paint caused by deformation and the tendency to blister formation.

41. Corrosion behavior of Laser Powder Bed Fusion Al-Mn-Mg-Sc-Zr Alloy

Corrosion behavior of Laser Powder Bed Fusion Al-Mn-Mg-Sc-Zr Alloy

Zequn Zhang¹, Bowei Zhang¹, Junsheng Wu¹

¹*Institute for Advanced Materials and Technology, University of Science and
Technology Beijing, Beijing 100083, China*

Presenter's e-mail address: zzq3971@163.com

Abstract Corrosion behavior of the laser powder bed fusion (LPBF) Al-Mn-Mg-Sc-Zr alloy was investigated based on microstructure characterization coupled with corrosion measurements. The results demonstrate that localized corrosion preferentially occurs at the molten pool boundaries of both planes, where the distribution of abundant micro-cathode $\text{Al}_3(\text{Sc}, \text{Zr})$ precipitates act as the predominant role. In contrast, the micro-anode $\text{Al}_6(\text{Mn}, \text{Fe})$ precipitates are more likely to be dissolved prior to the matrix nearby, thus showing little impact on the corrosion behavior of the LPBF alloy. The effect of heat treatments on the microstructure and corrosion behavior of LPBF Al-Mn-Mg-Sc-Zr alloy also were systematically investigated. The 300 °C/5 h heat-treatment doesn't alter the typical bimodal grain distribution of LPBF-fabricated alloy. However, the grains at molten pool boundaries experience a significant growth after a 500°C/5 h heat treatment, narrowing the gap of grain size between fine-grain (FG) region and coarse-grain (CG) region. It is also found that the heat treatments have an impact on $\text{Al}_3(\text{Sc}, \text{Zr})$ and $\text{Al}_6(\text{Mn}, \text{Fe})$ precipitates. Detailedly, the $\text{Al}_3(\text{Sc}, \text{Zr})$ precipitates undergo a slight growth in size and obvious increase in quantity after heat treatment whilst the $\text{Al}_6(\text{Mn}, \text{Fe})$ particles go through a rapid increase both in amount and size, especially for the alloy after being subject to a higher temperature heat treatment. As consequence, the heat-treated LPBF aluminum alloys exhibit worse corrosion resistance compared with their original state. The $\text{Al}_3(\text{Sc}, \text{Zr})$ precipitates acting as micro-cathodes at molten pool boundaries accelerate the preferential corrosion of fine grain regions of 300°C/5 h heat-treated alloy. In contrast, the 500°C/5 h heattreated alloy tends to promote a

more uniform corrosion due to the dissolution of the homogeneously distributed $\text{Al}_6(\text{Mn}, \text{Fe})$ anodes on the alloy surface.

Keywords LPBF, Al-Mn-Mg-Sc-Zr, heat treatment, precipitates, corrosion

42. Initial localized corrosion induced by multiscale precipitates in the new generation high-strength Al-Zn-Mg-Cu alloy

Initial localized corrosion induced by multiscale precipitates in the new generation
high-strength Al-Zn-Mg-Cu alloy

Wei Xue, Zequn Zhang, Bowei Zhang[#], Junsheng Wu[#]

*Institute of New Materials Technology, University of Science and Technology Beijing,
Beijing*

Presenter's e-mail address: xw_beike13@163.com

Abstract This work focuses on the distribution characteristics of harmful micron-scale precipitates and high-density nanoscale precipitates in the new generation high-strength Al-Zn-Mg-Cu alloy, as well as the electrochemical mechanism of initial localized corrosion. To this end, transmission electron microscopy (TEM) and field-emission scanning electron microscopy/energy dispersive spectroscopy (FE-SEM/ EDS) were employed to characterize the morphology, size, composition, and distribution of the precipitates. Scanning Kelvin probe force microscope (SKPFM) was then used to measure the Volta potential of the micro- and nano-sized precipitates, and the electrochemical mechanism of localized corrosion induced by precipitates was quantitatively studied by DFT theoretical calculations. Finally, the accuracy of the Volta potential measurement and DFT calculation results was confirmed by in-situ and quasi-in-situ observation of the corrosion behavior. The results demonstrate that the micron-scale harmful precipitates are mainly irregular shaped $\text{Al}_7\text{Cu}_2\text{Fe}$ phase with ~ 5 vol%. Main strengthening phase is rod-like and cube-shaped $\text{Mg}(\text{Zn}, \text{Al}, \text{Cu})_2$ nano-precipitates, which range in size from a few tens to several hundred nanometers. Opposite to the traditional view of

considering Mg-rich phase as micro-anodes, experimental and calculation results both suggest that Mg (Zn, Al, Cu)₂ precipitates exhibit higher Volta potential than the matrix due to the doping of Cu atoms. In aggressive conditions, the surrounding matrix is preferentially corroded while the Mg (Zn, Al, Cu)₂ particles undergo localized breakdowns by forming nano-pits ascribed to the Mg atoms dissolution. Compared with Mg (Zn, Al, Cu)₂ phases, a greater potential difference (approximately 600 mV) between Al₇Cu₂Fe micro-cathodes and matrix drives the earlier initiation of galvanic corrosion. In addition, the work functions of different precipitates are calculated by DFT. The work function values: Al₇Cu₂Fe > Mg₄Zn₄Cu₃Al > Al > MgZn₂, and the theoretical calculation results are highly consistent with the experimental results. In summary, while the localized corrosion induced by Al₇Cu₂Fe phase initiates earlier and causes more severe corrosion of the surrounding matrix, the limited presence of Al₇Cu₂Fe phase has minimal impact on the alloy's corrosion resistance. However, due to a significant number of Mg (Zn, Al, Cu)₂ phases present in the alloy, their impact on the corrosion resistance of the new generation high-strength Al-Zn-Mg-Cu alloy cannot be disregarded.

Keywords Al-Zn-Mg-Cu alloy, precipitated phase, surface potential, local corrosion, DFT

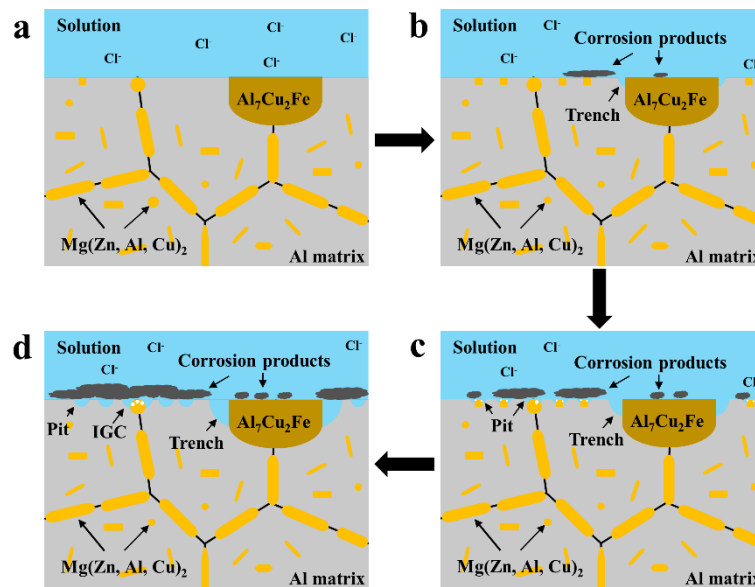


Fig. 1. Schematic representation of the localized corrosion initiation and propagation process induced by different

types of precipitates.

43. Initial Corrosion Behavior and Mechanism of Bogie Steel with Different Heat Treatment Structures in Industrial Polluted Environment Containing S

Initial Corrosion Behavior and Mechanism of Bogie Steel with Different Heat Treatment Structures in Industrial Polluted Environment Containing S

Jialiang Song, Kui Xiao*

University of Science and Technology Beijing, institute for advanced materials and technology, Beijing

Presenter's e-mail address: 1208566199@qq.com

Abstract China has a vast territory, with significant differences in climate and environment among different regions. As a means of transportation for long distances, trains' various components are affected by corrosion from different environments. As an important part of the train, the bogie plays a crucial role in carrying and driving the entire vehicle, and has a vital impact on the stability of train operation [1].

Since the Industrial Revolution in the 18th century, people have been using fossil fuels extensively, and the industrial pollution (mainly SO₂) caused has always been a serious threat to the service process of steel. Numerous studies [2] have shown that after being dissolved in water for a period of time, some of SO₂ will react with O₂ to form SO₄²⁻. The acidic solution will dissolve the weathering steel matrix to form FeSO₄, and Fe²⁺ will form FeOOH with dissolved oxygen. Then the solute will be recycled to produce sulfuric acid. Compared to carbon steel, the advantage of weathering steel is its lower sensitivity to SO₂ [3]. In addition, Wang et al. [2] found that a small amount of SO₂ promotes the formation of a crack-free and protective rust layer. But at the same time, Leygraf et al. [4] believe that a large amount of SO₂ can lead to severe acidification of the surface, which in turn dissolves the steel matrix.

Due to the high heat input received during the welding process at the connection part of the bogie, the local structure was significantly changed. Therefore, it is of great

significance to study the corrosion behavior and mechanism of different heat-treated structures.

At present, most research work on the corrosion resistance of weathering steel focuses on alloy elements and rust layer protection. However, comparative research on the corrosion initiation mechanism and rust layer characteristics of different heat-treated structures in S-containing environments is still relatively lacking. In this work, the microstructure and crystallographic information of the original and quenched structures of bogie steel G390NH were characterized by transmission electron microscopy (TEM), scanning Kelvin probe force microscopy (SKPFM) and electron backscatter diffraction (EBSD). The initial corrosion morphology was observed by field emission scanning electron microscopy (FE-SEM). Finally, based on the test results of electrochemical impedance spectroscopy and polarization curve, the relevant mechanisms and kinetic differences of initial corrosion between the two structures were analyzed from an electrochemical perspective.

This work mainly focuses on the initial corrosion behavior and mechanism of two different microstructures of bogie steel G390NH. After in-depth analysis, the following conclusions are drawn:

- (1) There is no obvious difference in the initial corrosion behavior between the F+P structure and the GB structure at the macro scale, including products and rates, but there are differences between the microscopic mechanisms.
- (2) There is the residual stress near the pearlite in the F+P structure, and micro-region galvanic effect is generated between the pearlite and the ferrite matrix during the corrosion process. The residual stress is evenly distributed in the ferrite phase of the GB structure, but there is no intense micro-region galvanic effect in the structure. The microdefects in the metal and the micro-region galvanic effect are the main factors inducing the initiation of corrosion.
- (3) When the two structures of G390NH are immersed in NaHSO₃ solution, the dense corrosion product layers will be formed on the surfaces, which have a blocking effect on the O₂ dissolved in the solution, thereby reducing the cathode reaction rate.

(4) In the initial stage of immersion, the corrosion of G390NH is mainly affected by dissolved O_2 and H^+ in the acidic environment. After the formation of the product layer, the dissolution of the metal becomes affected by H^+ and SO_4^{2-} / SO_3^{2-} . Among them, the F+P structure is more sensitive to the reduction of SO_4^{2-} / SO_3^{2-} .

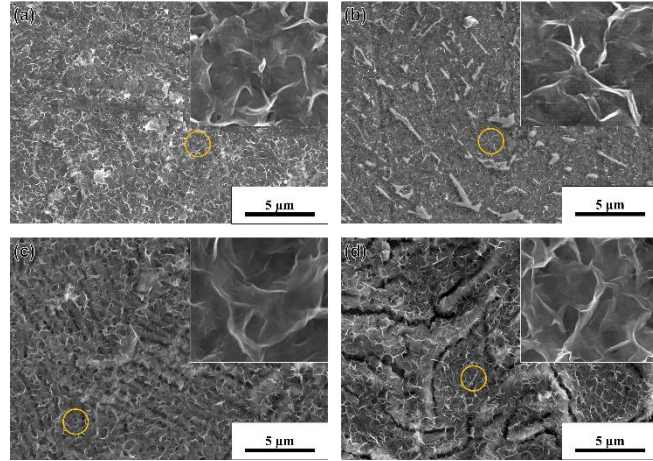


Fig. 1 Immersion test corrosion microstructure (before rust removal): immersion for 1 h (a) F + P and (b) GB structure; immersion for 12 h (c) F + P and (d) F + P structure.

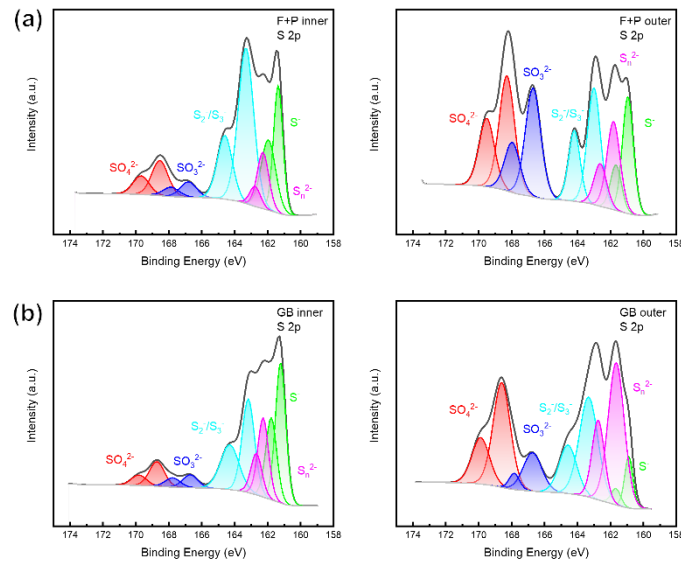


Fig. 2 XPS test results of surface products of two structures of G390NH immersed in 0.01 M $NaHSO_3$ for 12 h: (a) F+B structure and (b) GB structure.

Keywords bogie steel, initial corrosion, ferrite-pearlite, granular bainite, industrial polluted environment

Reference

- [1] J. Song, Z. Li, K. Xiao, H. Luo, J. Chen, W. Yu, X. Zhang, C. Dong, Study on the local corrosion behaviour and mechanism of bogie steel welded joints, *Corrosion Science*. 208 (2022) 110709. <https://doi.org/10.1016/j.corsci.2022.110709>.
- [2] J.H. Wang, F.I. Wei, Y.S. Chang, H.C. Shih, The corrosion mechanisms of carbon steel and weathering steel in SO₂ polluted atmospheres, *Materials Chemistry and Physics*. 47 (1997) 1–8. [https://doi.org/10.1016/S0254-0584\(97\)80019-3](https://doi.org/10.1016/S0254-0584(97)80019-3).
- [3] M. Morcillo, I. Díaz, H. Cano, B. Chico, D. de la Fuente, Atmospheric corrosion of weathering steels. Overview for engineers. Part I: Basic concepts, *Construction and Building Materials*. 213 (2019) 723–737. <https://doi.org/10.1016/j.conbuildmat.2019.03.334>.
- [4] THE ELECTROCHEMICAL SOCIETY SERIES, in: *Atmospheric Corrosion*, John Wiley & Sons, Inc., Hoboken, NJ, USA, 2016: p. a-c. <https://doi.org/10.1002/9781118762134.scard>.

44. Corrosion resistance of 12Cr1MoV and welded Inconel 625 coating on heat exchange surfaces with increasing steam parameters in waste incinerators

Corrosion resistance of 12Cr1MoV and welded Inconel 625 coating on heat exchange surfaces with increasing steam parameters in waste incinerators

李鉴全 刘欢

华中科技大学能源与动力工程学院

Abstract 12Cr1MoV is a widely used superheater material in waste incinerators in China. However, it's susceptible to high temperature corrosion due to the corrosive media(HCl, SO₂, ash, etc.) contained in the furnace. Therefore, Inconel 625 coating prepared by weld overlay is usually used, which provides good corrosion protection in the current medium-temperature boilers (i.e., 4.0MPa/400°C, 6.3MPa/450°C). With the co-incineration of industrial waste and the improvement of steam parameters becoming a new development trend, the temperature of heat exchange surfaces and the concentration of corrosive media are increasing. Thus, clarifying the

protectiveness of Inconel 625 in harsher corrosive environments is important. In this study, the corrosion test of the 12Cr1MoV and Inconel 625 coating was performed at elevated temperatures of 500-700°C. The sample was corroded by actual waste incinerator ash with high concentrations of HCl and SO₂. To further reveal the corrosion mechanism, we also conducted quantitative measurements of the concentrations of ions with different valence states (Ni²⁺/Cr³⁺/Cr⁶⁺/Mo⁴⁺/Fe³⁺). Results showed that in the absence of HCl and SO₂, the corrosion weight gain of 12Cr1MoV increased significantly with rising temperature, whereas the weight gain of the coating was only 31%-78% of this. Cr compounds were the main soluble corrosion products of the coating, with the mass of Cr ions increasing tenfold and the percentage of Cr⁶⁺ correspondingly rising from 27.9% to 75.5%, indicating a significant enhancement in the reactions of Cr/Cr₂O₃ with alkali metal salts in ash (such as NaCl/KCl) to form Na₂Cr₂O₄/K₂Cr₂O₄. Upon introduction of HCl and SO₂, no soluble Cr products were detected anymore, while soluble Ni compounds were detected from the coating. This suggests that HCl and SO₂ primarily exacerbate the corrosion by forming unprotected compounds such as NiCl₂ and NiSO₄. This means that when using Inconel 625 coating in high-parameter waste incinerators, inhibiting the formation of nickel compounds is crucial.

Keywords: Inconel 625; Weld; High-temperature corrosion; Soluble product; Waste incinerate

45. Title Ablation resistance of Ir/HfO₂ ultra-high temperature thermal protection coating

Title Ablation resistance of Ir/HfO₂ ultra-high temperature thermal protection coating

李发源 朱利安

国防科技大学

Abstract An Ir/HfO₂ ultra-high temperature thermal protection coating system was designed with the idea of functional modularization, using the Ir coating as an oxygen

barrier layer and the HfO₂ layer as an anti-ablation layer. The Re, Ir and HfO₂ coatings were successively prepared on the graphite substrate by chemical vapor deposition, molten salt electrodeposition and plasma spraying. The ablation resistance of the obtained graphite/Re/Ir/HfO₂ samples in short time at ultra-high temperature and long time at wide temperature range was tested by a high frequency plasma wind tunnel. The sample after ablation at 2700°C for 300s with a mass ablation rate of less than 0.12 mg·cm⁻²·s⁻¹ and a linear ablation rate of about -0.17 μm·s⁻¹ had no obvious defects. The sample after ablation at 2200°C~2800°C for 1800s was also free of obvious defects. Its mass ablation rate was about -0.057 mg·cm⁻²·s⁻¹ and the linear ablation rate was about -0.01 μm·s⁻¹, basically no ablation was achieved. The Ir/HfO₂ coating showed excellent ultra-high temperature ablation resistance characteristics, wide temperature range and no ablation during high frequency plasma wind tunnel tests, and has good application prospects for ultra-high temperature thermal protection.

Keywords ultra-high temperature; wind tunnel ablation; Ir coating; HfO₂ coating; anti-oxidation

46. High temperature corrosion resistance of enamel coating on 316L stainless steel in the environment of NaCl + water vapor + air

High temperature corrosion resistance of enamel coating on 316L stainless steel in the environment of NaCl + water vapor + air

Junan Pan, Shujiang Geng, Minghui Chen, Fuhui Wang

Shenyang National Laboratory for Materials Science, Northeastern University,

No.3-11 Wenhua Road, Shenyang, 110819, China

929539613@qq.com

Abstract 316L austenitic stainless steel has good toughness, plasticity, high-temperature strength and excellent welding performance^[1], is widely used in petrochemical industry, marine industry, agricultural production, energy development

and other fields^[2]. However, with the gradual increase in demand for its performance, 316L stainless steel itself has been unable to meet some of the service conditions^[3]. In order to improve its corrosion resistance, it is necessary to prepare protective coating on the surface of 316L stainless steel. The enamel coating provides excellent oxidation resistance and salt corrosion resistance in high temperature service.

In this paper, enamel coatings with thickness of 5 μm , 15 μm and 30 μm were prepared on the surface of 316L stainless steel, and the corrosion behavior of the coated stainless steel in 600 $^{\circ}\text{C}$ ~750 $^{\circ}\text{C}$ NaCl + water vapor + air environment was studied. The results showed that:

(1) The enamel coatings was dried at 250 $^{\circ}\text{C}$ for 15 min and finally heat-treated at 900 $^{\circ}\text{C}$ for 10 min. The coatings prepared under these conditions had uniform thickness, flat surface and bonded well with the substrate.

(2) After being corroded in 600 $^{\circ}\text{C}$ NaCl + water vapor + air environment for 10 h, the stainless steel matrix corroded seriously, while the coated stainless steel showed good corrosion resistance.

(3) After being corroded in 750 $^{\circ}\text{C}$ NaCl + water vapor + air environment for 10 h, both 15 μm and 30 μm enamel coatings effectively isolated the intrusion of NaCl and inhibited the internal diffusion of oxygen, and the mass changes per unit area of the sample after being corroded for 10 h was not obvious, while the protective effect of 5 μm coating was not good.

Keywords 316L stainless steel; enamel coating; NaCl; water vapor

Reference

- [1] E Edin, F Svahn, P Åkerfeldt, M Eriksson, M-L. Antti. Rapid method for comparative studies on stress relief heat treatment of additively manufactured 316L [J]. *Materials Science and Engineering: A*, 2022, 847: 143313
- [2] K.H. Lo, C.H. Shek, J.K.L. Lai. Recent developments in stainless steels [J]. *Materials Science and Engineering: R*, 2009, 65(4-6): 39-104

[3] Haixian Liu, Jiaqi He, Zhengyu Jin, Hongwei Liu. Pitting corrosion behavior and mechanism of 316L stainless steel induced by marine fungal extracellular polymeric substances [J].Corrosion Science, 2023, 224: 111485

47. (Fe,Co,Ni)₃O₄ Spinel Coating on Solid Oxide Fuel Cell Interconnect Steel

(Fe,Co,Ni)₃O₄ Spinel Coating on Solid Oxide Fuel Cell Interconnect Steel

Shujiang Geng, Maosen ZHao, Fuhui Wang

Northeastern University, No.3-11 Wenhua Road, Shenyang

Presenter's e-mail address: gengsj@smm.neu.edu.cn

Abstract Ferritic stainless steels have been widely employed as solid oxide fuel cell (SOFC) interconnects owing to their low cost, coefficient of thermal expansion match with other SOFC components, and good oxidation resistance and acceptable electrical conductivity of Cr₂O₃. However, they are confronted with several problems during operation in SOFC cathode working condition such as the evaporation of Cr₂O₃ which results in cathode Cr-poisoning and subsequent degradation of cell performance [1-3]. Therefore, it is necessary to develop electrically conductive coating on them in order to block Cr₂O₃ evaporation. So far, spinel coating is a promising coating to improve the electrical conductivity of the surface oxide scale thermally formed on the steel. In present paper, FeCoNi alloy layer has been deposited on ferritic stainless steel (SUS 430) by magnetron sputtering method. The coated steels were evaluated in air at 800°C corresponding to SOFC cathode environment. It was found that the coated steel initially experienced a large mass gain, followed by slight increase with time. The FeCoNi alloy layer was mainly converted into (Fe,Co,Ni)₃O₄ spinel layer beneath which a Cr-rich layer was grown from the steel substrate upon thermal exposure. The Cr-free outer layer not only suppressed Cr migration outward but also reduced the surface oxide scale area specific resistance (ASR) of the coated steel.

Keywords Solid oxide fuel cell; steel interconnect; spinel coating

Reference

[1] H. Falk-Windisch, J. E. Svensson, J. Froitzheim. Effect of temperature on chromium vaporization and oxide scale growth on interconnect steels for Solid Oxide Fuel Cells. *Journal of Power Sources*.287,25 (2015).

[2] S. P. Jiang, X. Chen. Chromium deposition and poisoning of cathodes of solid oxide fuel cells – A review. *International Journal of Hydrogen Energy*.39,505 (2014).

[3] Z. Xu, W. Xu, E. Stephens, B. Koeppel. Mechanical reliability and life prediction of coated metallic interconnects within solid oxide fuel cells. *Renewable Energy*.;113,1472 (2017).

48. Environmentally Assisted Cracking of Stainless Steels – From 3D/4D Time-lapse Imaging, Bipolar Electrochemistry, to Simulated Marine Environments

Environmentally Assisted Cracking of Stainless Steels – From 3D/4D Time-lapse Imaging, Bipolar Electrochemistry, to Simulated Marine Environments.

Dirk Engelburg¹

¹University of Manchester, United Kingdom

Abstract This presentation will provide novel insight of the relationship between environmental exposure parameters, the presence of applied and residual stress, microstructure surface film passivity and localised corrosion behaviour. Typical examples and innovative ways to advance our mechanistic understanding of localised corrosion and environmentally assisted cracking (EAC) are introduced, with the aim to obtain data to extend component lifetime, resilience & endurance. Novel techniques for measuring corrosion kinetic behaviour, passive film compositions, and crack nucleation propensities are explored and discussed. A range of novel ideas are presented, including the application of in-situ confocal microscopy, 2D/3D/4D corrosion and crack growth kinetic measurements, with associated chemical fingerprinting of corrosion products, with a focus on petrochemical and nuclear application.

49. Results Using a New Methodology to Test the Fatigue of Materials in Corrosive Media at High Pressures

Results Using a New Methodology to Test the Fatigue of Materials in Corrosive Media at High Pressures.

Rodrigo Garcia¹ and Oscar Rosa Mattos¹

*LNDC/COPPE, Federal University of Rio de Janeiro - UFRJ, Rio de Janeiro, RJ
21945-970, Brazil*

omattos@metalmat.ufrj.br

Abstract This article addresses a solution to a real engineering problem: a new algorithm to control Fatigue Testing Machines (FTMs) working in high pressure environments. Despite the various FTMs available on the market, customizations are sometimes necessary to perform special test conditions. This is the case, for example, of the requirements of the Brazilian pre-salt conditions, which involve pressures above 200 bars. Two factors are the main particularities of these tests causing considerable differences between the actual load on the specimen and that measured by traditional external load cells when a pressurized vessel is used. The first is the sealing system, causing a frictional force on the shaft, and the other is the high pressure inside the vessel, expelling the shaft. Therefore, to accurately measure the actual force on the sample, LNDC designed a system using a set of strain gauges to measure both the crack length and the applied load (EFS technique). This work presents an alternative to use such a system to produce a complementary feedback signal to improve the FTMs control algorithm. In short, a feedback signal from a load cell is used to produce the sinusoidal shape, while the EFS technique provides additional feedback for amplitude and bias correction. Experimental results demonstrate the efficiency of this methodology. In this way, it was possible to perform a control that meets the requirements of the ASTM E647 standard in high pressure corrosion fatigue tests. New results are presented and compared with others obtained

by the classical methodology used in the literature, in particular, the so-called DCPD method to measure crack propagation will be compared with the results obtained using this new methodology.

Keywords Corrosion Fatigue, Crack propagation

Reference

A critical insight on the use of external load cells for fatigue tests in pressurized systems. <https://doi.org/10.1016/j.engfracmech.2017.06.015>.

Corrosion Fatigue Tests Using Strain Gauges for Measuring Load and Crack length, Rodrigo R.A. Garcia; Felipe Cristaldi C. Caldas; Oscar Rosa Mattos. CORROSION (2016) 72 (12): 1547–1555.

50. Atomic-scale analysis of hydrogen embrittlement in high-strength Al alloys

Atomic-scale analysis of hydrogen embrittlement in high-strength Al alloys

Huan Zhao^{*}, Poulami Chakraborty, Dirk Ponge, Tilmann Hickel, Binhan Sun,
Chun-Hung Wu, Baptiste Gault, Dierk Raabe

¹*Max-Planck-Institut für Eisenforschung, Düsseldorf, Germany.*

Email: h.zhao@xjtu.edu.cn

** Current address: State Key Laboratory for Mechanical Behavior of Materials, Xi'an Jiaotong University, Xi'an, China*

Abstract Environmentally assisted embrittlement of high-strength Al alloys hinders their wide applications. The important role of hydrogen (H) associated with the H “embrittlement” mechanism occurs. However, the challenge of assessing the precise trapping sites of H makes the mechanisms remain ambiguous. We used atom probe tomography to investigate H associated with specific microstructural features in a high-strength 7xxx Al alloy ^[1]. We successfully achieved visualization and assessment of H at second-phases and grain boundaries, with the enrichment of one order of magnitude higher as opposed to the Al matrix. We used these observations to guide atomistic ab initio calculations, which show that the co-segregation of alloying

elements and H favours grain boundary decohesion, and the strong partitioning of H into the second-phase particles removes solute H from the matrix, hence preventing H embrittlement. Our insights further advance the mechanistic understanding of H-assisted embrittlement in Al alloys, emphasizing the role of H traps in minimizing cracking and guiding new alloy design.

Keywords Hydrogen embrittlement, 7xxx Al alloy, Mechanical properties, Atom probe tomography, Ab-initio calculations

Reference

[1]. Zhao, H. *et al.* Hydrogen trapping and embrittlement in high-strength Al alloys. *Nature* 602, 437-441, doi:10.1038/s41586-021-04343-z (2022).

51. Correlating oxidation, localized oxidation and stress corrosion cracking of austenitic alloys and weldments in pressurized water reactor primary coolants

Correlating oxidation, localized oxidation and stress corrosion cracking of austenitic alloys and weldments in pressurized water reactor primary coolants

Zhanpeng Lu¹

¹ *Institute of Materials, School of Materials Science and Engineering, Shanghai University, Shanghai, 200072, China*

² *State Key Laboratory of Advanced Special Steels, Shanghai University, Shanghai, 200444, China*

Zhanpeng lu: zplu@t.shu.edu.cn

Abstract The oxidation behavior and localized oxidation penetration at the inner oxide-alloy matrix were investigated by exposure tests in high temperature water followed by Optical-SEM surface observation as well as FIB sampling/TEM cross-section observation and analyses, using the materials for stress corrosion cracking tests. Stress corrosion cracking (SCC) growth rate tests with various kinds of base metals and weldments were conducted in high temperature water environments. The approach for characterizing SCC growth behaviors of highly SCC-resistant alloys

has been developed by proposing two parameters, average SCC growth rate in terms of SCC band and maximum SCC growth rates in terms of distribution and size of locally intergranular cracks and interdendritic cracks. It has been found that local chemical composition and local deformation at the microscopic level contribute to both the general stress corrosion band and the locally penetrating cracking along the grain boundaries or phase boundaries. The results are interpreted by the formulation of the transient oxidation kinetics at the crack tip under stress/strain and the resultant crack growth.

Keywords Nuclear power plant, austenitic alloys, high temperature water, oxidation, localized oxidation, stress corrosion cracking

References

- [1]. T.M. Cui, J.R. Ma, K. Zhang, Z.P. Lu, Y.J. Tang, X.H. Xu, S. L. Perez, T. Shoji. *J. Electrochemical Society*, 167(16)(2020)161502.
- [2]. T.M. Cui, X.H. Xu, J.R. Ma, Z.P. Lu, Y.J. Tang, K. Zhang, S.L. Yang, Z.M. Zhong, S. L. Perez, T. Shoji. *J. Nuclear Materials*, 553(2021)153057.
- [3]. T.M. Cui, H.Y. Dong, X.H. Xu, J.R. Ma, Z.P. Lu, Y.J. Tang, D. Pan, S. L. Perez, T. Shoji. *J. Nuclear Materials*, 557(2021)153209.
- [4]. T.M. Cui, Q. Xiong, J.R. Ma, K. Zhang, Z.P. Lu, J.J. Chen, Y.B. Jia, H. Zheng, S.L. Yang, Z.M. Zhong, S. L. Perez, T. Shoji. *Corrosion*, 77(8)(2021)878-895.
- [5]. T.M. Cui, X.H. Xu, D. Pan, J.R. Ma, Z.P. Lu, J.J. Chen, X. Liang, S. L. Perez, T. Shoji. *J. Nuclear Materials*, 565(2022)153741.
- [6]. T.M. Cui, X.H. Xu, D. Pan, Z.P. Lu, X.H. Li, J.R. Ma, Y.P. Zhang, S.L. Yang, T. Shoji. *J. Nuclear Materials*, 569(2022)153913.
- [7]. T.M. Cui, X.H. Xu, D. Pan, Z.P. Lu, J.R. Ma, S.L. Yang, H. Zheng, Z.M. Zhong, T. Shoji. *J. Nuclear Materials*, 561(2022)153509.
- [8]. Q. Xiao, J.J. Chen, Z.P. Lu, J. Xu, T. Shoji. *Corrosion*, 78(8)(2022) 711-725.
- [9]. X.H. Xu, Y.B. Jia, D. Pan, T.M. Cui, Z.P. Lu, S. L. Perez, J.J. Chen, S.Y. Li, T. Shoji. *J. Nuclear Materials*, 588(2024) 154753.
- [10]. T.M. Cui, X.H. Xu, D. Pan, J.J. Chen, Z.P. Lu, Y.P. Zhang, S.L. Yang, T. Shoji. *J. Nuclear Materials*, 588 (2024) 154796.

52. Corrosion challenges of the supercritical CO₂ transportation pipeline

Corrosion challenges of the supercritical CO₂ transportation pipeline

Kaiyan Li^{1,2}, Naiqiang Zhang¹, Yimin Zeng²

¹*School of Energy Power and Mechanical Engineering, North China Electric Power University, Beijing, 102206, P.R. China*

²*Natural Resources Canada, CanmetMATERIALS, Hamilton, Ontario L8P 0A5, Canada*

Presenter's e-mail address: kaiyang.li@ncepu.edu.cn

Abstract The pipeline transportation of supercritical CO₂ (S-CO₂) is a crucial part to achieve Carbon Capture, Utilization, and Storage (CCUS). The captured S-CO₂ always contain certain impurities (like H₂O, O₂, H₂S, SO₂, etc.), which cause corrosion and stress corrosion cracking of the pipeline steels. However, how these impurities induce degradation and the related mechanisms are still unclear. Therefore, the following works have been conducted: analyzing the corrosion mechanisms of different impurities; identifying the synergistic effects of these impurities; purposing the threshold concentrations of impurities for corrosion control; evaluating stress corrosion cracking susceptibility of pipelines in various S-CO₂ environments; employing in situ electrochemical noise for corrosion detection; setting up long-term corrosion prediction model. It is intended to understand the pipeline corrosion in S-CO₂ environments and provide theoretical foundation and technical support for the related corrosion control.

Keywords Supercritical CO₂; pipeline steel; impurity; stress corrosion cracking

Reference

[1] Li K, Zeng Y*, Luo J-L*. Influence of H₂S on the general corrosion and sulfide stress cracking of pipelines steels for supercritical CO₂ transportation. *Corrosion Science* 2021;190:109639.

[2] Li K, Zeng Y*. Long-term Corrosion and Stress Corrosion Cracking of X65 Steel in H₂O-saturated Supercritical CO₂ with SO₂ and O₂ Impurities. *Construction and*

Building Materials. 2023;362: 129746.

[3] Kaiyang Li, Yimin Zeng*. Advancing the mechanistic understanding of corrosion in supercritical CO₂ with H₂O and O₂ impurities. Corrosion Science. 2023;213:110981.

[4] Zeng Y*, Li K. Influence of SO₂ on the corrosion and stress corrosion cracking susceptibility of supercritical CO₂ transportation pipelines. Corrosion Science 2020;165:108404.

[5] Effect of Cr on Corrosion Performance of Steels in Supercritical CO₂ Environments. AMPP 2022.

[6] Corrosion Behaviors of Carbon Steels and Cr-Bearing Steels in Supercritical CO₂. PR-280-002-2021. American Steel Properties & Applications Conference 2021.

[7] Effect of Impurity SO₂ on Corrosion and Stress Corrosion Cracking of X65 Steel in Supercritical CO₂ Streams. CORROSION 2019, Nashville, TN, USA.

[8] Impacts of Impurities on Corrosion of Supercritical CO₂ Transportation Pipeline Steels. CORROSION 2018, Phoenix, AZ, USA. (Highlighted by Materials Performance magazine)

53. Corrosion test result on Rotating Cage Autoclave (RCA) and comparison of some configuration of cage to wall shear stress of corrosion test sample to achieve the better accuracy

Corrosion test result on Rotating Cage Autoclave (RCA) and comparison of some configuration of cage to wall shear stress of corrosion test sample to achieve the better accuracy.

Bambang Widyanto^{1,2}, Irma Pratiwi¹, Raden Dadan Ramdan¹

¹*Institute of Technology Bandung,*

²*University of General Achmad Yani - Indonesia*

Abstract The existing Rotating Cage Autoclave for corrosion test was used currently to simulate corrosion phenomenon in the oil and gas transmission pipeline and well

tubing materials especially in the brine solution and introduced by the mixture of H₂S-CO₂ gas environment. Some parameters which were used are gas composition, gas pressure, temperature and rotation of the cage, and the duration of the test is 30 days. The autoclave was free from leaks due to special construction dedicated for corrosion test in H₂S environment.

In fact, this experiment is an approach that was used to understand the corrosion resistance of the pipe materials in the field especially in corrosion erosion mechanisms. In the pipeline or well tubing, the materials were situated in the fixed condition and oil and gas and other constituent flowing inside the pipe with certain flow speed, while in rotating cage autoclave, the samples which are fixed in the cage or cylinder sample holder immersed in brine solution that was injected by premix gas containing CO₂ and H₂S and turning with certain rotation speed. The cage rotation was adjusted according to the value of shear stress that wanted to be attained.

Some disadvantages were observed in the test results. Because the sample holder was built in two pieces of disks that handle some pieces of test samples, and there are some millimeters of distance among those samples, it permits the penetration of the solution behind the samples and stay at the center of the cage and finally attack the back surface of the samples. Because the movement of the solution at the center of the cage could not be determined precisely, it disturbs the measure of weight change due to corrosion that occurs to the back surface of the samples. Ideally all solution movement at the sample surface must be determined accurately to obtain a good understanding of corrosion phenomena.

Some ideas were taken to improve the accuracy of corrosion measurements for example, using a solid sample cage, or with placing the samples at the autoclave wall. Those ideas could limit the corrosion mechanism only to one surface and protect the other surface from contamination with the corrosion environment. At the beginning, some simulations using Computational Fluid Dynamic (CFD) were done, but after that, it needs confirmation with the experimental results in corrosion loop or rotating cage autoclave.

Keyword RCA corrosion test, CO₂-H₂S environment, CFD

54. Defeating hydrogen-induced grain-boundary embrittlement via triggering unusual interfacial segregation in FeCrCoNi-type high-entropy alloys

Defeating hydrogen-induced grain-boundary embrittlement via triggering unusual interfacial segregation in FeCrCoNi-type high-entropy alloys

Qian Li¹, Weihong Liu², Shijun Zhao³, Tao Yang¹

¹*Department of Materials Science and Engineering, City University of Hong Kong, Hong Kong, China*

²*School of Materials Science and Engineering, Harbin Institute of Technology, Shenzhen, China*

³*Department of Mechanical Engineering, City University of Hong Kong, Hong Kong, China*

Presenter's e-mail address: taoyang6@cityu.edu.hk

Abstract Metallic materials are mostly susceptible to hydrogen embrittlement (HE), which severely deteriorates their mechanical properties and causes catastrophic failures with poor ductility. In this study, we found that such a long-standing HE problem can be effectively eliminated in the Fe_x(CrCoNi)_{1-x} face-centered-cubic (fcc) high-entropy alloys (HEAs) by triggering the localized segregation of Cr at grain boundaries (GBs). It was revealed that increasing the Fe concentration from 2.5 to 25 at. % leads to substantially improved HE resistance, i.e., the ductility loss decreases from 70% to 6%. Meanwhile, the fracture mode transformed from the intergranular to the transgranular mode. Multiscale microstructural analyses demonstrated that the Fe_{2.5}Cr_{32.5}Co_{32.5}Ni_{32.5} and Fe₂₅Cr₂₅Co₂₅Ni₂₅ alloys show negligible differences in the phase structure, grain size, and grain-boundary (GB) character. However, interestingly, the near atomic-resolution elemental mapping revealed that an increased Fe concentration promotes the nanoscale Cr segregation at the GBs, which is primarily motivated by the strong repulsive force between Cr and Fe and the low

self-binding energy of Cr. Such unusual interfacial segregation of Cr, which has not been reported before in the Fe₂₅Cr₂₅Co₂₅Ni₂₅ alloy, helps enhance the GBs' cohesive strength and suppresses the local hydrogen segregation at GBs due to the decreased GB energy, leading to the outstanding HE resistance. These findings decipher the origins of the vastly-improved HE resistance in current FeCrCoNi-type HEAs, and meanwhile, provide new insight into the future development of novel high-performance structural alloys with extraordinary immunity to hydrogen-induced damages.

Keywords High-entropy alloys; Hydrogen embrittlement; Grain-boundary segregation; Mechanical properties

Reference

- [1] Li, Q., et al. "Defeating hydrogen-induced grain-boundary embrittlement via triggering unusual interfacial segregation in FeCrCoNi-type high-entropy alloys." *Acta Materialia* 241 (2022): 118410.
- [2] Xiao B, et al. Environmental embrittlement behavior of high-entropy alloys. *Microstructures* 2023;3:2023006.
- [3] Chen, X. H., et al. "Enhanced resistance to hydrogen embrittlement in a CrCoNi-based medium-entropy alloy via grain-boundary decoration of boron." *Materials Research Letters* 10.4 (2022): 278-286.

55. Effect of cold work on stress corrosion cracking behavior of 316L and 316NG stainless steels in high temperature water

Effect of cold work on stress corrosion cracking behavior of 316L and 316NG
stainless steels in high temperature water

Caibo Xie^{1,2}, Deng Pan^{1,2}, Xinhe Xu^{1,2}, Tongming Cui^{1,2}, Zhanpeng Lu^{1,2}, Tetsuo
Shoji³

¹*Institute of Materials, School of Materials Science and Engineering, Shanghai
University, Shanghai 200072, China*

²*State Key Laboratory of Advanced Special Steel, Shanghai University, Shanghai,
200444, China*

³*New Industry Creation Hatchery Center, Tohoku University, Sendai, 980-8579, Japan*

Presenter's e-mail address: Xie_caibo@shu.edu.cn

Corresponding author: zplu@t.shu.edu.cn

Abstract The stress corrosion cracking growth rates of uniaxially 20% (reduction in thickness) cold worked 316L and 316NG stainless steels (SSs) in 320 °C high temperature water are measured. Cold worked 316L SS exhibited nearly continuous and uniform intergranular stress corrosion cracking front and band on the fracture surface. 316NG only exhibited locally intergranular stress corrosion cracking sites. Stress corrosion cracking growth rate of cold worked 316L SS is significantly higher than that of the cold worked 316NG SS. The oxides of the two materials are evenly distributed. The oxide particles on the surface of 316L are small and relatively densely packed. The size of oxide particles on the surface of 316NG are large and relatively sparsely distributed. The Vickers hardness values and the local deformation degree of 316L SS in terms of Kernel Average Misorientation are higher than those of 316NG SS, which tend to results in the differences of stress corrosion cracking growth in high temperature water.

Keywords Nuclear power plant, Stainless steels, stress corrosion cracking, crack growth rate, high temperature water

56. Effect of gradient microstructure induced pre-torsion on hydrogen embrittlement of pure iron

Effect of gradient microstructure induced pre-torsion on hydrogen embrittlement of
pure iron

Xinfeng Li 李新锋

¹ 中山大学

Abstract The common problem of metal materials is that as the strength of the alloy

increases, its hydrogen embrittlement (HE) resistance decreases. In this study, we have proposed to use gradient structure to solve the inverted relationship between strength and HE resistance. Gradient-structured pure iron was prepared by pre-torsion tests with various pre-torsional angles and their HE behaviors were studied by slow strain rate tensile tests, microstructural analysis and time-of-flight secondary ion mass spectrometry. The results show that a change in pre-torsion angles can produce different gradient microstructures of pure iron, including gradient dislocations and sub-grains, and high pre-torsion angles correspond to large slopes between hardness vs. r/R along radial direction of samples. With an increase in pre-torsion angle from 0° to 1400° , yield strength of the alloys linearly increases, whereas the HE susceptibility first decreases and then increases. For the sample pre-torsioned at 400° , yield strength and HE-resistance are simultaneously improved, demonstrating that the construction of a suitable gradient microstructure is a potential strategy to maximize strength and HE-resistance synergy. The susceptibility to HE of pre-torsioned samples is related to the gradient distribution of grain boundary and dislocation hydrogen traps. At low pre-torsion angles (0° , 150° , 400°), hydrogen atoms are dispersed by these traps, with improvement of HE-resistance, whereas high pre-torsion angles (700° , 1000° , 1400°) correlates with a local high grain boundary and dislocation traps around the periphery, leading to high HE susceptibility. A strength predication model of gradient-structured pure iron is proposed. The predictive yield strength is in accordance with experimental results. With an increase in pre-torsion angle, the increments of dislocation strengthening and grain boundary strengthening increase. Compared with other strengthening mechanism, the contribution of dislocation strengthening dominates.

Keywords hydrogen embrittlement; pure iron; gradient microstructure

57. Effect of microstructure and reversed austenite on the hydrogen embrittlement susceptibility of Ni-Cr-Mo-V/Nb high strength steel

Effect of microstructure and reversed austenite on the hydrogen embrittlement
susceptibility of Ni-Cr-Mo-V/Nb high strength steel

Chao Hai, Cuiwei Du*

¹*Institute of Advanced Materials and Technology, University of Science and
Technology Beijing, Beijing, 100083, China*

email address: dcw@ustb.edu.cn

Abstract Ni-Cr-Mo-V/Nb steel is widely used in deep sea structural material for their interesting combination of excellent good properties such as high strength, good lower-temperature toughness, good weld property and outstanding corrosion resistance. Unlike traditional heat treatment, several novel process for quenching-lamellarizing-tempering (QLT) or Quenching -Partitioning-tempering (Q-P-T) heat treatments are proposed and applied to improve the strength and ductility of steel by obtaining multiphases microstructure. The enrichment of austenite stabilizing elements (C, or Mn) forms the austenite can enhance the ductility and toughness of steel. Similarly, the same intention could be carried through to the high Ni content of Ni-Cr-Mo-V/Nb steel by the enrichment of austenite stabilizing elements (Ni) to form the austenite under suitable heat treatment process. It is generally considered that the Ni-enrichment of film-like austenite can greatly improve the low-temperature toughness of the steel. Unfortunately, when used in deep-sea environment, especially under cathodic protection, high-strength steel is most susceptible to hydrogen embrittlement (HE) [1-4]. However, the role of reversed austenite (RA) on the HE in this Ni-Cr-Mo-V multiphase steel has not been fully understood.

Herein, we present the interesting study on the hydrogen embrittlement behavior of three kinds of steel with the same composition and different heat treatment process. Hydrogen diffusivity and activation energy between hydrogen and trapping sites were measured by hydrogen permeation test and TDS. The microstructure and fracture morphology were observed by scanning electron microscopy (SEM). Transmission

electron microscopy (TEM), electron backscattered diffraction (EBSD) analysis and X-ray diffraction (XRD) were used to analyze the microstructure of steel and RA. On this basis, the effects of different microstructures and RA content on the hydrogen embrittlement resistance of NiCrMoV/Nb steel were studied.

The Microstructure and RA significantly affect the hydrogen permeation behavior. The hydrogen diffusion rate of the three steels decreases in the following order: $D_{\text{eff}}(\text{Q}) > D_{\text{eff}}(\text{QLT}) > D_{\text{eff}}(\text{QT})$. The QT steel shows a noble HE resistance for the lowest hydrogen diffusion and maximum apparent hydrogen concentration. TDS results confirms that RA has a higher the activation energy as 32.5 kJ/mol in NiCrMoV/Nb steels, which can act as a stable hydrogen trapping site. However, RA can also transform to martensite under the combined action of sufficient hydrogen and tensile force which deteriorates the HE resistance. Thus, QLT steel containing more RA was found to have more hydrogen embrittlement susceptibility. With the difference of heat treatment in the following orders: Q, QT and QLT, the main fracture mode changes from typical intergranular fracture to quasi-cleavage fracture, and dimples were also observed in the tensile fracture surface of QT specimen. QT specimen exhibits the best resistance to hydrogen embrittlement with the lowest hydrogen diffusion and good austenite stability.

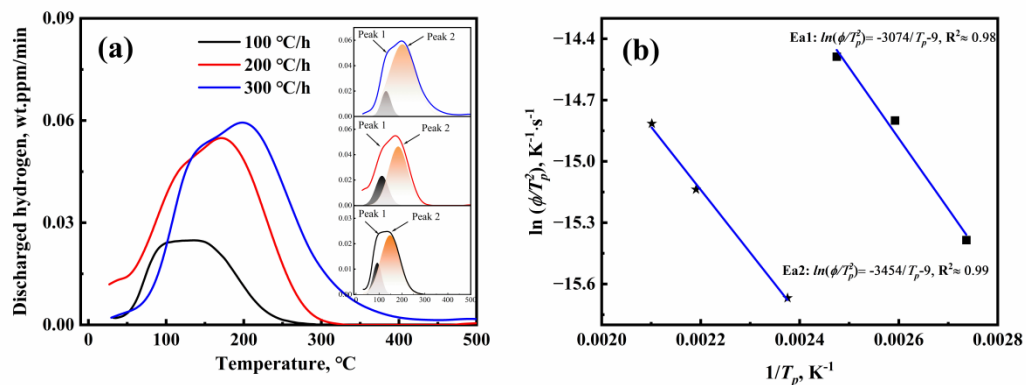


Figure 1 H desorption rate curves obtained from the TDS at different heat rates of 100°C/h, 200°C/h and 300°C/h for QLT with H-charging. (b) plot of $\ln(\Phi/T_p^2)$ vs. $1/T_p$ to calculate E_a for hydrogen desorption

Table1 Peaking temperature of specimens at different heating rates and activation

energy (E_a).

Specimen	Heating rate (°C/h)	Temperature of Desorption peak (°C)	Accumulated of hydrogen content (wt. ppm)	E_a , kJ/mol
Q	100	349.95	0.458	23
	200	373.25	0.526	
	300	393.45	0.506	
QT	100	383.55	3.402	19
	200	423.55	3.543	
	300	441.85	3.545	
QLT	100	peak1=365.38	3.013	$E_{a1}=25.6$ $E_{a2}=32.4$
		peak2=420.95		
	200	peak1=385.70	3.039	
		peak2=456.49		
300	peak1=404.01	3.121		
	peak2=475.90			

Corresponding author: Cuiwei Du, Processor,(1972-).Her research directions include corrosion in soil environment and microbiologically influenced corrosion.

Keywords NiCrMoV/Nb steel; Reversed austenite; Hydrogen embrittlement; TDS.

References:

[1] Venezuela J, Lim F Y, Liu L, et al. Hydrogen embrittlement of an automotive 1700 MPa martensitic advanced high-strength steel [J]. Corrosion Science, 2020, 171.

[2] Venezuela J, Blanch J, Zulkiply A, et al. Further study of the hydrogen embrittlement of martensitic advanced high-strength steel in simulated auto service conditions [J]. Corrosion Science, 2018, 135: 120-135.

[3] Venezuela J, Liu Q, Zhang M, et al. The influence of hydrogen on the mechanical and fracture properties of some martensitic advanced high strength steels studied using the linearly increasing stress test [J]. Corrosion Science, 2015, 99: 98-117.

[4] Tsay L, Hu Y, Chen C. Embrittlement of T-200 maraging steel in a hydrogen sulfide solution [J]. Corrosion Science, 2005, 47(4): 965-976.

58. Effect of Nb alloying on resistance to hydrogen embrittlement in multiphase stainless steel

Effect of Nb alloying on resistance to hydrogen embrittlement in multiphase stainless steel

Menghao Liu^{1,2}, Cuiwei Du^{1,2*}, Xiaogang Li^{1,2}

¹*Key Laboratory for Corrosion and Protection of the Ministry of Education, Institute of Advanced Materials & Technology, University of Science and Technology Beijing, Beijing, China*

²*National Materials Corrosion and Protection Data Center, University of Science and Technology Beijing, Beijing, China*

Email address: dcw@ustb.edu.cn.

Abstract Owing to the intricate interfacial structure and the presence of metastable austenite, multiphase stainless steel is susceptible to hydrogen embrittlement, mandating the control of hydrogen embrittlement resistance. The addition of Nb significantly enhances the hydrogen embrittlement resistance of single-phase steels. Therefore, this investigation aims to examine the impact of Nb alloying on the hydrogen embrittlement behavior of multiphase stainless steel and expound upon its underlying mechanisms. The following conclusions were drawn from this study: The hydrogen embrittlement sensitivity of multiphase stainless steel is reduced by 10% upon the incorporation of Nb. Nanoscale NbC precipitates within the austenite phase and at the austenite/martensite phase interfaces, impeding hydrogen diffusion and thus inhibiting crack initiation. NbC also precipitates within the ferrite phase and martensite phase, impeding crack propagation. Residual austenite in Nb-containing steels also possesses higher stacking fault energy, contributing to a reduction in hydrogen embrittlement sensitivity.

Corresponding author: Cuiwei Du, professor at University of Science and Technology Beijing. Her research directions include corrosion in soil environment and microbiologically influenced corrosion.

Keywords Hydrogen embrittlement; Multiphase stainless steel; Stacking fault energy

59. Enhancing Effect of High-Temperature Water on Crack Growth of 316LN Stainless Steel Under Various Loading Frequencies

Enhancing Effect of High-Temperature Water on Crack Growth of 316LN Stainless Steel Under Various Loading Frequencies

Panpan Wu^{1,2}, Chen Li^{1,2}, Xinhe Xu^{1,2}, Tongming Cui^{1,2}, Zhanpeng Lu^{#, 1,2}, Tetsuo Shoji³

¹ *Institute of Materials, School of Materials Science and Engineering, Shanghai University, Shanghai, 200072, China*

² *State Key Laboratory of Advanced Special Steels, Shanghai University, Shanghai, 200072, China*

³ *New Industry Creation Hatchery Center, Tohoku University, Sendai, 980-8579, Japan*

Presenter: wupanpan@shu.edu.cn

Corresponding author: +86-21-56336107; Email: zplu@t.shu.edu.cn.

Abstract Fatigue crack growth rates of 316LN stainless steel were determined in pressurized water at various loading frequencies with 12 compact tension specimens. The fatigue crack growth rate was higher for longer load-rising time. The environmental-enhancement factor on da/dN by primary water increases with increasing load rising time from 5s to 500s at 320 °C. A higher stress intensity amplitude tends to result in a lower environmental effect on da/dN .

Keywords 316LN stainless steel; Primary water reactor; Environmentally assisted fatigue; Crack growth rate; Various loading frequencies.

Reference

[1] L. Zhang, J. Wang, Effect of temperature and loading mode on environmentally

assisted crack growth of a forged 316L SS in oxygenated high-temperature water, Corrosion Science, 87 (2014): p.278-287.

[2] Y. Hu, C. Sun, J. Xie, Y. Hong, Effects of Loading Frequency and Loading Type on High-Cycle and Very-High-Cycle Fatigue of a High-Strength Steel, Materials (Basel), 11 (2018): p.1456.

[3] V. Igwemezie, A. Mehmanparast, Waveform and frequency effects on corrosion-fatigue crack growth behaviour in modern marine steels, International Journal of Fatigue, 134 (2020): p.105484.

60. New insights and experimental/modeling confirmations of the HELP+HEDE model for the synergistic action of hydrogen embrittlement in metallic materials

New insights and experimental/modeling confirmations of the HELP+HEDE model for the synergistic action of hydrogen embrittlement in metallic materials

Milos B. Djukic¹

¹ Full Professor, University of Belgrade, Faculty of Mechanical Engineering, Department for Engineering Materials and Welding, Tribology, Fuels and Combustion, Kraljice Marije 16, 11200 Belgrade, Serbia

¹ Head of the Hydrogen-Materials Interactions Laboratory

¹ Assistant Subject Editor, International Journal of Hydrogen Energy by Elsevier

¹ Executive Committee Member of the ESIS (European Structural Integrity Society)

¹ Member of the team for preparation of the Hydrogen Strategy of the Republic of Serbia

Email (Prof. Dr. Milos B. Djukic): mdjukic@mas.bg.ac.rs

Authors: Milos B. Djukic¹, Gordana M. Bakic¹, Vera Sijacki Zeravcic¹, Bratislav

Rajcic¹,

Aleksandar Sedmak ¹, Muhammad Wasim ² and Jovana Perisic ¹

¹ *University of Belgrade, Faculty of Mechanical Engineering, Kraljice Marije 16,
11120 Belgrade, Serbia*

² *School of Engineering, Infrastructure Engineering Department, The University of
Melbourne, 3010 Melbourne, VIC, Australia*

Abstract A selection of suitable materials is critical for the safety of any hydrogen application. Most engineers know that hydrogen embrittlement and other hydrogen-specific damaging mechanisms of various metallic materials represent serious threats. The deleterious hydrogen effects and provoked degradation of mechanical properties of steel are expressed in diverse forms and often in opposite ways, including both softening and hardening phenomena, depending on three main factors: material, mechanic, and environmental. The HELP+HEDE model for synergistic action of hydrogen embrittlement (HE) mechanisms defined that the previous HELP mechanism activity is not always necessary for the activation and the observed complete predominance of the HEDE mechanism (“non-HELP mediated decohesion” process activation) at high local/global hydrogen concentrations in steels [1-8].

According to the HELP+HEDE model, the degree and nature of decreases in the material’s resistance to the crack propagation (steady-state linear decrease or the sudden drop) in steel are strictly related to the local/global hydrogen concentration in metals. Therefore, the synergistic effects of HE mechanisms are reflected through the corresponding predominance of HELP (at lower hydrogen concentration) or HEDE mechanism (at higher hydrogen concentration after reaching the critical local/global concentration) of hydrogen embrittlement. In our recent attempt to provide further progress in understanding the synergy of HE mechanisms, we proposed the unified HELP+HEDE model [9]. Accordingly, the "local HEDE micro-incidents" (grain boundary decohesion, fissures, and initial IG micro-cracks) as discrete micro-scale incidents, appear at a high local hydrogen concentration, but at still moderate global concentration, lower than the critical [9]. In such a case, the HELP mechanism is still

predominant (HELP+HEDE, HELP>HEDE), macroscopically speaking. According to the unified HELP+HEDE model, for the full macro HEDE mechanism manifestation (sharp drop in macro-mechanical properties and crack propagation resistance) and its dominance (HELP+HEDE, HEDE>>HELP), the necessary prerequisite is “the macro-volume effects” of HEDE. This means the appearance and accumulation of a large enough number of local HEDE micro incidents in a small volume. The new "local HEDE micro-incidents" concept at the local hydrogen concentration above the critical one, tries to bridge the gap between the various scales (macro, micro-meso, and nano-atomic) in the understanding of the physics of HE.

This Invited talk provides the summary of new insights and experimental and modeling confirmations [10,11] about the HELP+HEDE model for the synergistic action of hydrogen embrittlement in metallic materials.

Reference

- [1] B.N. Popov, J-W. Lee, **M.B. Djukic**, *Chapter 7 - Hydrogen Permeation and Hydrogen Induced Cracking*, in: Handbook of Environmental Degradation of Materials, Third Edition, edited by Myer Kutz, 2018, William Andrew, Elsevier (2018), pp. 133-162. <https://doi.org/10.1016/B978-0-323-52472-8.00007-1>
- [2] M.B. Djukic, V. Sijacki Zeravcic, G.M. Bakic, A. Sedmak, B. Rajicic, *The synergistic action and interplay of hydrogen embrittlement mechanisms in steels and iron: Localized plasticity and decohesion*, Engineering Fracture Mechanics 216 (2019), p. 106528. <https://doi.org/10.1016/j.engfracmech.2019.106528>
- [3] M.B. Djukic, V. Sijacki Zeravcic, G.M. Bakic, A. Sedmak, B. Rajicic, *Hydrogen damage of steels: A case study and hydrogen embrittlement model*, Engineering Failure Analysis, 58 (2015), pp. 485-498. <https://doi.org/10.1016/j.engfailanal.2015.05.017>
- [4] M.B. Djukic, G.M. Bakic, V. Sijacki Zeravcic, A. Sedmak, B. Rajicic, *Hydrogen embrittlement of industrial components: prediction, prevention, and models*, Corrosion, 72 (2016), pp. 943-961. <https://doi.org/10.5006/1958>
- [5] M. Wasim, M.B. Djukic, *Hydrogen embrittlement of low carbon structural steel at*

macro-, micro- and nano-levels, *International Journal of Hydrogen Energy* 45(3) (2020), pp. 2145-2156. <https://doi.org/10.1016/j.ijhydene.2019.11.070>

[6] M.B. Djukic, W.A. Curtin, Z. Zhang, A. Sedmak, Recent Advances on Hydrogen Embrittlement Understanding and Future Research Framework, Editorial, *Engineering Fracture Mechanics* 241 (2021), p. 107439. <https://doi.org/10.1016/j.engfracmech.2020.107439>

[7] M. Wasim, M.B. Djukic, External corrosion of oil and gas pipelines: A review of failure mechanisms and predictive preventions, *International Journal of Natural Gas Science and Engineering* 100 (2022), p. 104467. <https://doi.org/10.1016/j.jngse.2022.104467>

[8] O. Bouledroua, Z. Hafsi, M.B. Djukic, S. Elaoud, The synergistic effects of hydrogen embrittlement and transient gas flow conditions on integrity assessment of a precracked steel pipeline, *International Journal of Hydrogen Energy* 45(35) (2020), p. 18010 - 18020. <https://doi.org/10.1016/j.ijhydene.2020.04.262>

[9] M. Wasim, M.B. Djukic, T.D. Ngo, Influence of hydrogen-enhanced plasticity and decohesion mechanisms of hydrogen embrittlement on the fracture resistance of steel, *Engineering Failure Analysis* 123 (2021), p. 105312. <https://doi.org/10.1016/j.engfailanal.2021.105312>

[10] H.W. Lee, N.B. Jamal, H. Fakhri, R. Ranade, H. Egner, A. Lipski, M. Piotrowski, S. Mroziński, C.L. Rao, M.B. Djukic, C. Basaran, Unified Mechanics of Metallic Structural Materials. in: *Reference Modul in Materials Science and Materials Engineering*, Elsevier (2023) <https://doi.org/10.1016/B978-0-323-90646-3.00006-X>

[11] H.W. Lee, M.B. Djukic, C. Basaran, Modeling fatigue life and hydrogen embrittlement of bcc steel with unified mechanics theory, *International Journal of Hydrogen Energy* 48(54) (2023), p. 20773-20803. <https://doi.org/10.1016/j.ijhydene.2023.02.110>

61. Microscopic criteria for stress corrosion crack initiation of Monel 400 alloy in hydrofluoric acid vapor

Microscopic criteria for stress corrosion crack initiation of Monel 400 alloy in hydrofluoric acid vapor

Hailong Dai^{1,2,3}, Shouwen Shi^{1,2,3}, Xu Chen^{1,2,3}

¹*School of Chemical Engineering and Technology, Tianjin University, Tianjin 300072, China*

²*Tianjin Key Laboratory of Chemical Process Safety and Equipment Technology, Tianjin 300350, China*

³*Zhejiang Institute of Tianjin University, Ningbo, Zhejiang, 315201, China*

Abstract Monel 400 alloy has extremely high reactivity in hydrofluoric acid (HF) vapor and can rapidly cause stress corrosion cracking (SCC) [1-4]. Stress corrosion crack initiation is the main part of the stress corrosion life of serviced materials, so understanding the law of stress corrosion crack initiation and quantitative evaluation will provide an important reference for stress corrosion life prediction. The stress corrosion crack initiation rule of Monel 400 alloy in HF vapor environment was studied using SEM-DIC technology, and effective micromechanical parameters were extracted to identify crack initiation. The results show that neither the crystallographic index nor the existing microscopic crack initiation criterion can effectively predict the stress corrosion crack initiation of Monel 400 alloy in HF vapor [5-13]. In this study, a new index based on the microscopic strain field is proposed, and the crack initiation is highly correlated with the microscopic normal strain. For intergranular cracking (IGC), when the normal strain difference in grain boundary (GB) is greater than 2%, the crack initiation probability is as high as 95%. For transgranular cracking (TGC), the probability of crack initiation exceeds 95% when the normal strain in TG is greater than 4.4%. Furthermore, according to the geometric characteristics of GB and slip plane, the normal strain of GB and intra crystal are normalized respectively, and a parameter F is proposed which can accurately predict IGC and TGC initiation with a

prediction accuracy of 100%.

Keywords Monel 400 alloy; Stress corrosion cracking; Crack initiation; SEM-DIC; Transgranular cracking;

Reference

[1] H. Dai, S. Shi, C. Guo, X. Chen, Detrimental Effect of Surface Mechanical Grinding on Stress Corrosion Behavior of Monel 400 alloy in Hydrofluoric Acid Vapor, *Corrosion*, 79 (2023), pp. 1166–1178, <https://doi.org/10.5006/4382>.

[2] H. Dai, S. Shi, C. Guo, Z. Ning, Y. Kuang, X. Chen, The synergistic effect between fluoridation degradation and dislocation sliding on stress corrosion failure of Monel 400 alloy in HF vapor, *Corros. Sci.*, 224 (2023), Article 111489, <https://doi.org/10.1016/j.corsci.2023.111489>.

[3] H. Dai, S. Shi, J. Tang, C. Guo, Z. Ning, X. Chen, Revealing the effect of heat treatment on stress corrosion cracking behavior of Monel 400 alloy in hydrofluoric acid vapor environment, *Corros. Sci.*, 215 (2023), Article 111046, <https://doi.org/10.1016/j.corsci.2023.111046>.

[4] C. Guo, S. Shi, H. Dai, X. Sun, J. Yu, X. Chen, The deterioration effects of corrosion product deposition on Ni-Cu alloy in hydrofluoric acid vapor phase, *Corros. Sci.*, 219 (2023), Article 111256, <https://doi.org/10.1016/j.corsci.2023.111256>.

[5] G. Was, B. Alexandreanu, J. Busby, Localized deformation induced IGSCC and IASCC of austenitic alloys in high temperature water, in: *Key Eng. Mater.*, Trans Tech Publ, 2004, pp. 885-902.

[6] G.S. Was, D. Farkas, I.M. Robertson, Micromechanics of dislocation channeling in intergranular stress corrosion crack nucleation, *Curr. Opin. Solid State Mater. Sci.*, 16 (2012), pp. 134-142, <https://doi.org/10.1016/j.cossms.2012.03.003>.

[7] T. Fujii, Y. Hisada, K. Tohgo, Y. Shimamura, Investigation on nucleation of intergranular stress corrosion cracking in austenitic stainless steel by in situ strain measurement, *Mater. Sci. Eng. A*, 773 (2020), Article 138858, <https://doi.org/10.1016/j.msea.2019.138858>.

[8] T. Fujii, T. Sawada, K. Tohgo, Y. Shimamura, Mechanical criterion for nucleation

of intergranular stress corrosion cracking in austenitic stainless steel, *Forces in Mechanics*, 3 (2021), Article 100013, <https://doi.org/10.1016/j.finmec.2021.100013>.

[9] T. Fujii, M. Suzuki, Y. Shimamura, Susceptibility to intergranular corrosion in sensitized austenitic stainless steel characterized via crystallographic characteristics of grain boundaries, *Corros. Sci.*, 195 (2022), Article 109946, <https://doi.org/10.1016/j.corsci.2021.109946>.

[10] T. Fujii, K. Tohgo, Y. Mori, Y. Miura, Y. Shimamura, Crystallographic and mechanical investigation of intergranular stress corrosion crack initiation in austenitic stainless steel, *Mater. Sci. Eng. A*, 751 (2019), pp. 160-170, <https://doi.org/10.1016/j.msea.2019.02.069>.

[11] T. Fujii, K. Tohgo, Y. Mori, Y. Shimamura, Crystallography of intergranular corrosion in sensitized austenitic stainless steel, *Mater. Charact.*, 144 (2018), pp. 219-226, <https://doi.org/10.1016/j.matchar.2018.07.014>.

[12] T. Fujii, R. Yamakawa, K. Tohgo, Y. Shimamura, Strain-based approach to investigate intergranular stress corrosion crack initiation on a smooth surface of austenitic stainless steel, *Mater. Sci. Eng. A*, 756 (2019), pp. 518-527, <https://doi.org/10.1016/j.msea.2019.04.083>.

[13] A.S.T.M. B127, Standard Specification for Nickel-Copper Alloy (UNS N04400) Plate, Sheet, and Strip, in, 2005.

62. Non-steady electrochemical mechanism of stress corrosion cracking and its protection techniques

Non-steady electrochemical mechanism of stress corrosion cracking and its protection techniques

Zhiyong Liu^{1,2}, Cuiwei Du^{1,2}, Chaofang Dong^{1,2}, Xiaogang Li^{1,2}

¹ *National Materials Corrosion and Protection Data Center, University of Science and Technology Beijing, Beijing 100083, China*

² *Key Laboratory for Corrosion and Protection (MOE), University of Science and*

Technology Beijing, Beijing 100083, China

E-mail address: liuzhiyong7804@126.com

Abstract Stress corrosion cracking (SCC) is one of the major threats to the operational safety of load-bearing structure or materials in many industrial fields. SCC mechanism has been widely emphasized by the industry and is the basis of SCC diagnosis, assessment and protection. Authors of this work conducted an in-depth study on the electrochemical mechanism of stress corrosion and its applications for decades. They found that SCC of steels is an interactive process of fracture and electrochemical reactions, and its two-dimensional characteristics of cracking and expansion determine that SCC has non-stationary electrochemical properties. The fresh metal surface continuously exposed by crack expansion and the non-stationary electrochemical process caused by dislocation outcrop movement are the two main non-stationary electrochemical processes in the SCC process, which have a decisive influence on the SCC and its mechanism. Due to the above two mechanisms, SCC in aqueous phase media is generally characterized as controlled by a mixture of anodic dissolution and hydrogen embrittlement mechanisms (AD+HE). Based on the above understanding, a quantitative theoretical model for SCC sensitivity and life prediction is proposed, and various SCC monitoring and detection techniques as well as composition design methods for SCC-resistant steels are established and have been applied in a large number of engineering applications.

Keywords Stress corrosion cracking, Non stationary electrochemistry, Prediction model, SCC-resistant steel

Reference

- [1] X.X. Xu, H.L. Cheng, W. Wu, Z.Y. Liu, X.G. Li, Stress corrosion cracking behavior and mechanism of Fe-Mn-Al-C-Ni high specific strength steel in the marine atmospheric environment[J]. *Corrosion Science*, 191 (2021) 109760.
- [2] W. Wu, Z.Y. Liu, Q.Y. Wang, X.G. Li, Improving the resistance of high-strength steel to SCC in a SO₂-polluted marine atmosphere through Nb and Sb microalloying[J]. *Corrosion Science*, 170 (2020) 108693.

- [3] T.L. Zhao, Z.Y. Liu, X.X. Xu, Y. Li, C.W. Du, X.B. Liu, Interaction between hydrogen and cyclic stress and its role in fatigue damage mechanism[J]. *Corrosion Science*, 157 (2019) 146-156.
- [4] Z.Y. Liu, W.K. Hao, W. Wu, H. Luo, X.G. Li, Fundamental investigation of stress corrosion cracking of E690 steel in simulated marine thin electrolyte layer[J]. *Corrosion Science*, 148 (2019) 388-396.
- [5] T.L. Zhao, Z.Y. Liu, C.W. Du, C. Liu, X.X. Xu, X.G. Li, Modeling for corrosion fatigue crack initiation life based on corrosion kinetics and equivalent initial flaw size theory[J]. *Corrosion Science*, 142 (2018) 277-283.
- [6] Z.Y. Liu, Q. Li, Z.Y. Cui, W. Wu, Z. Li, C.W. Du, X.G. Li, Field experiment of stress corrosion cracking behavior of high strength pipeline steels in typical soil environments[J]. *Construction and Building Materials*, 148 (2017) 131-139.
- [7] Z.Y. Liu, W. Wu, W.K. Hao, X.G. Li, C.W. Du, K. Xiao, Technical Note: Stress Corrosion Cracking Mechanism of 304L under a Glycine Environment[J]. *Corrosion*, 72 (2016) 332-341.
- [8] Z.Y. Liu, Z.Y. Cui, X.G. Li, C.W. Du, Y.Y. Xing, Mechanistic aspect of stress corrosion cracking of X80 pipeline steel under non-stable cathodic polarization[J]. *Electrochemistry Communications*, 48 (2014) 127-129.
- [9] Z.Y. Liu, L. Lu, Y.Z. Huang, C.W. Du, X.G. Li, Mechanistic Aspect of Non-Steady Electrochemical Characteristic During Stress Corrosion Cracking of an X70 Pipeline Steel in Simulated Underground Water[J]. *Corrosion*, 70 (2014) 678-685.
- [10] Z.Y. Liu, X.G. Li, Y.F. Cheng, Mechanistic aspect of near-neutral pH stress corrosion cracking of pipelines under cathodic polarization[J]. *Corrosion Science*, 55 (2012) 54-60.
- [11] Z.Y. Liu, X.G. Li, Y.F. Cheng, Electrochemical state conversion model for occurrence of pitting corrosion on a cathodically polarized carbon steel in a near-neutral pH solution[J]. *Electrochimica Acta*, 56 (2011) 4167-4175.
- [12] Z.Y. Liu, X.G. Li, C.W. Du, Y.F. Cheng, Local additional potential model for effect of strain rate on SCC of pipeline steel in an acidic soil solution[J]. *Corrosion*

Science, 51 (2009) 2863-2871.

[13] Z.Y. Liu, X.G. Li, C.W. Du, L. Lu, Y.R. Zhang, Y.F. Cheng, Effect of inclusions on initiation of stress corrosion cracks in X70 pipeline steel in an acidic soil environment[J]. Corrosion Science, 51 (2009) 895-900.

[14] Z.Y. Liu, X.G. Li, C.W. Du, G.L. Zhai, Y.F. Cheng, Stress corrosion cracking behavior of X70 pipe steel in an acidic soil environment[J]. Corrosion Science, 50 (2008) 2251-2257.

63. Progress in Design of Hydrogen Embrittlement-Resistance High Strength Steel and Prospects

Progress in Design of Hydrogen Embrittlement-Resistance High Strength Steel and
Prospects

LIU Jing^{1,2} Huang Feng², zhang Shiqi², Zhixian Peng², Qian Hu²

¹*College of Materials Science and Engineering, Shenzhen University, Shenzhen
518000, China*

²*The State Key Laboratory of Refractories and Metallurgy, Wuhan University of
Science and Technology, Wuhan, Hubei 430081, China*

Corresponding author, E-mail: liujing@wust.edu.cn

Abstract Under the background of carbon peaking and carbon neutralization, there is an increasing demand for advanced hydrogen embrittlement (HE) resistant high strength steels and novel mitigation methods. This report briefly reviews the discovery and recognition of HE, the three-step processes of HE, and gives a comprehensive description of HE mitigation strategies. In the aspect of the permeation of hydrogen into high-strength steel, the influences corrosion product film and alternating stress on the hydrogen permeation are reported, which verifies the feasibility of using corrosion film to actively mitigate hydrogen permeation and HE. Regarding the hydrogen trap design in high strength steel, the recent advances in the design and fabrication of second phases-induced hydrogen traps, such as inclusions and precipitates are described in detail. In the section of hydrogen-induced cracking

control, the progress of using grain boundary engineering and segregation to suppress hydrogen cracking in recent years are discussed. Finally, based on the above contents, the future developing directions of HE research are prospected.

Keywords high strength steel; hydrogen embrittlement; hydrogen permeation

64. Rendering a predictive and protecting mechanism on stress corrosion cracking: Cleavage dissolution model

Rendering a predictive and protecting mechanism on stress corrosion cracking:
Cleavage dissolution model

ZHU Long-Kui *

*Academy of Advanced Technology, Beijing Peace-Test Tech. Co. Ltd., Beijing China,
100084*

Abstract As a significant cause of disastrous accidents, stress corrosion cracking (SCC) has delayed for a century since the so-called season cracking attacked metallic structures. The SCC is akin to a cancer in materials and equipments owing to no systematic insight into the predictive and protecting mechanisms. In this work, the SCC under elastic and plastic loads was investigated in type 316L stainless steel during immersion of a boiling 45 wt.% MgCl₂ solution. Two- and three-dimensional microcrack morphologies, characterized using synchrotron-based X-ray computed tomography and so on, indicate that the SCC cracks advanced along the cleavage planes (1 0 0) without accompanying surface slipping at the elastic stress levels, and switched to the intergranular mode at the high plastic stress levels. The first-principles simulations show that synergistic adsorption of H and Cl atoms in the octahedral interstices minimized the surface energy of the cleavage planes (0 0 1) owing to a 73% reduction, in comparison to a 28% reduction only under the H-adsorbed condition. On the basis, the cleavage-dissolution mechanism has been put forward, proposing that the SCC essentially originates from brittle rupture of corrosive environment particles assisted low-surface-energy cleavage facets, and anodic dissolution along the crack fronts, which is unnecessarily dominated by or depends on dislocation emission.

Wherein, the corrosive environment particles primarily consist of the hydrogen atoms and the electronegative ions such as the chlorine ions during the SCC of stainless steel in chloride environment. Quantitatively, the resistance, R_{SCC} , of SCC initiation and propagation can be redefined as: $R_{SCC} = 2\gamma_s - W_e$ or $R_{SCC} = 2\gamma_s + \gamma_p - W_e + W_p$, where W_e is the environmental work including the Gibbs' adsorption energy, the elastic strain energy as well as the diffusion activation energy, while W_p is the additional plastic deformation work related to local dislocation pinning.

Keywords Stress corrosion cracking; Brittle cleavage; Crack growth resistance; Corrosive environment particle

65. Hydrogen embrittlement susceptibility of X80 pipeline steel in hydrogen-blended natural gas environments

Hydrogen embrittlement susceptibility of X80 pipeline steel in hydrogen-blended natural gas environments

Cailin Wang^{1,2}, Cuiwei Liu^{1,2}, Yuxing Li^{1,2}

¹*College of Pipeline and Civil Engineering, China University of Petroleum (East China), Qingdao, Shandong, 266580, China*

²*Shandong Provincial Key Laboratory of Oil & Gas Storage and Transportation Security, China University of Petroleum (East China), Qingdao, Shandong, 266580, China*

clwang0330@163.com

Abstract Blending gaseous hydrogen into the existing natural gas pipelines provides an economical and efficient approach for large-scale hydrogen energy transportation. Hydrogen atoms can be generated and adsorbed on the steel surface by dissociative adsorption [1], followed by the absorption, diffusion and accumulation, and finally may lead to hydrogen embrittlement [2]. The above steps are highly influenced by the gas components [3]. Thus it is necessary to investigate the effects of gas components on the hydrogen embrittlement susceptibility of pipeline steel. In-situ high-pressure

gaseous hydrogen permeation tests and slow strain rate tensile tests of X80 pipeline steel were conducted in the simulated hydrogen blended natural gas environments with different H₂/CH₄/CO contents. The permeability characteristics, mechanical properties and fracture morphologies were further analyzed. Results show that the subsurface hydrogen concentration, ductility loss and hydrogen embrittlement susceptibility increased significantly as hydrogen contents increased from 10% to 15%. Moreover, a positive correlation between subsurface hydrogen concentration and hydrogen embrittlement index was revealed. The hydrogen embrittlement susceptibility of X80 steel can be inhibited by the presence of CH₄/CO, and the inhibition mechanisms were discussed. When the CH₄ contents increased above 20%, the inhibition on hydrogen embrittlement of X80 steel was stabilized. By comparison, the inhibitory effect of CO was more significant.

Keywords Hydrogen embrittlement; Hydrogen permeation; CH₄; CO

Reference

- [1] Y. Sun, Y.F. Cheng, Thermodynamics of spontaneous dissociation and dissociative adsorption of hydrogen molecules and hydrogen atom adsorption and absorption on steel under pipelining conditions, *Int. J. Hydrogen Energy*. 46 (2021) 34469–34486.
- [2] C. Wang, J. Zhang, C. Liu, Q. Hu, R. Zhang, X. Xu, H. Yang, Y. Ning, Y. Li, Study on hydrogen embrittlement susceptibility of X80 steel through in-situ gaseous hydrogen permeation and slow strain rate tensile tests, *Int. J. Hydrogen Energy*. 48 (2023) 243–256.
- [3] C. Liu, H. Yang, C. Wang, H. Zhang, R. Ding, L. Ai, X. Fan, R. Zhang, X. Xu, Y. Ning, Y.F. Cheng, Y. Li, Effects of CH₄ and CO on hydrogen embrittlement susceptibility of X80 pipeline steel in hydrogen blended natural gas, *Int. J. Hydrogen Energy*. 48 (2023) 27766–27777.

66. Superwetting Coatings inside Capillary Tubes for in-vitro Diagnosis Lidong Sun

Superwetting Coatings inside Capillary Tubes for in-vitro Diagnosis

Lidong Sun

*School of Materials Science and Engineering, Chongqing University, Chongqing
400044, PR China*

Abstract Metal tubes are the key components for heat and mass transfer in precision instrument and advanced equipment. Superwetting coating plays an essential role in drag reduction, corrosion resistance, heat transfer enhancement, and so on. However, it remains a great challenge to prepare such a coating of superwettability inside capillary tubes, in view of the spatial limitation. This presentation introduces the fabrication of uniform and superwetting coatings at capillary tubes (inner diameter 0.3–10 mm). The method of coaxial anodization is discussed. Theoretical equations are derived to compute the intrinsic contact angles at the tubular system. Their applications in drag reduction and in-vitro diagnosis are demonstrated and discussed.

67. The role of Mg/MgO interfaces in the accelerated corrosion of additive manufactured Mg alloys

The role of Mg/MgO interfaces in the accelerated corrosion of additive manufactured
Mg alloys

Daniel J. Blackwood¹, Kai Xiang Kuah¹, Man-Fai Ng²

¹*Department of Materials Science & Engineering, National University of Singapore, 9
Engineering Drive 1, Singapore, 117575, Singapore*

²*Institute of High Performance Computing, Agency for Science, Technology and
Research, 1 Fusionopolis Way, #16-16 Connexis, Singapore 138632*

Presenter's e-mail address: msedjb@nus.edu.sg

Abstract Recent interest has been shown in using additive manufactured magnesium alloys in a range of different applications, from biomedical implants to aerospace. However, corrosion rates of additive manufactured Mg alloys have been reported to be higher than their as cast counterparts, and it is postulated that this due to increased kinetics for the supporting cathodic reaction on secondary phases [1,2]. MgO particulates are the main secondary phase in found additive manufactured alloys that are absent from cast alloy and it has been shown that attempts to remove these does impact the kinetics of the cathodic hydrogen evolution reaction [3]. However, the low

electrical conductivity of MgO (bandgap 7.8 eV) would seem to preclude it from acting as an effective cathode surface. Nevertheless, density of state calculations through density function theory using hybrid HSE06 functional revealed overlapping electronic states at the Mg/MgO interface, which facilitates electron transfers and participate in redox reactions. Subsequent determination of the hydrogen absorption energy at the Mg/MgO interface reveal it to be an excellent catalytic site, with HER being found to be a factor of 23x more efficient at the interface than on metallic Mg. The results not only support the plausibility of Mg/MgO interface being an effective cathode to the adjacent anodic Mg matrix during corrosion, but also contribute to the understanding of the enhanced cathodic activities observed during the anodic dissolution of magnesium.

Keywords magnesium, additive manufacturing, corrosion

References

- [1] KX Kuah, DJ Blackwood, WK Ong, M Salehi, HL Seet, MLS Nai, S. Wijesinghe. “Analysis of the corrosion performance of binder jet additive manufactured magnesium alloys for biomedical applications” *Journal of Magnesium and Alloys* **10** (2022) 1296-1310
- [2] M. Esmaily, Z. Zeng, A. N. Mortazavi, A. Gullino, S. Choudhary, T. Derra, F. Benn, F. D'Elia, M. Mütter, S. Thomas, A. Huang, A. Allanore, A. Kopp, N. Birbilis, “A detailed microstructural and corrosion analysis of magnesium alloy WE43 manufactured by selective laser melting”, *Additive Manufacturing* **35** (2020)101321
- [3] KX Kuah, M Salehi, WK Ong, HL Seet, MLS Nai, S Wijesinghe, DJ Blackwood, .Insights into the influence of oxide inclusions on corrosion performance of additive manufactured magnesium alloys”, *npj Materials Degradation* **6** (2022) 36.

68. Corrosion in low carbon energy technologies Gareth Hinds

Corrosion in low carbon energy technologies

Gareth Hinds

Electrochemistry Group, National Physical Laboratory, UK

Presenter's e-mail address: gareth.hinds@npl.co.uk

Abstract Corrosion science and engineering has always played a critical role in the energy sector due to the challenges associated with long term exposure of materials and components to harsh environments. Similar issues exist for low carbon technologies that are required in the global energy transition. For electrochemical energy conversion and storage devices such as fuel cells, electrolyzers and batteries, the presence of a cell voltage adds a further driving force for degradation. It is critical that corrosion expertise from established industrial sectors is transferred effectively to the research communities developing these emerging technologies. In this talk, a case study will be presented to demonstrate how transfer of knowledge from an established industry (oil and gas) to an emerging technology (water electrolysis) can lead to major breakthroughs.

Keywords corrosion, energy transition, oil and gas, water electrolysis

69. Insight into physical interpretation of electrochemical impedance spectra of Mg

Insight into physical interpretation of electrochemical impedance spectra of Mg
Linqian Wang¹, Darya Snihirova¹, Min Deng¹, Sviatlana V. Lamaka¹, Mikhail L.
Zheludkevich^{1,2}

¹*Institute of Surface Science, Helmholtz-Zentrum Hereon, 21502 Geesthacht,
Germany*

²*Institute of Materials Science, Faculty of Engineering, Kiel University, 24143 Kiel,
Germany*

Presenter's e-mail address: linqian.wang@hebut.edu.cn

Abstract The Electrochemical Impedance Spectroscopy (EIS) has been widely applied to study the corrosion behavior and mechanism of different bare and coated Mg-based materials. However, the analysis and interpretation of Mg-EIS results are

controversial. Assignment of the observed time constants to the specific processes is still debated. Despite wide application of EIS on Mg, diverse equivalent circuits are used by different researchers to fit similar impedance spectra. The ambiguous interpretations of the origin of time constants may cause the misleading explanations for Mg corrosion behavior. Hence, it is essential to reveal the physical interpretations of Mg impedance spectra for a better understanding of respective corrosion mechanisms.

In this work, we thoroughly discussed the physical interpretations of time constants in Mg impedance spectra, which are revealing for the investigating the corrosion behavior of Mg and its alloys. Conventional [1] and Tribo-EIS measurements [2] were performed to investigate the evolution of high frequency (HF) and middle frequency (MF) capacitive loops in impedance spectra of pure Mg under different surface states. The assignment of the HF time constant is confirmed through investigation of the oxide/hydroxide films formed at Mg surface in NaCl solution with different initial pH. Tribo-EIS measurements were performed to identify the origin of the HF and MF time constants of Mg. The results indicate that the HF time constant originates from the barrier properties of the MgO-based surface film and the MF time constant stems from the charge transfer process. Additionally, the non-stationarity of EIS measurement on several Mg-based materials in number of electrolytes was studied [3]. The results indicate that the impedance spectra of Mg-based materials in aqueous electrolytes is influenced by the internal non-stationarity of Mg-electrolyte system and the external non-stationarity induced by EIS measurement. Accordingly, the origin of inductive behavior of Mg-based materials is discussed.

Keywords EIS, magnesium, corrosion

Reference

[1] L. Wang, D. Snihirova, M. Deng, C. Wang, B. Vaghefinazari, G. Wiese, M. Langridge, D. Höche, S.V. Lamaka, M.L. Zheludkevich, Insight into physical interpretation of high frequency time constant in electrochemical impedance spectra of Mg, *Corrosion Science*, (2021) 109501.

[2] L. Wang, D. Snihirova, M. Deng, B. Vaghefinazari, D. Höche, S.V. Lamaka, M.L. Zheludkevich, Revealing physical interpretation of time constants in electrochemical impedance spectra of Mg via Tribo-EIS measurements, *Electrochimica Acta*, 404 (2022) 139582.

[3] L. Wang, D. Snihirova, M. D. Havigh, M. Deng, S.V. Lamaka, H. Terry, M.L. Zheludkevich, Non-stationarity in electrochemical impedance measurement of Mg-based materials in aqueous media, *Electrochimica Acta*, 468 (2023) 143140.

70. Interpretation on the fast corrosion process of Mg-alloys using electrochemical impedance spectroscopy

Interpretation on the fast corrosion process of Mg-alloys using electrochemical impedance spectroscopy

Yong Xingyue, Ji Haotian, Li Zhuoxuan, Xie Lili

State Key Lab. of Organic-Inorganic Composites, Beijing University of Chemical Technology, Beijing 100029, P. R. China

Presenter's e-mail address: yongxy@mail.buct.edu.cn

Abstract Magnesium is a very active metal. Similarly, the corrosion process of Mg-alloys in a 3.5% NaCl solution is very fast. Thus, it is very important to determine its stationary when EIS measurement was used to study the corrosion process of Mg-alloys in a 3.5% NaCl solution. In this study, the EIS characteristics of the Mg-alloys with or without coating in a 3.5% NaCl solution were studied based on the EIS measurement. Then, the equivalent electric circuits were set up on the EIS spectra in accordance with the physical-chemical features of Mg-alloy electrodes with or without coating in a 3.5% NaCl solution, and that they were used to fit the EIS spectra. Finally, the stationary of the corrosion process of Mg-alloy electrodes with or without coating was discussed on the basis of the function of real and imaginary part of the impedance as frequencies. The results showed that the non-stationary of Mg-alloy electrodes with or without coating in a 3.5% NaCl solution resulted from the

reactivity of the material with the electrolyte, the very low frequency domain of the EIS response showed a small tail, which is a typical behavior of a system that is not at steady-state. This was proved by fitting goodness and the departure of the slopes in plots of Z_r or Z_{im} vs. f from ± 1 . Therefore, it should be careful to analyze and interpret the EIS spectra.

Keywords Mg-alloys, chloride solution, corrosion process, EIS, SEM

References

- [1] G. Baril, G. Galicia, C. Deslouis, N. Pebere, B. Tribollet, V. Vivier, An impedance investigation of the mechanism of pure magnesium corrosion in sodium sulfate solution. *J. Electrochem. Soc.*, 154(2) (2007) C108-C113, <http://doi.org/10.1149/1.2401056>.
- [2] G. Galicia, N. Pebere, B. Tribollet, V. Vivier, Local and global electrochemical impedance applied to the corrosion behavior of an AZ91 magnesium alloy. *Corrosion Sci.* 51 (2009) 1789-1794. <https://doi.org/10.1016/j.corsci.2009.05005>.
- [3] M. Jamesh, S. Kumar, T. S. N. S. Narayanan, Corrosion behavior of commercially pure Mg and ZM21 Mg alloy in Ringer's solution – Long term evaluation by EIS, *Corros. Sci.* 53 (2011) 645-654, <https://doi.org/10.1016/j.corsci.2010.10.011>.

71. on Corrosion Behavior of Fe-Ga Alloy in Simulated Marine Environment

Research on Corrosion Behavior of Fe-Ga Alloy in Simulated Marine Environment

Peiyang Jiao, Pei Gong*, Bochen Li[#]

School of Materials Science and Engineering, Inner Mongolia University of Technology, Hohhot, Inner Mongolia 010051, China

Presenter's e-mail address: gongpei123@163.com

Abstract Fe-Ga alloy, as a new type of magnetostrictive material, has broad application prospects in fields such as sonar transducers, ocean exploration and development, and micro displacement drives. This article investigates the corrosion behavior of Fe-Ga alloy in seawater environment. Using static corrosion full

immersion experiments, combined with morphology observation, corrosion product analysis, open circuit potential, dynamic potential polarization curve, and electrochemical impedance spectroscopy testing. The corrosion morphology, corrosion products, and corrosion rate of Fe₈₁Ga₁₉ alloy immersed in simulated seawater environment for different times were compared to analyze the corrosion behavior of Fe₈₁Ga₁₉ alloy in simulated seawater environment. The experimental results show that the rust layer on the surface of Fe₈₁Ga₁₉ alloy changes from yellow to reddish brown, and the corrosion products gradually thicken. By observing the cross-sectional morphology of Fe₈₁Ga₁₉ alloy through SEM, it was found that the corrosion products of Fe₈₁Ga₁₉ alloy were distributed in a needle like manner, with corrosion products ranging from 5 μm gradually thickens to 20 μm. At the same time, the corrosion pits on the substrate surface tend to gradually deepen. EDS, XRD, and XPS characterization of the surface products of the sample showed that the corrosion products were mainly composed of γ-FeOOH, Ga₂O₃, Fe₂O₃. The corrosion rates of Fe₈₁Ga₁₉ alloy soaked for 5 days, 10 days, 15 days, and 20 days in static corrosion full immersion experiments were calculated using the weight loss method to be 0.060 g/(m² · h), 0.070 g/(m² · h), 0.066 g/(m² · h), and 0.080 g/(m² · h), respectively. As the corrosion time increases, the capacitance arc radius gradually decreases, and the self corrosion current density value first increases and then decreases. There is a clear passivation plateau in the potentiodynamic polarization curve. The results indicate that as the corrosion time prolongs, the corrosion resistance of Fe₈₁Ga₁₉ alloy in simulated seawater gradually weakens, and the corrosion rate continues to increase. It mainly exhibits uniform corrosion in simulated seawater, and the oxide film and corrosion products generated on the surface can have a certain protective effect on the substrate.

Keywords Fe-Ga alloy, simulate seawater, corrosion behavior, electrochemical testing

72. Sequential dual-passivation of Cr and Mn in stainless steel and its applications at high potentials

Sequential dual-passivation of Cr and Mn in stainless steel and its applications at high potentials

YU Kaiping¹, Huang Mingxin¹

¹*Department of Mechanical Engineering, The University of Hong Kong, Pokfulam Road, Hong Kong, China*

Presenter's e-mail address: kpyu20@hku.hk

Abstract Expensive setup materials have imposed substantial restrictions on the commercialization of green hydrogen production from water electrolysis. One crucial material for the porous transport layers and bipolar plates of the setup is costly pure Ti, which has superior corrosion resistance at the potentials above oxygen evolution [1-3]. In addition, Ti-based components are coated with noble Au or Pt to decrease contact resistance and insulated oxidation, further enhancing the setup cost. Stainless steel is significantly less expensive compared to pure Ti, and it has demonstrated its vital role in a wide variety of industries. Unfortunately, the current development of stainless steel has reached a stagnant stage due to the fundamental limitation of the conventional Cr-based single-passivation mechanism. Owing to the further oxidation of stable Cr₂O₃ into soluble Cr(VI) species, transpassive corrosion often occurs at ~1000 mV, which is below the potential required for water oxidation [4].

Here, we show that, by using a sequential dual-passivation mechanism, substantially enhanced anti-corrosion properties can be achieved in Mn-contained stainless steel, with a high breakdown potential of ~1700 mV (saturated calomel electrode, SCE) in a 3.5 wt.% NaCl solution [5]. Specifically, the conventional Cr-based and counter-intuitive Mn-based passivation is sequentially activated during potentiodynamic polarization. The Cr-based passive layer prevents corrosion at low potentials below ~720 mV(SCE), while the Mn-based passive layer resists corrosion at high potentials up to ~1700 mV(SCE). The present “sequential dual-passivation” strategy enlarges the passive region of stainless steel to high potentials above water oxidation, enabling them as potential anodic materials for green hydrogen production via water electrolysis.

Keywords sequential dual-passivation, chromium, manganese, corrosion resistance, water electrolysis

Reference

- [1] Q. Chen, Y. Wang, F. Yang, H. Xu, Two-dimensional multi-physics modeling of porous transport layer in polymer electrolyte membrane electrolyzer for water splitting, *International Journal of Hydrogen Energy*, 45 (2020) 32984-32994.
- [2] P. Kim, J. Lee, C. Lee, K. Fahy, P. Shrestha, K. Krause, H. Shafaque, A. Bazylak, Tailoring catalyst layer interface with titanium mesh porous transport layers, *Electrochimica Acta*, 373 (2021) 137879.
- [3] M. Bernt, C. Schramm, J. Schröter, C. Gebauer, J. Byrknes, C. Eickes, H. Gasteiger, Effect of the IrOx conductivity on the anode electrode/porous transport layer interfacial resistance in PEM water electrolyzers, *Journal of The Electrochemical Society*, 168 (2021) 084513.
- [4] I. Betova, M. Bojinov, T. Laitinen, K. Mäkelä, P. Pohjanne, T. Saario, The transpassive dissolution mechanism of highly alloyed stainless steels: II. Effect of pH and solution anion on the kinetics, *Corrosion science*, 44 (2002) 2699-2723.
- [5] K. Yu, S. Feng, C. Ding, M. Gu, P. Yu, M. Huang, A sequential dual-passivation strategy for designing stainless steel used above water oxidation, *Materials Today*, (2023).

73. Spatially Resolved Local Electrochemical *In Operando* Techniques Visualize the Interface of biodegradable Metals

Spatially Resolved Local Electrochemical *In Operando* Techniques Visualize the Interface of biodegradable Metals

Cheng Wang¹, Chenglin Chu¹, Feng Xue¹, Jing Bai¹,
Mikhail Zheludkevich², Sviatlana Lamaka²

¹ *School of Materials Science and Engineering, Southeast University, Nanjing, 211189, China*

² Institute for Surface Science, Helmholtz-Zentrum Hereon, Geesthacht, 21502,
Germany

Presenter's e-mail address: cheng.wang@seu.edu.cn

Abstract The degradation of biodegradable metals typically initiates locally and evolves variably, which is difficult to be captured by general experimental methods. The advancement of spatially resolved local *in operando* techniques enables a powerful *in situ* approach to study the degradation mechanism of biodegradable metals at the metal interface, especially following the evolution of interfacial pH and O₂ concentration, which are substantial factors during the metal biodegradation. The degradation behavior of biodegradable Mg, Zn, and Fe alloys are systematically characterized by spatially resolved local techniques that measure local pH, O₂ levels, and H₂ concentration at the metal interface. The local pH indicates anodic/cathodic process and formation of pH-dependent degradation products at metal interface. The local O₂/H₂ concentrations demonstrate typical cathodic reactions accompanying metal degradation, including hydrogen evolution reaction (HER) and oxygen reduction reaction (ORR).

The results reveal interfacial electrochemical processes of biodegradable Mg, Zn, and Fe alloys. Counterintuitively, ORR, a secondary cathodic process for Mg, contributes higher to the corrosion of slowly degrading ultra-high-purity Mg (16.5%) than in fast corroding commercially-pure-Mg (1.3%). The dissolution of Mg typically induces high local pH (10.4-10.6 in NaCl), which yet gets relatively low and stable (7.5-8.0) in Ca²⁺-containing Hanks' balanced salt solution (HBSS, pH=7.4) without synthesis pH buffers at 37 °C under hydrodynamic conditions. In contrast, Zn and Fe alloys experience significant O₂ consumption and localized acidification because dissolved metal cations hydrolyze in HBSS at 37 °C. The interfacial pH variation is buffered in Ca²⁺-containing HBSS due to Ca-P-containing precipitates. The addition of synthetic pH buffers stabilizes the interfacial pH for Zn alloys but not for Mg. The Ca-P-containing products layer protects Mg, Zn, and Fe alloys from water and oxygen in Ca²⁺-containing HBSS, slowing ORR as the layer densify. These findings

emphasize the importance of understanding the interactions at metal-fluid interface during metal biodegradation.

Keywords local *in operando* techniques, interfacial pH, local oxygen consumption, local hydrogen evolution, biodegradable metals

Reference

[1] **Cheng Wang**, Christabelle Tonna, Di Mei, Joseph Buhagiar, Mikhail L. Zheludkevich, Sviatlana V. Lamaka, Biodegradation behaviour of Fe-based alloys in Hanks' Balanced Salt Solutions Part II. The evolution of local pH and dissolved oxygen concentration at metal interface, *Bioactive Materials*, 7 (2022) 412-425.

[2] **Cheng Wang**, Ci Song, Di Mei, Linqian Wang, Wenhui Wang, Ting Wu, Darya Snihirova, Mikhail L. Zheludkevich, Sviatlana V. Lamaka, Low interfacial pH discloses the favorable biodegradability of several Mg alloys, *Corrosion Science*, 197 (2022) 110059.

[3] **Cheng Wang**, Xiao Liu, Di Mei, Min Deng, Yufeng Zheng, Mikhail L. Zheludkevich, Sviatlana V. Lamaka, Local pH and oxygen concentration at the interface of Zn alloys in Tris-HCl or HEPES buffered Hanks' balanced salt solution, *Corrosion Science*, 197 (2022). 110061.

[4] **Cheng Wang**, Wen Xu, Daniel Höche, Mikhail L. Zheludkevich, Sviatlana V. Lamaka, Exploring the contribution of oxygen reduction reaction to Mg corrosion by modeling assisted local analysis, *Journal of Magnesium and Alloys*, 2022.

[5] **Cheng Wang**, Di Mei, Gert Wiese, Linqian Wang, Min Deng, Sviatlana V. Lamaka, Mikhail L. Zheludkevich, High rate oxygen reduction reaction during corrosion of ultra-high-purity magnesium, *npj Materials Degradation*, 4 (2020) 42.

74. Chloride Susceptibility Index (CSI): an *ab initio* based corrosion resistance indicator

Chloride Susceptibility Index (CSI): an *ab initio* based corrosion resistance indicator

Huibin Ke^{1,2*}, Tianshu Li^{1,3}, Pin Lu⁴, Gerald S. Frankel¹, Christopher D. Taylor^{1,5}

¹ Fontana Corrosion Center, Department of Materials Science & Engineering, The Ohio State University, Columbus, USA

² School of Materials Science and Engineering, Beijing Institute of Technology, Beijing, China

³ Xi'an Jiaotong University, Xi'an, China

⁴ QuesTek Innovations LLC, Evanston, USA

⁵ Materials Technology & Development, DNV GL USA, Dublin, USA

Presenter's e-mail address: kehuibin@bit.edu.cn

Abstract Many properties have been used to indicate the corrosion resistance of metallic materials. However, there is still no single property that can be used to compare across different alloy system and predict the corrosion resistance of metallic materials. Here, a universal scientifically based quantitative indicator called chloride susceptibility index (CSI) is introduced based on a multi-scale modeling framework. This framework can be applied to study the effect of different factors on corrosion resistance of alloys, including alloy composition, solution pH, Cl⁻ concentration and temperature. Commonly used Ni-Cr-based alloys and stainless steels will be used as examples for this study. Firstly, *ab initio* modeling is used to study the adsorption energy of O and Cl to alloy surfaces with different solutes. Then, a Langmuir model is used to study the competitive adsorption of Cl vs. O under different conditions, from which CSI will be calculated. By connecting atomic scale properties with environmental conditions, CSI allows the predictable quantitative measurement of one aspect of the corrosion resistance of metallic materials, namely the sensitivity of the alloy surface to complexation with chloride versus oxide formation, which is related to the repassivation property of alloys. Finally, experimental measured repassivation potential is compared with CSI and a strong linear relationship is found between these two.

75. Effect of Heat Flow on the Corrosion Behavior of Carbon Steel H₂SO₄ Solution Interface

Effect of Heat Flow on the Corrosion Behavior of Carbon Steel H₂SO₄ Solution
Interface

Zeyu Zhou

Guangzhou University

Abstract Heat exchange processes and heat exchange devices are most widely used in production and life. Convective heat transfer is a typical heat exchange process. In order to find out the influence of heat flow on the corrosion behavior of heat transfer surface, this study combined COMSOL simulation analysis to design and build an electrochemical testing system, then the corrosion behavior of Q235 carbon steel in 0.5 M sulfuric acid solution under different heat transfer conditions was investigated by weight loss method and electrochemical method. Based on the transition-state equation, the enthalpy and entropy changes of transition-state formation in the corrosion reaction control step were analyzed. The results show that positive heat flow (flowing from metal to solution) reduces the corrosion rate of the heat transfer surface, while negative heat flow (flowing from solution to metal) accelerates the corrosion rate of the heat transfer surface. Under the test condition without heat flow, the enthalpy change and entropy change of the transition-state formation in the corrosion reaction control step don't change significantly. However, when heat flows through the heat transfer interface, the enthalpy change and entropy change have changed significantly. The heat flux is linearly related to the entropy and enthalpy change, and the change rate under the condition of negative heat flow is significantly higher than that of positive heat flow. These results indicate that heat flow not only changes the concentration of reactants near the interface, but also affects the rate and mechanism of the corrosion reaction, and the effect of negative heat flow is greater than that of positive heat flow. This study provides an experimental basis and theoretical method for determining the corrosion rate in heat transfer environments.

(This work was supported by the grant from NSFC, No. 51971067)

Keywords COMSOL simulation analysis, heat flow, heat transfer surface, corrosion behavior, mechanism

76. Effects of temperature and acetic acid on electrochemical corrosion behavior of X80 steel

Effects of temperature and acetic acid on electrochemical corrosion behavior of X80 steel

Yadong Li¹, Wanpeng Yao¹, Siquan Wang¹, JianJun Pang², Yan Li^{1,*}

¹*School of Materials Science and Engineering, China University of Petroleum (East China), Qingdao 266580, China*

²*School of Mechanical and Automotive Engineering, Zhejiang University of Water Resources and Electric Power, Hangzhou 310018, China*

Abstract The effects of temperature and HAc on the corrosion behavior of X80 steel were investigated by electrochemical measurements, including electrochemical impedance spectroscopy and potentiodynamic polarization curves. Results showed that the corrosion current density of X80 steel increased with the increased of temperature. The near-surface pH values of X80 steel revealed that due to the formation conditions of the corrosion film, differences existed between electrochemical measurements and weight loss method results. The changes of cathodic and anodic charge transfer resistance indicating that the mechanism of HAc that affects the cathodic reaction process was found to be the buffering effect, and HAc served as the source of H⁺.

Keywords Pipeline steel; Electrochemical impedance spectroscopy; Near-surface pH; CO₂ corrosion

Reference

[1] S.X. Zhang, F.Q. Xie, X.M. Li, J.H. Luo, G.G. Su, L.X. Zhu, Q.G. Chen, Failure analysis of the leakage in girth weld of bimetal composite pipe. Eng. Fail. Anal., 2023,

143, p 106917.

[2] E. Basilico, S. Marcelin, R. Mingant, J. Kittel, M. Fregonese, F. Ropital, The effect of chemical species on the electrochemical reactions and corrosion product layer of carbon steel in CO₂ aqueous environment: A review. *Mater. Corros.*, 2021, 72, p 1-16.

[3] T. das Chagas Almeida, M.C.E. Bandeira, Moreira R M, O.R. Mattos, New insights on the role of CO₂ in the mechanism of carbon steel corrosion. *Corros. Sci.*, 2017, 120, p 239-250.

77. Cellular automaton simulation of electrochemical behavior of B30 copper-nickel alloy in seawater environment

Cellular automaton simulation of electrochemical behavior of B30 copper-nickel alloy
in seawater environment

Yuanqing Jin¹, Hong Chen¹, Yifan Jiang¹, Shiyu Hu¹, Meili Wu¹, Baikang Zhu¹,
Zhiwei Chen^{1*}, Wei Zhang², Weihua Li³

*1 College of Petrochemical Engineering and Environment, Zhejiang Ocean University,
Zhoushan*

2 School of Chemical Engineering and Technology, Sun Yat-sen University, Zhuhai

*3 School of Civil Engineering and Communication, North China University of Water
Resources and Electric Power, Zhengzhou*

Abstract B30 copper-nickel alloy has excellent corrosion resistance in seawater environment, and the oxide film formed on the surface of the alloy has an important effect on its electrochemical behavior. The electrochemical behavior of the oxide film on the surface of B30 copper-nickel alloy was investigated by using the AC impedance spectrum test with Gamry. In seawater environment, the electrochemical behavior of B30 Cu-Ni alloy is divided into four stages, which are the incomplete forming stage, the development and stability stage, the unstable stage and the local

failure stage. A cellular automaton model was established to simulate and verify the corrosion electrochemical behavior of B30 copper-nickel alloy in seawater environment. The results show that the oxide film of the alloy has different effects on the corrosion rate at different stages. With the increase of soaking time, the corrosion rate increases first and then decreases, and then gradually becomes stable. At the same time, the cellular automata model also visualizes the surface topography at mesoscale.

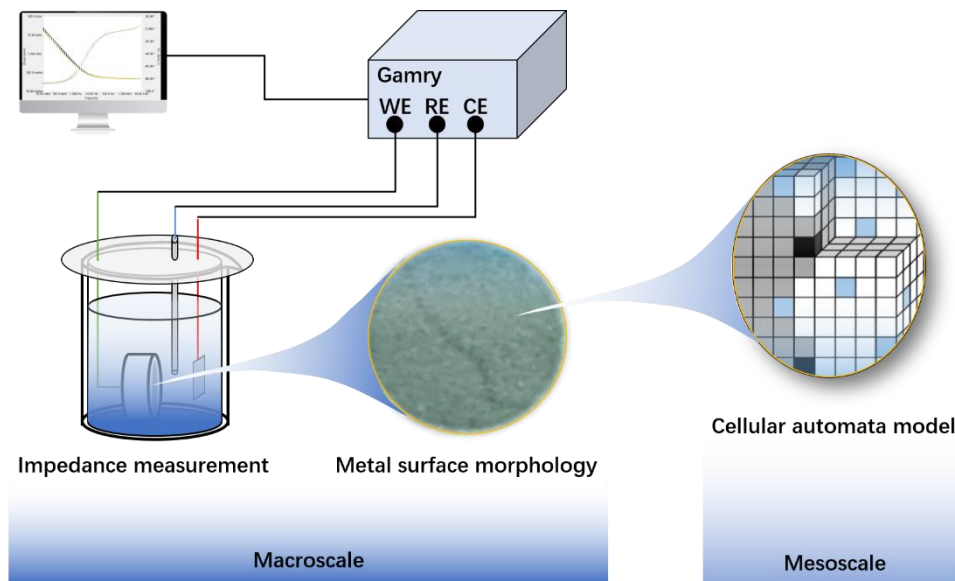


Figure.1 B30 copper-nickel alloy surface morphology and mesoscopic cellular automata model diagram

Keywords B30 copper-nickel alloy; Electrochemical behavior; Alternating current impedance; Seawater corrosion; cellular automaton

References

- [1] BARARPOUR S M, JAMSHIDI AVAL H, JAMAATI R. Cellular automaton modeling of dynamic recrystallization in Al-Mg alloy coating fabricated using the friction surfacing process [J]. Surf Coat Technol, 2021, 407: 126784.
- [2] HASHEMI S, KALIDINDI S R. A machine learning framework for the temporal evolution of microstructure during static recrystallization of polycrystalline materials simulated by cellular automaton [J]. Comput Mater Sci, 2021, 188: 110132.
- [3] DI CAPRIO D, STAFIEJ J. Simulations of passivation phenomena based on

- discrete lattice gas automata [J]. *Electrochim Acta*, 2010, 55(12): 3884-3890.
- [4] WANG H, HAN E. Mesoscopic Simulation of Diffusion Characteristics in the Corrosion Film [J]. *J Mater Sci Technol*, 2012, 28(5): 427-432.
- [5] CUI C, MA R, CHEN A, et al. Experimental study and 3D cellular automata simulation of corrosion pits on Q345 steel surface under salt-spray environment [J]. *Corros Sci*, 2019, 154: 80-89.
- [6] STĘPIEŃ J, DI CAPRIO D, STAFIEJ J. 3D simulations of the metal passivation process in potentiostatic conditions using discrete lattice gas automaton [J]. *Electrochim Acta*, 2019, 295: 173-180.
- [7] GUIZO S, DI CAPRIO D, DE LAMARE J, et al. Intergranular corrosion: Comparison between experiments and cellular automata [J]. *Corros Sci*, 2020, 177: 108953.

78. Effect of Er addition on the microstructure and corrosion performance of zinc aluminum magnesium coating

Effect of Er addition on the microstructure and corrosion performance of zinc
aluminum magnesium coating

LIU Guanghui, XU Chengliang, JIANG Guangrui

*Shougang Research Institute of Technology, Shougang Group Co., Ltd., Beijing,
100043, China*

Abstract Hot dip galvanized products are widely used in various aspects of production and life due to their excellent corrosion resistance. Some studies have added a fourth trace alloying element to the zinc aluminum magnesium coating to form a quaternary alloy for better performance. This article prepared four different compositions of Zn-Al-Mg alloy ingots with trace amounts of Er added by induction melting, including 1 #: Zn-1.7% Al-1.1% Mg-0.1% Er, 2 #: Zn-1.7% Al-1.1% Mg-0.5%

Er, 3 #: Zn-7% Al-2% Mg-0.1% Er, and 4 #: Zn-7% Al-2% Mg-0.5% Er. Four compositions of alloys were melted in a heating furnace with argon gas protection atmosphere and solidification experiments were carried out under water cooling conditions to obtain the solidification structure. The solidification structure and corrosion behavior of Zn-Al-Mg alloy with Er addition were studied through microstructure characterization and electrochemical testing. The type of precipitation of Er compounds was predicted through phase diagram calculation. The microstructure and phase types of the alloy were analyzed using scanning electron microscopy (SEM), electron probe microanalysis (EPMA), and field emission scanning electron microscopy (JSM-7001F). With the addition of Er, the solidification structure of the alloy has been refined to a certain extent. From energy spectrum analysis, the precipitated compound system $\text{Er}_2\text{Zn}_{17}$ has a density greater than that of zinc liquid, which may generate bottom slag in actual hot dip plating processes, which needs to be comprehensively considered. Finally, electrochemical testing was conducted on various alloy samples using electrochemical methods. The Tafel polarization curve test results and AC impedance spectrum test results show that the corrosion resistance of low aluminum and low magnesium alloys added with Er is still generally lower than that of magnesium products in medium aluminum. For similar samples, the addition of Er is beneficial for improving corrosion resistance. Based on the possible surface quality issues and the generation of zinc slag in actual products, the effect of Er addition needs further evaluation. At present, there is little research on the microstructure and properties of quaternary alloys containing Er. Therefore, studying the influence of Er content on the microstructure and properties of alloys is of great significance.

Keywords Er containing zinc aluminum magnesium alloy; Solidification structure; Corrosion resistance; $\text{Er}_2\text{Zn}_{17}$

79. Deterioration corrosion of steel affected by *Shewanella algae* under degradation and transformation of oil in marine rust layer

Deterioration corrosion of steel affected by *Shewanella algae* under degradation and transformation of oil in marine rust layer

Ding Guo^{1,2,3,4}, Jizhou Duan^{1,2,4,*}, Yimeng Zhang^{1,2,4}

¹ *Key Laboratory of Marine Environmental Corrosion and Biofouling, Institute of Oceanology, Chinese Academy of Sciences, No.7 Nanhai Road, 266071, Qingdao, China*

² *Open Studio for Marine Corrosion and Protection, Pilot National Laboratory for Marine Science and Technology (Qingdao), No.168 Wenhazhong Road, Qingdao, China*

³ *University of Chinese Academy of Sciences, No. 380 Huaibeizhen Road, Beijing, 101408, China*

⁴ *Center for Ocean Mega-Science, Chinese Academy of Sciences, No.7 Nanhai Road, Qingdao, 266071, China*

*Email: duanjz@qdio.ac.cn (J.z. Duan)

Abstract Nearshore oil hydrocarbon pollution, offshore oil spill, marine oil and gas development and utilization would all let metal materials that will be used in oil-water environment exposed to the risk of corrosion damage by synergistic effects of microorganisms and marine environment. Microbial corrosion in oilfield environment is up to 50% of corrosion loss, and crude oil mainly affects corrosion damage of metal materials through affecting microbial activities. Crude oil exposure increases the abundance of hydrocarbon-degrading microorganisms in seawater and steel rust layers, and the nitrate reduction and petroleum degradation functions of microorganisms play a critical role in the microbial deterioration corrosion processes of metal materials, especially for long-term anaerobic corrosion by sulfate reducing bacteria. According to the microbial cell extraction and microbial diversity analysis of

the rust layer, *Shewanella* sp. was found to exist in the X70 steel rust layer exposed to marine oil-water environment for a long period, and belongs to the dominant microorganism closely related to the long-term evolution mechanisms of steel corrosion products. A strain of *Shewanella algae* with oil degradation function was purified using the aerobic mineral salt solid agar plate from the rust layer, which could catalyze the coupling processes of oxidation acid-producing of oil and X70 steel pitting corrosion with oil as sole carbon source and iron ion as energy source. The degradation substrates of *S. algae* are diverse, and the morphological expression of flagellum and cilia on the cell membrane surface may form a tight metabolic relationship between cells and between cells and iron minerals. In water layers containing oil, the humic acid and oil species and content are related to the biofilm formation and surface adhesion of *S. algae* in the deterioration corrosion system. And the conversion of nitrogen containing compounds in petroleum and the deposition of C and P elements on surface of X70 steel show the potential of microorganisms to inhibit metal corrosion. As a facultative anaerobic microorganism, *S. algae* also functions in degradation of anaerobic petroleum hydrocarbons, and may play a significant role in the interface of aerobic and anaerobic rust layers in the long-term oil-water immersion corrosion of steel materials.

Keywords *Shewanella algae*; Deterioration corrosion; Oil degradation; Microbial corrosion; Rust layer mineral

Reference

- Yimeng Z, Xiaofan Z, Fang G, Xucheng D, Jiawen S, Ruiyong Z, Jizhou D, Binbin Z, Baorong H. Microbiologically influenced corrosion of steel in coastal surface seawater contaminated by crude oil [J]. npj Materials Degradation, 2022, 6(35):1-12.
- Ding G, Yimeng Z, Xucheng D, Xiangju L, Yingying P, Jizhou D, Fang G. Accelerated deterioration corrosion of X70 steel by oxidation acid-producing process catalyzed by *Acinetobacter soli* in oil-water environment [J]. Bioelectrochemistry, 2023, 154:108539.

80. Electrochemical behaviour of corrosion products and their effect on structural alloy in molten fluoride salt

Electrochemical behaviour of corrosion products and their effect on structural alloy in molten fluoride salt

Hua Ai¹, Xiang-Xi Ye¹, Miao Shen¹

¹ *Shanghai Institute of Applied Physics, Chinese Academy of Sciences, Shanghai 201800, China*

E-mail address: aihua@sinap.ac.cn

Abstract Molten Salt Reactor (MSR), one of the candidate reactor of the “International Generation IV Nuclear Reactors”, adopts molten fluoride salt as the fuel carrier and heat transfer media [1-3]. The molten fluoride salt circulates in the reactor core and circuit piping at 600°C ~ 700°C. However, the strong corrosivity of molten fluoride salt is a challenge to structural materials [4-9], threatening the safe operation of MSRs. In practice, sparging a gas mixture of H₂ and HF is used to purify the molten fluoride salt to reduce its corrosivity [10]. Meanwhile, purification treatment in the metallic containers and the corrosion of metallic materials during the operation of MSRs both can introduce metallic fluorides [11, 12]. Iron fluorides are the common corrosion products, and their electrochemical behaviour is crucial to the properties of molten fluoride salt. We experimentally found that relatively high concentration of iron ions in LiF-NaF-KF (FLiNaK) salt results in the deposition of metallic Fe on the alloy surface [13, 14]. Accordingly, the chemical valence state of iron fluorides was analyzed through high-temperature ultraviolet-visible (UV-vis) absorption spectroscopy, results suggest that Fe(II) is unstable and gets converted to more stable Fe (III) through the disproportionation reaction: $3\text{Fe (II)} = 2\text{Fe (III)} + \text{Fe}$ in FLiNaK salt [15]. The electrochemical behaviour of iron ions was studied through CV and SWV. The conversion ratio of Fe (II) to Fe (III) in molten FLiNaK salt was approximately 81.9% by calculation. Based on above chemical valence state analysis, the corrosivity of iron fluorides on structural alloy was investigated and elaborated.

The corrosion of Ni-based alloy in molten FLiNaK salt was aggravated by iron fluorides due to the redox reaction: $\text{Fe (III)} + \text{Cr} = \text{Fe} + \text{Cr (III)}$, resulting in the formation of the Cr-depletion layer and Fe-rich layer [14, 15].

Keywords Molten salts; Molten salt reactor; Corrosion products; Electrochemical analysis; High temperature corrosion

Reference

- [1] J.F. R. Serrano-López, S. Cuesta-López, Molten salts database for energy applications, *Chemical Engineering and Processing*, 14 (2013) 1-29.
- [2] H. Boussier, S. Delpéch, V. Ghetta, D. Heuer, D.E. Holcomb, V. Ignatiev, E. Merle-Lucotte, J. Serp, The Molten Salt Reactor in Generation IV: Overview and Perspectives, in: *Generation4 International Forum Symposium*, 2012.
- [3] D. Leblanc, Molten salt reactors: A new beginning for an old idea, *Nuclear Engineering & Design*, 240 (2009) 1644-1656.
- [4] H. Ai, M. Shen, H. Sun, K.P. Dolan, C. Wang, M. Ge, H. Yin, X. Li, H. Peng, N. Li, L. Xie, Effects of O^{2-} additive on corrosion behavior of Fe–Cr–Ni alloy in molten fluoride salts, *Corrosion Science*, 150 (2019) 175-182.
- [5] S.S. Raiman, S. Lee, Aggregation and data analysis of corrosion studies in molten chloride and fluoride salts, *Journal of Nuclear Materials*, 511 (2018) 523-535.
- [6] S. Guo, J. Zhang, W. Wu, W. Zhou, Corrosion in the molten fluoride and chloride salts and materials development for nuclear applications, *Progress in Materials Science*, 97 (2018) 448-487.
- [7] H. Ai, J. Hou, X.-X. Ye, C.L. Zeng, H. Sun, X. Li, G. Yu, X. Zhou, J.-Q. Wang, Influence of graphite-alloy interactions on corrosion of Ni-Mo-Cr alloy in molten fluorides, *Journal of Nuclear Materials*, 503 (2018) 116-123.
- [8] G. Zheng, K. Sridharan, Corrosion of Structural Alloys in High-Temperature Molten Fluoride Salts for Applications in Molten Salt Reactors, *Jom*, 70 (2018) 1535-1541.
- [9] K.M. Sankar, P.M. Singh, Effect of oxide impurities on the corrosion behavior of structural materials in molten LiF-NaF-KF, *Corrosion Science*, 206 (2022) 110473.

- [10] G. Zong, Z.-B. Zhang, J.-H. Sun, J.-C. Xiao, Preparation of high-purity molten FLiNaK salt by the hydrofluorination process, *Journal of Fluorine Chemistry*, 197 (2017) 134-141.
- [11] H. Yin, J. Qiu, H. Liu, W. Liu, Y. Wang, Z. Fei, S. Zhao, X. An, J. Cheng, T. Chen, P. Zhang, G. Yu, L. Xie, Effect of CrF₃ on the corrosion behaviour of Hastelloy-N and 316L stainless steel alloys in FLiNaK molten salt, *Corrosion Science*, 131 (2018) 355-364.
- [12] W. Xue, X. Yang, J. Qiu, H. Liu, B. Zhao, H. Xia, X. Zhou, P. Huai, H. Liu, J. Wang, Effects of Cr³⁺ on the corrosion of SiC in LiF–NaF–KF molten salt, *Corrosion Science*, 114 (2017) 96-101.
- [13] H. Ai, S. Liu, X.-X. Ye, L. Jiang, B. Zhou, X. Yang, B. Leng, Z. Li, Metallic impurities induced corrosion of a Ni-26W-6Cr alloy in molten fluoride salts at 850 °C, *Corrosion Science*, 178 (2021) 109079.
- [14] H. Ai, X.-X. Ye, L. Jiang, B. Leng, M. Shen, Z. Li, Y. Jia, J.-Q. Wang, X. Zhou, Y. Xie, L. Xie, On the possibility of severe corrosion of a Ni-W-Cr alloy in fluoride molten salts at high temperature, *Corrosion Science*, 149 (2019) 218-225.
- [15] H. Ai, Y. Liu, M. Shen, H. Liu, Y. Chen, X. Yang, H. Liu, Y. Qian, J. Wang, Dissolved valence state of iron fluorides and their effect on Ni-based alloy in FLiNaK salt, *Corrosion Science*, 192 (2021) 109794.

81. How to estimate the stable pitting transition according to the electrochemical noise transient

How to estimate the stable pitting transition according to the electrochemical noise transient

Wei Liu

School of Physics and Electronic Information Engineering, NingXia Normal University, Guyuan 756000, People's Republic of China

Liuwei_0043@163.com

Abstract Some approach or parameters were employed to indicate the state of stable pitting such as the energy distribution obtained by the wavelet analysis or the Hilbert spectra, the recurrence quantitative parameters obtained from the recurrence analysis, and the noise resistance as well in the electrochemical noise analysis. The pitting current density may be the key parameter for the stable pitting estimation which determined the dissolution-diffusion sustainable dynamic balance in the pit according to the theoretical framework proposed by Li, Scully, and Frankel. While the critical pit stable product defined the accumulative effect under the high pitting current density. The pitting current growth rate as well as its cumulative time was adopted to indicate the stable pitting transition according to the electrochemical current transient analysis in the stainless steel pitting process, which may provide the quantitative indicator agreed with the theoretical framework.

Keywords Electrochemical noise; Stable pitting; Pitting current growth rate; Stainless steel

Reference

- [1] Z. Zhang, X. Li, Z. Zhao, et al. In-situ monitoring of pitting corrosion of Q235 carbon steel by electrochemical noise: Wavelet and recurrence quantification analysis[J]. *Journal of Electroanalytical Chemistry*, 2020, 879: 114776.
- [2] L. Xie, W. Zhou, S. Zou. Pitting behavior of Ti-15-3 titanium alloy with different surface in salt spray studied using electrochemical noise[J]. *Journal of Materials Research and Technology*, 2021, 14: 2865-2883.
- [3] C. Wang, Y. Cai, C. Ye, et al. In situ monitoring of the localized corrosion of 304 stainless steel in FeCl₃ solution using a joint electrochemical noise and scanning reference electrode technique[J]. *Electrochemistry Communications*, 2018, 90: 11-15.
- [4] Y. Zhao, E. Zhou, D. Xu, et al. Laboratory investigation of microbiologically influenced corrosion of 2205 duplex stainless steel by marine *Pseudomonas aeruginosa* biofilm using electrochemical noise[J]. *Corrosion Science*, 2018, 143: 281-291.
- [5] M.N. Bajestani, J. Neshati, M.H. Siadati. Development of time-frequency analysis

in electrochemical noise for detection of pitting corrosion[J]. *Corrosion*, 2019, 75(2): 183-191.

[6] Z. Zhang, X. Wu, J. Tan. Laboratory-scale identification of corrosion mechanisms by a pattern recognition system based on electrochemical noise measurements[J]. *Journal of The Electrochemical Society*, 2019, 166(12): C284.

[7] M.A. Amin. Metastable and stable pitting events on Al induced by chlorate and perchlorate anions—Polarization, XPS and SEM studies[J]. *Electrochimica acta*, 2009, 54(6): 1857-1863.

[8] M.H. Moayed, R.C. Newman. Evolution of current transients and morphology of metastable and stable pitting on stainless steel near the critical pitting temperature[J]. *Corrosion science*, 2006, 48(4): 1004-1018.

[9] Y. Tang, N. Dai, J. Wu, et al. Effect of surface roughness on pitting corrosion of 2205 duplex stainless steel investigated by electrochemical noise measurements[J]. *Materials*, 2019, 12(5): 738.

[10] T. Li, J.R. Scully, G.S. Frankel. Localized corrosion: passive film breakdown vs pit growth stability: part v. validation of a new framework for pit growth stability using one-dimensional artificial pit electrodes[J]. *Journal of The Electrochemical Society*, 2019, 166(11): C3341.

82. Corrosion behavior of pure metals (Ni and Ti) and alloys (316H SS and GH3535) in liquid GaInSn

Corrosion behavior of pure metals (Ni and Ti) and alloys (316H SS and GH3535) in
liquid GaInSn

Jianhui Yu^{1,2}, Hongxia Xu², Xiangxi Ye², Bin Leng², Hanxun Qiu¹, Xingtai Zhou²

¹ *School of Materials and Chemistry, University of Shanghai for Science and
Technology, Shanghai 200093, China*

² *Shanghai Institute of Applied Physics, Chinese Academy of Sciences, Shanghai
201800, China*

Abstract In this study, the interactions between a Ga-based liquid metal (GLM)-GaInSn and some metal materials, including pure metals (Ni and Ti) as well as alloys (316H stainless steel (SS) and GH3535), at 650 °C were investigated. The goal was to evaluate their corrosion performance and select a suitable candidate material for use as a molten salt manometer diaphragm in a thermal energy storage system. The results indicate that the alloys (316H SS and GH3535) exhibited less corrosion in the liquid GaInSn, relative to the pure metals (Ni and Ti). For all the tested materials exposed to the liquid GaInSn, Ga-rich binary intermetallic compounds (IMCs) were found to form on the surface of the metal materials as a result of the decomposition of the liquid GaInSn and the reaction with the constituent elements of the metal materials. The corrosion mechanism for all tested materials exposed to the liquid GaInSn is also discussed and proposed, which may aid in selecting the optimal candidate material when liquid GaInSn is used as the pressure sensing medium.

Keywords Metal materials, liquid GaInSn, Corrosion, Intermetallic compounds, thermal energy storage system

Reference

- [1] H. Wang, S. Chen, B. Yuan, et al., Liquid Metal Transformable Machines. *Accounts Mater. Res.* 2(12), 1227-1238 (2021). <https://doi.org/10.1021/accountsmr.1c00182>
- [2] Q. Wang, C. Pan, Y. Zhang, et al., Magnetoactive liquid-solid phase transitional matter. *Matter* 6(3), 855-872 (2023). <https://doi.org/10.1016/j.matt.2022.12.003>
- [3] R. Matsuzaki, K. Tabayashi, Highly Stretchable, Global, and Distributed Local Strain Sensing Line Using GaInSn Electrodes for Wearable Electronics. *Adv. Funct. Mater.* 25(25), 3806-3813 (2015). <https://doi.org/10.1002/adfm.201501396>
- [4] Y. Sohn, K. Chu, Flexible hybrid conductor comprising eutectic Ga-In liquid metal and Ag nanowires for the application of electronic skin. *Mater. Lett.* 265,

- 127223 (2020). <https://doi.org/10.1016/j.matlet.2019.127223>
- [5] M. Zhang, S. Yao, W. Rao, et al., Transformable soft liquid metal micro/nanomaterials. *Mater. Sci. Eng. R-Rep.* 138, 1-35 (2019). <https://doi.org/10.1016/j.mser.2019.03.001>
- [6] Y. Lin, J. Genzer, M.D. Dickey, Attributes, Fabrication, and Applications of Gallium-Based Liquid Metal Particles. *Adv. Sci.* 7(12), 2000192 (2020). <https://doi.org/10.1002/advs.202000192>
- [7] M.D. Dickey, Stretchable and Soft Electronics using Liquid Metals. *Adv. Mater.* 29(27), 1606425 (2017). <https://doi.org/10.1002/adma.201606425>
- [8] J. Tounonen, M. Männistö, D. Richon, et al., Application of GaInSn Liquid Metal Alloy Replacing Mercury in a Phase Equilibrium Cell: Vapor Pressures of Toluene, Hexylbenzene, and 2-Ethyl-naphthalene. *J. Chem. Eng. Data* 65(7), 3270-3276 (2020). <https://doi.org/10.1021/acs.jced.9b01208>
- [9] D.-H. Kim, J.A. Rogers, Stretchable Electronics: Materials Strategies and Devices. *Adv. Mater.* 20(24), 4887-4892 (2008). <https://doi.org/10.1002/adma.200801788>
- [10] N.B. Morley, J. Burris, L.C. Cadwallader, et al., GaInSn usage in the research laboratory. *Rev. Sci. Instrum.* 79(5), 056107 (2008). <https://doi.org/10.1063/1.2930813>
- [11] G. Yun, S.-Y. Tang, S. Sun, et al., Liquid metal-filled magnetorheological elastomer with positive piezoconductivity. *Nat. Commun.* 10(1), 1300 (2019). <https://doi.org/10.1038/s41467-019-09325-4>
- [12] T. Daeneke, K. Khoshmanesh, N. Mahmood, et al., Liquid metals: fundamentals and applications in chemistry. *Chem. Soc. Rev.* 47(11), 4073-4111 (2018). <https://doi.org/10.1039/C7CS00043J>
- [13] Q. Li, B.-D. Du, J.-Y. Gao, et al., Liquid metal gallium-based printing of Cu-doped p-type Ga₂O₃ semiconductor and Ga₂O₃ homojunction diodes. *Appl. Phys. Rev.* 10(1), 011402 (2023). <https://doi.org/10.1063/5.0097346>
- [14] Q. Li, B.-D. Du, J.-Y. Gao, et al., Room-Temperature Printing of Ultrathin Quasi-2D GaN Semiconductor via Liquid Metal Gallium Surface Confined

- Nitridation Reaction. *Adv. Mater. Technol.* 7(11), 2200733 (2022).
<https://doi.org/10.1002/admt.202200733>
- [15] Q. Zhang, Y. Zheng, J. Liu, Direct writing of electronics based on alloy and metal (DREAM) ink: A newly emerging area and its impact on energy, environment and health sciences. *Front. Energy* 6(4), 311-340 (2012).
<https://doi.org/10.1007/s11708-012-0214-x>
- [16] X. He, T. Xuan, J. Wu, et al., Flexible and Stretchable Elastomer Composites Based on Lightweight Liquid Metal Foam Spheres with Pod-like Contacts. *ACS Appl. Mater. Interfaces* 15(4), 5856-5869 (2023). <https://doi.org/10.1021/acsami.2c19621>
- [17] J.-H. So, J. Thelen, A. Qusba, et al., Reversibly Deformable and Mechanically Tunable Fluidic Antennas. *Adv. Funct. Mater.* 19(22), 3632-3637 (2009).
<https://doi.org/10.1002/adfm.200900604>
- [18] A. AlHazzaa, N. Haneklaus, Diffusion Bonding and Transient Liquid Phase (TLP) Bonding of Type 304 and 316 Austenitic Stainless Steel—A Review of Similar and Dissimilar Material Joints. *Metals* 10(5), 613 (2020).
<https://doi.org/10.3390/met10050613>
- [19] F. Alnaimat, Y. Rashid, Thermal Energy Storage in Solar Power Plants: A Review of the Materials, Associated Limitations, and Proposed Solutions. *Energies* 12(21), 4164 (2019). <https://doi.org/10.3390/en12214164>
- [20] W. Ding, A. Bonk, T. Bauer, Corrosion behavior of metallic alloys in molten chloride salts for thermal energy storage in concentrated solar power plants: A review. *Front. Chem. Sci. Eng.* 12(3), 564-576 (2018).
<https://doi.org/10.1007/s11705-018-1720-0>
- [21] A. Ravi Shankar, S. Mathiya, K. Thyagarajan, et al., Corrosion and Microstructure Correlation in Molten LiCl-KCl Medium. *Metall. Mater. Trans. A-Phys. Metall. Mater. Sci.* 41(7), 1815-1825 (2010).
<https://doi.org/10.1007/s11661-010-0223-5>
- [22] H. Li, X. Yang, X. Yin, et al., Effect of Chloride Impurity on Corrosion Kinetics of Stainless Steels in Molten Solar Salt for CSP Application: Experiments and

- Modeling. Oxid. Met. 95(3), 311-332 (2021).
<https://doi.org/10.1007/s11085-021-10025-y>
- [23] E. Hamdy, J.N. Olovsson, C. Geers, Perspectives on selected alloys in contact with eutectic melts for thermal storage: Nitrates, carbonates and chlorides. *Sol. Energy* 224, 1210-1221 (2021). <https://doi.org/10.1016/j.solener.2021.06.069>
- [24] W. Ren, G. Muralidharan, D.F. Wilson, et al., Considerations of Alloy N for Fluoride Salt-Cooled High-Temperature Reactor Applications. Paper presented at ASME 2011 Pressure Vessels and Piping Conference (Baltimore, Maryland, USA, July 17-21, 2011)
- [25] J. Serp, M. Allibert, O. Beneš, et al., The molten salt reactor (MSR) in generation IV: Overview and perspectives. *Prog. Nucl. Energy* 77, 308-319 (2014).
<https://doi.org/10.1016/j.pnucene.2014.02.014>
- [26] L.C. Olson, J.W. Ambrosek, K. Sridharan, et al., Materials corrosion in molten LiF–NaF–KF salt. *J. Fluorine Chem.* 130(1), 67-73 (2009).
<https://doi.org/10.1016/j.jfluchem.2008.05.008>
- [27] X.-X. Ye, H. Ai, Z. Guo, et al., The high-temperature corrosion of Hastelloy N alloy (UNS N10003) in molten fluoride salts analysed by STXM, XAS, XRD, SEM, EPMA, TEM/EDS. *Corros. Sci.* 106, 249-259 (2016).
<https://doi.org/10.1016/j.corsci.2016.02.010>
- [28] L. Jiang, X.-X. Ye, D.-J. Wang, et al., Synchrotron radiation-based materials characterization techniques shed light on molten salt reactor alloys. *Nucl. Sci. Tech.* 31(1), 6 (2019). <https://doi.org/10.1007/s41365-019-0719-7>
- [29] F. Barbier, J. Blanc, Corrosion of martensitic and austenitic steels in liquid gallium. *J. Mater. Res.* 14(3), 737-744 (1999).
<https://doi.org/10.1557/JMR.1999.0099>
- [30] S.H. Shin, J.J. Kim, J.A. Jung, et al., A study on corrosion behavior of austenitic stainless steel in liquid metals at high temperature. *J. Nucl. Mater.* 422(1), 92-102 (2012). <https://doi.org/10.1016/j.jnucmat.2011.12.007>
- [31] J. Guo, J. Cheng, H. Tan, et al., Ga-based liquid metal: Lubrication and corrosion

behaviors at a wide temperature range. *Materialia* 4, 10-19 (2018).
<https://doi.org/10.1016/j.mtla.2018.09.007>

[32] R.W. Cahn, *Binary Alloy Phase Diagrams*—Second edition. *Adv. Mater.* 3(12), 628-629 (1991). <https://doi.org/10.1002/adma.19910031215>

[33] E.M. Summers, T.A. Lograsso, M. Wun-Fogle, Magnetostriction of binary and ternary Fe–Ga alloys. *J. Mater. Sci.* 42(23), 9582-9594 (2007).
<https://doi.org/10.1007/s10853-007-2096-6>

[34] A. Belgacem-Bouzida, Y. Djaballah, M. Notin, Calorimetric measurement of the intermetallic compounds Cr₃Ga and CrGa₄ and thermodynamic assessment of the (Cr–Ga) system. *J. Alloys Compd.* 397(1), 155-160 (2005).
<https://doi.org/10.1016/j.jallcom.2005.01.026>

[35] Y. Cui, F. Liang, S. Xu, et al., Interfacial wetting behaviors of liquid Ga alloys/FeGa₃ based on metallic bond interaction. *Colloid Surf. A-Physicochem. Eng. Asp.* 569, 102-109 (2019). <https://doi.org/10.1016/j.colsurfa.2019.01.079>

[36] S.P. Yatsenko, N.A. Sabirzyanov, A.S. Yatsenko, Dissolution rates and solubility of some metals in liquid gallium and aluminum. *J. Phys. Conf. Ser.* 98(6), 062032 (2008). <https://doi.org/10.1088/1742-6596/98/6/062032>

[37] Y. Miyakawa, M. Kondo, Corrosion behaviors of various steels and nickel-based alloys in liquid Sn media. *Nucl. Mater. Energy* 30, 101154 (2022).
<https://doi.org/10.1016/j.nme.2022.101154>

[38] O. Nishikawa, A.R. Saadat, Field emission and field ion microscope study of Ga, In and Sn on W: Structure, work function, diffusion and binding energy. *Surf. Sci.* 60(2), 301-324 (1976). [https://doi.org/10.1016/0039-6028\(76\)90319-8](https://doi.org/10.1016/0039-6028(76)90319-8)

[39] A.R. Saadat, Activation energies for surface diffusion and polarizabilities of gallium, indium and tin on a molybdenum surface. *J. Phys. D: Appl. Phys.* 27(2), 356 (1994). <https://doi.org/10.1088/0022-3727/27/2/026>

[40] S.P. Yatsenko, Y.A. Anikin, Solubility of metals of the fifth period in liquid gallium. *Mater. Sci.* 6(3), 333-337 (1973). <https://doi.org/10.1007/BF00720616>

[41] J. Guo, J. Cheng, S. Wang, et al., A Protective FeGa₃ film on the steel surface

prepared by in-situ hot-reaction with liquid metal. Mater. Lett. 228, 17-20 (2018).
<https://doi.org/10.1016/j.matlet.2018.05.111>

83.Preparation and performance study of environmentally responsive microencapsulated self-healing coatings

Preparation and performance study of environmentally responsive microencapsulated self-healing coatings

Shudi Zhang^{1,*}, Xinya Wei¹, Jialin Dong¹, Jiahui Bing¹, Linkun Liu¹ and Tao Zhang^{2,*}

¹*School of Environmental and Chemical Engineering, Shenyang Ligong*

University, Shenyang 110159, China

²*Chinese Academy of Sciences (Shenyang) Metal Research, Shenyang 110016, China*

zhangshudi@163.com(S.Z.); zhangtao@mail.neu.edu.cn(T.Z.)

Abstract Environmentally responsive self-repairing coating is a kind of coating with self-repairing function when the surface coating film is damaged. In this paper, the solvent evaporation method was used to prepare slow-release agent microcapsules, which were added into the anticorrosion coating based on E-51 epoxy resin and matching curing agent to obtain the self-repairing anticorrosion coating. The self-repairing anti-corrosion performance of the coating was characterized and evaluated by optical microscopy, scanning electron microscopy, thermogravimetric analysis, Fourier infrared spectroscopy, etc. The self-repairing anti-corrosion performance of the coating was also analyzed by the mechanical property test, the corrosive solution immersion test as well as the electrochemical polarization curves and the AC impedance test. The results showed that when the core-wall mass ratio was 1.2:1, the stirring rate was 800 r/min, and the temperature was 38 °C was the optimal process conditions for synthesizing microcapsules. The coating with microcapsules has obvious signs of healing, and the current density is of a lower order of magnitude, and the impedance modulus is large indicating better corrosion resistance.

Keywords Environmental response; Self-healing; Microcapsule; Epoxy resin

Reference

- [1] HE Z, JIANG.S, LI Q, et al. Facile and cost-effective synthesis of isocyanate microcapsules via polyvinylalcohol-mediated interfacial polymerization and their application in self-healing materials[J]. *Composites Science and Technology*,2017, 138: 15-23.
- [2] Zhu D Y, Rong M Z, Zhang M Q. Self-healing polymeric materials based on microencapsulated healing agents: From design to preparation[J]. *Progress in Polymer Science*, 2015, 49: 175-220.
- [3] Patrick J F, Robb M J, Sottos N R, et al. Polymers with autonomous lifecycle control[J]. *Nature*, 2016, 540 (7633):363-370.
- [4] Zheng N, Qiao L, Liu J, et al. Microcapsules of multilayered shell structure synthesized via one-part strategy and their application in self-healing coatings[J]. *Composites Communications*, 2019, 12: 26-32.
- [5] YUAN L, LIANG G, XIE J, et al. Preparation and Characterization of Poly (Urea-formaldehyde) Microcapsules Filled with Epoxy Resins[J]. *Polymer*, 2006, 47(15): 5338—5349.
- [6] YUAN L, LIANG G Z, XIE J Q, et al. The Permeability and Stability of Microencapsulated Epoxy Resins[J]. *Journal of Materials Science*, 2007, 42(12): 4390—4397.
- [7] Wang Jixing, Tang Junlei, Zhang Hailong, et al. A CO₂-re-sponsive anti corrosion ethyl cellulose coating based on the pH-response mechanism [J]. *Corrosion Science*, 2021, 180.109194.
- [8] Bai Z H, Sun Y, Li C, et al. Novel intelligent self-responsive function fillers to enhance the durable anticorrosion performance of epoxy coating[J]. *Progress in Organic Coatings*, 2022, 170: 106963.
- [9] Zhu Q S, Zhang K, Huang Y X, et al. Hydrothermally synthesized ZnO-reduced grapheneoxide nanocomposite for enhanced anticorrosion performance of waterborne epoxy coating[J]. *Journal of Nanostructure in Chemistry*, 2022, 12 (2): 277-289.

[10] Cai Y H, Meng F D, Liu L, et al. The effect of the modification of mica by high-temperature mechanochemistry on the anticorrosion performance of epoxy coatings[J]. *Polymers*, 2021, 13 (3): 378.

84. 6061 galvanic corrosion behavior in simulated seawater

6061 galvanic corrosion behavior in simulated seawater

Shudi Zhang^{1,*}, Wenkang Jing¹, Shuyan Zhao², Hang Song¹, Yong Guan^{2*}

¹*School of Environmental and Chemical Engineering, Shenyang Ligong*

University, Shenyang 110159, China;

²*Chinese Academy of Sciences (Shenyang) Metal Research, Shenyang 110016, China*

zhangshudi@163.com(S.Z.); yguan@imr.ac.cn(T.Z.)

Abstract 6061 aluminum alloy is a material commonly used in Marine equipment. 6061 aluminum alloy is a material commonly used in Marine equipment. The galvanic corrosion behavior of 6061 aluminum alloy in simulated seawater was studied by electrochemical method and surface analysis technique. The results show that when aluminum alloy is used in contact with metal, it is usually anode, and the coupling contact accelerates the pitting process, and the acceleration tendency of galvanic corrosion becomes more serious with the increase of potential difference and surface area of contact metal. The galvanic corrosion behavior of 6061 aluminum alloy in simulated seawater was studied by electrochemical method and surface analysis technique. The results show that when aluminum alloy is used in contact with metal, it is usually anode, and the coupling contact accelerates the pitting process, and the acceleration tendency of galvanic corrosion becomes more serious with the increase of potential difference and surface area of contact metal.

Key words galvanic corrosion; Aluminum alloy; EIS

Reference

- [1] WANG L, XUAN W F, MOU X L. Corrosion characteristics of 2A11 aluminum alloy/carbon steel coupling under enhanced natural environment [J]. Surface technology, 2011, 40(5): 1-4.
- [2] SHI P A, SHUAI M B, LIU D X, et al. The influence factors of galvanic corrosion study [J]. Journal of weapon materials science and engineering, 2013, 4 (5) : 68-73. .
- [3] YAO X, CAI C, LI J F, et al. Planar distribution of galvanic corrosion between 5383 aluminum alloy and 907 steel and aluminum bronze[J]. Corrosion Science and Protection Technology, 2015, 27(05): 419-424
- [4] LIU Y, SHI Y, LI N, et al. Galvanic corrosion behavior of 5083 aluminum alloy and 2205 stainless steel in natural seawater [J]. Corrosion and Protection, 2012, 33(06): 532-534.
- [5] WANG S S, YANG L, XIAO K, et al. Galvanic corrosion of anodized 6061 aluminum alloy in an industrial-marine atmospheric environment [J]. J. Chin. Eng., 2018, 40: 833
- [6] Ma J L, Wen J B, Lu X W et al. Study on electrochemical impedance spectroscopy of Aluminum alloy anode corrosion process [J]. Corrosion and Protection, 2009, 30(06): 373-376.
- [7] ZHANG Z Q, CHEN Z B, DONG Q J, et al. Study on galvanic corrosion behavior of low alloy steel, stainless steel and aluminum-magnesium alloy in simulated deep sea environment [J]. Chinese Journal of Corrosion and Protection, 2022(003): 042
- A. Ruiz-Garcia, V. Esquivel-Peña, J. Genesca, R. Montoya. Advances in galvanic corrosion of aluminum alloys. [J] Electrochimica Acta, 2023, 449 (5), 142227.

85. Anisotropic Corrosion and Discharge behavior of Mg-Y Binary Alloys with High Rare Earth Content in Natural Seawater

Anisotropic Corrosion and Discharge behavior of Mg-Y Binary Alloys with High

Rare Earth Content in Natural Seawater

Quantong Jiang^{1,2}, Siwei Wu^{1,2}, Jizhou Duan^{1,2}, Baorong Hou^{1,2}

¹ CAS Key Laboratory of Marine Environmental Corrosion and Bio-fouling, Institute of Oceanology, Chinese Academy of Sciences, No. 7 Nanhai Road, Qingdao, 266071, China

² Sanya Institute of Ocean Eco-Environmental Engineering, Zhenzhou Road, Sanya, 572000, China

Presenter's e-mail address: jiangquantong@qdio.ac.cn

Abstract Magnesium alloy anode materials for seawater battery were prepared by adding high content of yttrium element, multiple free forging and hot extrusion. The microstructure, crystallographic preferred orientation, electrochemical corrosion performance, environmental discharge performance and microscopic corrosion morphology in different directions of magnesium alloy anodes were studied. The results showed that the grain orientation of Mg-10Y and Mg-20Y alloys along the ED direction mainly consisted of (0 0 0 1) base plane, and the samples in TD direction and ED direction were mainly composed of (1 0-1 0) and (2-1-1 0) crystal planes, respectively. The different energy levels of dissimilar crystal planes lead to great differences in electrochemical stability and corrosion resistance. The electrochemical dissolution activity of (1 0-1 0) and (2-1-1 0) crystal plane was much larger than that of (0 0 0 1) base plane. The corrosion dissolution mechanism of magnesium alloys with high rare earth content was explained by different crystal surface activity models.

Keywords Corrosion, Discharge, Anisotropic, Magnesium alloy, Natural seawater

Reference

- [1]Sun C, Liu H, Wang C, et al. Anisotropy investigation of an ECAP-processed Mg-Al-Ca-Mn alloy with synergistically enhanced mechanical properties and corrosion resistance[J]. Journal of Alloys and Compounds, 2022, 911: 165046.
- [2] Xie Q, Ma A, Jiang J, et al. Tailoring the corrosion behavior and mechanism of AZ31 magnesium alloys by different Ca contents for marine application[J]. Corrosion

Science, 2021, 192: 109842.

[3] Gerashi E, Alizadeh R, Langdon T G. Effect of crystallographic texture and twinning on the corrosion behavior of Mg alloys: A review[J]. Journal of Magnesium and Alloys, 2022, 10(2): 313-325.

86. Mitigation of stress corrosion cracking of X80 steel induced by sulfate reducing *Desulfovibrio vulgaris* biofilm using THPS

Mitigation of stress corrosion cracking of X80 steel induced by sulfate reducing
Desulfovibrio vulgaris biofilm using THPS

Jike Yang^{1,2}, Junlei Wang³, Yuntian Lou^{1,2}, Yue Pan^{1,2}, Zhong Li^{1,2*}

¹*University of Science and Technology Beijing, Beijing 100083*

²*National Materials Corrosion and Protection Data Center, Beijing 100083*

³*Defense Engineering Institute, AMS, PLA Luoyang 471000 China*

ABSTRACT Microbiologically influenced corrosion (MIC) is a relative recent research area in corrosion field. The most common corrosive microorganism in MIC is sulfate reducing bacteria (SRB), *Desulfovibrio vulgaris*. Meanwhile, stress corrosion cracking (SCC) which induced by both applied stress on the metal and corrosive circumstance, always cause ruptures in industrial fields such as pipelines or storage tanks, leading to severe economic losses. The metabolic activities of *D. vulgaris* provides corrosion on metal surfaces. Disaster accident in the industry often occur when pipelines are subjected to both SCC and MIC. To solved this problem, biocide, such as Tetrakis hydroxymethyl phosphonium sulfate (THPS) was used to inhibit microbial growth. X80 pipeline steel is a widely used material for oil and gas pipelines which is susceptible to the both MIC and SCC. Hence, it is important to investigate the how to mitigate the SCC behavior of X80 steel induced by MIC under continuous mechanical stress, using X80 U-bend coupon which provide the continuous stress on the X80 steel. X80 U-bend coupons were immersed in ATCC

1249 culture medium (250 mL in 450 mL anaerobic bottles) inoculated with *D. vulgaris*. Following a 14-day incubation period of *D. vulgaris* in ATCC 1249 culture medium at 37 °C with X80 U-bend coupons, the weight losses results were 2.7 mg cm⁻² (0 ppm), 1.4 mg cm⁻² (15 ppm), 1.1 mg cm⁻² (30 ppm), 0.7 mg cm⁻² (45 ppm) and 0.5 mg cm⁻² (60 ppm), respectively. The sessile cell counts were 9.3×10⁷ cells cm⁻² (0 ppm), 3.9×10⁶ cells cm⁻² (15 ppm), 1.6×10⁶ cells cm⁻² (30 ppm), 3.0×10⁵ cells cm⁻² (45 ppm), 1.0×10⁵ cells cm⁻² (60 ppm) , respectively. The planktonic cell counts were 2.1×10⁶ cells mL⁻¹ (0 ppm), 2.8×10⁵ cells mL⁻¹ (15 ppm), 1.2×10⁵ cells mL⁻¹ (30 ppm), 5.0×10⁴ cells mL⁻¹ (45 ppm), 2.0×10⁴ cells mL⁻¹ (60 ppm) , respectively. The SEM images of cracking on the X80 U-bend illustrated that the cracks on the X80 U-bend that induced by *D. vulgaris* decreased with increasing THPS concentration. Open circuit potential (OCP), electrochemical impedance spectroscopy (EIS), linear polarization resistance (LPR), and potentiodynamic polarization results corroborated the increasing THPS concentration corresponding decreasing MIC rate, which mitigate the SCC activity of X80 steel. Meanwhile, depending on the theoretical calculation, the adsorption mechanism of THPS and X80 U-bend are both physical absorption and chemical absorption.

Key words Microbiologically influenced corrosion, Sulfate reducing bacteria, Stress corrosion cracking, THPS.

87. Study on hydrogen compatibility and influencing factors of hydrogen transport pipe

Study on hydrogen compatibility and influencing factors of hydrogen transport pipe

Ba Li^{1*}, Yu Hou², Jian Zheng², Bing Wang¹, Shujun Jia¹, Qingyou Liu¹

¹Central Iron and Steel Research Institute Co., Ltd., Beijing 100081 China

² Construction Project Management Branch of China National Petroleum Pipeline

Network Group Co., Ltd., Langfang 065000 China

Presenter's e-mail address: balicugb@sina.com

Abstract Hydrogen energy is a secondary energy source that meets the requirements of resources, the environment and sustainable development. Hydrogen transport is an essential part of hydrogen energy utilization, such as hydrogen production, hydrogen storage, hydrogen transport and hydrogen use, and pipeline transportation is the most economical and efficient transportation method. The research and development of hydrogen transport pipeline is a typical example of realizing the national "dual carbon" strategic goal through scientific and technological innovation. With the urgent need for safe long-distance and large-scale transport of hydrogen, there is a pressing need to investigate the compatibility of pure hydrogen and natural gas/hydrogen mixtures long-distance pipelines. In this paper, we focus on hydrogen-doped pipes with high steel grade and low hydrogen pressure, and pure hydrogen pipes with intermediate or low steel grade and high pressure. Partly research works on the safety evaluation of X80 hydrogen-containing pipelines for simulated coal-to-gas transmission and on the factors affecting the hydrogen brittle resistance of pure hydrogen pipelines were introduced, respectively. The results show that, for high-grade pipes in service, hydrogen compatibility tests should be performed before hydrogen mixing to prevent various defects from causing hydrogen damage during hydrogen mixing. Under the high-pressure hydrogen environment, the acicular ferrite microstructure had better hydrogen embrittlement resistance than the polygonal ferrite + bainite microstructure. Metallurgical defects such as large M/A constituent, strip microstructure, and MnS inclusions could lead to hydrogen damage in medium and low-grade pipe steel in different hydrogen pressure environments under stress coupling.

Keywords hydrogen transmission, hydrogen doped, pure hydrogen, hydrogen compatibility

88. Evading the Efficiency-Voltage Trade-off in Magnesium-Air Batteries

Evading the Efficiency-Voltage Trade-off in Magnesium-Air Batteries

Hongxing Liang¹, Liang Wu², Wenbo Du¹

¹ *Beijing University of Technology, 100 Pingleyuan, Chaoyang District, Beijing
100124, China.*

² *Chongqing University, No.174, Shapingba Street, Chongqing City, 400044, China.*

Presenter's e-mail address: hongxingliang@bjut.edu.cn

Abstract The magnesium-air (Mg-air) battery, known for its exceptional energy density and cost-effectiveness, holds the potential to revolutionize applications that conventional rechargeable batteries have yet to conquer [1]. This includes serving as range extenders for electric vehicles and powering long-range drones. However, the long-standing barrier of the efficiency-voltage trade-off has hindered its widespread adoption, impeding further advancements in energy density [2]. We surmounted this obstacle by pioneering a novel active learning framework specifically tailored to screen high performance magnesium anodes. The innovative framework integrates the physically interpretable variables, machine learning, Pareto front exploration, experimental feedback, and feedback from generated data. Within an extensive compositional space (~350,000 possibilities), we have pinpointed a novel anode, Mg-1Ga-1Ca-0.5In, with exceptional energy density ($2548 \pm 220 \text{ W h kg}^{-1}$). We have identified that the excellent performance of Mg-1Ga-1Ca-0.5In is attributed to the concept of "grain boundary activation" and "intra-grain inhibition". This concept stands apart from the conventional design concept commonly reported in existing studies, which primarily emphasize the influence of second phases on discharge behavior, with the impact of solute atoms on discharge behavior overlooked. We believe that our findings hold immense promise for the future of energy storage.

Keywords Magnesium anode; Corrosion; Machine learning; Theoretical calculation

References

- [1] Y. Li, J. Lu, Metal-air batteries: will they be the future electrochemical energy storage device of choice?, *ACS Energy Letters* 2(6) (2017) 1370-1377.
- [2] Z. Liu, J. Bao, J. Sha, Z. Zhang, Modulation of the discharge and corrosion properties of aqueous Mg-air batteries by alloying from first-principles theory, *The Journal of Physical Chemistry C* 127(21) (2023) 10062-10068.

89. Study on the influence of magnetic induction heating parameters on the temperature gradient of thermal-mechanical fatigue

Study on the influence of magnetic induction heating parameters on the temperature gradient of thermal-mechanical fatigue

Xie Bing^{1,2}, Hao Xuelong^{1,2}

¹*Guobiao(Beijing) Testing & Certification Co., Ltd, 11 Xingke East Street, Yanqi Economic Development Zone, Huairou District, Beijing 101407, China*

²*National Center of Analysis and Testing for Nonferrous Metals and Electronic Materials, General Research Institute for Nonferrous Metals, Beisanhuanzhong Road, Xicheng District, Beijing 100088, China*

xiebing@cutc.net, haoxuelong@gbtcgroup.com

Abstract The control of temperature gradient determines the accuracy of thermal-mechanical fatigue test results. There are no clear regulations on the types of magnetic induction coils, the distribution of thermocouples, and the definition of temperature gradients in the testing methods for thermal-mechanical fatigue both domestically and internationally. In this study, the individual and hybrid effects of different types of magnetic induction coils and the distribution of thermocouples on the temperature gradient of thermal-mechanical fatigue were investigated. Thermal strain and zero pressure tests are measured under different turns of the induction coil and spacing between thermocouples. The significant finding of this study is the effect law of magnetic induction heating parameters on the temperature gradient of thermomechanical fatigue.

Keywords thermal-mechanical fatigue, temperature gradient

Reference

[1] Huo Shiyu, Yan Qun, Gao Xiang. The influence of induction heating coil parameters on the temperature field of engine blades [J] Hot working process, 2018, 47 (18): 70-4

- [2] Chen Jingyang, Jing Fulei, Yang Junjie. Thermal-mechanical fatigue behavior and life modeling of nickel-based single crystal superalloys [J]. Journal of Aerodynamics, 2021,36 (05): 897-906
- [3] Sun J, Yuan H, Vormwald M. Thermal gradient mechanical fatigue assessment of a nickel-based superalloy[J]. International Journal of Fatigue, 2020, 135(Jun.):105486.1-105486.14.DOI:10.1016/j.ijfatigue.2020.105486.
- [4] Gao Shengyong, Wang Yiwen, Su Ru, Wu Dayong, Kang Jie, Bao Yanping. Low-Cycle Fatigue Behavior of GH4169 Superalloy. Chinese Journal of Rare Metals. 2022,46(3):289-296.
- [5] Li Jingnan, Dong Ruifeng, Chen Zishuai, Huang Dongnan, Qu Jinglong. Formability of Free Forging GH4720Li Superalloy with Different Gradient Heating Process. Chinese Journal of Rare Metals. 2022,46(2):162-168.

90.Study on hydrogen compatibility and influencing factors of hydrogen transport pipe

Study on hydrogen compatibility and influencing factors of hydrogen transport pipe

Ba Li^{1*}, Yu Hou², Jian Zheng², Bing Wang¹, Shujun Jia¹, Qingyou Liu¹

¹Central Iron and Steel Research Institute Co., Ltd., Beijing 100081 China

² Construction Project Management Branch of China National Petroleum Pipeline

Network Group Co., Ltd., Langfang 065000 China

Presenter's e-mail address: balicugb@sina.com

Abstract Hydrogen energy is a secondary energy source that meets the requirements of resources, the environment and sustainable development. Hydrogen transport is an essential part of hydrogen energy utilization, such as hydrogen production, hydrogen storage, hydrogen transport and hydrogen use, and pipeline transportation is the most economical and efficient transportation method. The research and development of hydrogen transport pipeline is a typical example of realizing the national "dual carbon" strategic goal through scientific and technological innovation. With the urgent need for safe long-distance and large-scale transport of hydrogen, there is a pressing

need to investigate the compatibility of pure hydrogen and natural gas/hydrogen mixtures long-distance pipelines. In this paper, we focus on hydrogen-doped pipes with high steel grade and low hydrogen pressure, and pure hydrogen pipes with intermediate or low steel grade and high pressure. Partly research works on the safety evaluation of X80 hydrogen-containing pipelines for simulated coal-to-gas transmission and on the factors affecting the hydrogen brittle resistance of pure hydrogen pipelines were introduced, respectively. The results show that, for high-grade pipes in service, hydrogen compatibility tests should be performed before hydrogen mixing to prevent various defects from causing hydrogen damage during hydrogen mixing. Under the high-pressure hydrogen environment, the acicular ferrite microstructure had better hydrogen embrittlement resistance than the polygonal ferrite + bainite microstructure. Metallurgical defects such as large M/A constituent, strip microstructure, and MnS inclusions could lead to hydrogen damage in medium and low-grade pipe steel in different hydrogen pressure environments under stress coupling.

Keywords hydrogen transmission, hydrogen doped, pure hydrogen, hydrogen compatibility

91.A Modified Polyurea Platform with Nano Titanium Dioxide for Antibacterial and Drag-Reducing Applications in Marine Structures

A Modified Polyurea Platform with Nano Titanium Dioxide for Antibacterial and Drag-Reducing Applications in Marine Structures

Yuanzhe Li ^{1, 2, *}

¹ *Transportation Design Institution, China Academy of Art, Hangzhou, 310002*

² *School of Materials Science & Engineering, Nanyang Technological University, Singapore, 639798, Singapore yuanzhe001@e.ntu.edu.sg (Y.Z. Li) &*

wchoo004@e.ntu.edu.sg (W.L. Choo)

Presenter's e-mail address: yuanzhe001@e.ntu.edu.sg

Abstract Marine structures are commonly affected by biofouling problems caused by

marine microorganisms like marine worms and sea squirts. However, the practical application of traditional Reactive Oxygen Species (ROS) materials for anti-biofouling purposes is limited due to inadequate underwater lighting. Additionally, photocatalytic materials often possess hydrophilic and porous properties that can promote biofilm adhesion. To address these challenges, a modified polyurea platform with nano-microstructure and low surface energy is developed. This platform reduces biofilm and bacterial adhesion while simultaneously reducing resistance between the fluid and the coating surface. The antibacterial and drag reduction mechanism of nano titanium dioxide in the polyurea system has been systematically studied through surface characterization, biological analysis, and microchannel fluid drag reduction experiments. A certain weight percentage of nano titanium dioxide was able to form a uniformly riblet structure similar to shark skin grooves on the polyurea surface, which ensures that the surface morphology of the coating facilitates fluid flow in the same direction, thereby minimizing momentum transfer and outward jetting of eddies in the boundary layer and enhancing the drag reduction effect in microchannels. Additionally, nano titanium dioxide can produce ROS, which has a photocatalytic degradation effect on biofilm proteins, destroying cell membranes and reducing their adhesion. By adjusting the formula of different components in the coating system, biofilm adhesion can be sustained below 5×10^5 CFU/ml, and the coating surface drag reduction rate can be maintained above 3.0 %. The modified polyurea platform with nano titanium dioxide can effectively reduce biofilm adhesion and drag resistance, and the mechanism of photocatalytic degradation of biofilm proteins by ROS can further improve the anti-biofouling performance. This research provides a novel approach to preparing functional antibacterial and drag-reducing composite surfaces and has potential applications in marine structures to reduce biofouling problems and improve their performance in drag reduction.

Keywords Marine Structures, Antibiofouling, Reactive Oxygen Species, Nanotitanium Dioxide, Polyurea, Drag Reduction

92. Advanced surface analytical methods for corrosion research Philippe Marcus

Advanced surface analytical methods for corrosion research

Philippe Marcus

*PSL University, CNRS-Chimie ParisTech, Institut de Recherche de Chimie Paris,
Research Group of Physical Chemistry of Surfaces, Paris, France*

philippe.marcus@chimieparistech.psl.eu

Abstract In this lecture the use of advanced surface analytical methods for corrosion research will be exemplified for different topics in which fundamental understanding of mechanisms of corrosion is required to then design new highly corrosion resistant alloys, new corrosion inhibitors or new surface treatments.

The contents of the lecture will be as follows:

- high resolution techniques for corrosion research
- new alloys containing Cr and Mo for enhanced passivity
- replacement of CrVI in conversion layers on Al alloys
- corrosion inhibition by organic molecules

93. A case study on a failed superheater used in a biomass thermal power plant:

Metallurgical investigation

A case study on a failed superheater used in a biomass thermal power plant:

Metallurgical investigation.

Thee Chowwanonthapunya

Abstract This case study presents the metallurgical investigation on the failed superheater tube used in a biomass power plant. To analyze the causes of the superheater tube failure, visual inspection, microstructural examination, chemical analysis, and hardness measurement were employed. Results from the investigation indicate that the main cause of this failure was related to the long-term overheating, subsequently leading to the occurrence of excessive thermal oxidation and

graphitization. The excessive thermal degradation accelerated the loss of the wall tube thickness, thus raising the stress acting on the tube. Graphitization degraded the microstructure of the tube, reducing the mechanical performance of the tube. The combination of two negative effects contributed to the premature rupture of the tube. Materials with higher high temperature degradation, such as SA213 T22 , are suggested to replace the failed tube. Temperature monitoring and mapping in such high temperatures is also recommended.

94.All-In-One passive, active and self-healing properties control of epoxy coating by microenvironment regulation for long-term anticorrosion

All-In-One passive, active and self-healing properties control of epoxy coating by
microenvironment regulation for long-term anticorrosion

程孟, 胡松青

中国石油大学 (华东)

Abstract With excellent mechanical strength and structural stability, metal materials have played an important role in the development of social modernization. However, the inevitable corrosion phenomenon in the service process not only causes direct economic losses, but also seriously endangers public security and restricts the in-depth development of social economy, which has become a major problem to be solved urgently.[1] For a long time, coating technology has made irreplaceable contributions to metal corrosion protection because of its convenient operation and excellent anticorrosion performance.[2] In essence, the coating relies on the shielding effect of its own structure for the corrosive medium to realize the corrosion protection of metal, and its anticorrosion ability gradually weakens with the extension of time.[3] Stimuli-responsive coatings can self-repair their own anticorrosion function in response to environmental changes, but they do not exhibit ideal long-term protective effect due to the lack of ability to regulate corrosive media, while this is vital to practical metal protection.[4] Herein, a novel “coating microenvironment regulation”

concept based on well-designed nanofiller is proposed to realize long-term anticorrosion. The introduced nanofiller is to simultaneously endow coatings with corrosive media shielding, active oxygen consumption and stimuli-responsive functions, thus “three birds with one stone”. The target nanofiller exhibits excellent oxygen depletion performance and is uniformly dispersed in the coating to construct steric hindrance against corrosive media. This dual effect allows composite coating to maintain the excellent anticorrosion performance over 60 days under oxygen environment. In addition, the nanofiller can release inhibitor at corrosion sites in response to environment change when coating is damaged, so as to restore the protective ability of coating. Such multifunctional coating exploration overcomes the protective limitation of current self-healing coatings and sheds light on the design of intelligent long-term anticorrosion coatings.

Keywords coating; long-term protection; microenvironment regulation; stimuli-responsive self-healing.

95. Transformational Discovery Methods for Corrosion Protection in a Circular Economy

Transformational Discovery Methods for Corrosion Protection in a Circular Economy

Ivan Cole¹, Patrick Keil², Pablo Ordejón³, Ernane de Freitas Martins^{1,3}, José María Castillo Robles^{1,3}, Steffen Jeschke¹, Rou Jun Toh¹, Jim Jose¹, Qiushi Deng¹, Paul White¹, Xiaobo Chen¹, Chathumini Samarawickrama¹, Philip Eiden⁴, Tomas Prosek⁵,
Milan Patel¹

¹ *RMIT University, Melbourne, Australia*

² *BASF Coatings GmbH, Muenster, Germany*

³ *ICN2, Barcelona, Spain*

⁴ *BASF SE, Ludwigshafen, Germany*

⁵ *University of Chemistry and Technology, Prague*

Abstract In this decade, fresh demands from law makers and the public are challenging how we design our traditional corrosion protection systems for metals. This applies to both active polymeric coatings and hard metallic coatings (such as galvanising). It is now expected that such protection systems contain no toxins, but also be “sustainable” and at the end of their life be able to be processed to begin again a new life. Thus, consumer and legislative demands have shifted past the performance demands from the 60-90’s and even the non-toxicity requirements from the 90-10’s. To meet these enhanced demands, we need new design and discovery methods that can allow us to shift away from incremental adjustments to our standard systems but look to see if totally different systems may provide corrosion protection. However, when we broaden the potential systems, the design possibility or the discovery spaces expands dramatically, and we thus need fast experimental, digital, or a combination of these methods to select the optimum solutions. In this paper, the development of transformational discovery methods applied to corrosion inhibitors and aluminium-based coatings to galvanically protect galvanised steel will be discussed.

The restriction or banning of chromates (such as strontium chromate) as inhibitors in paints to protect a wide range of metals (structural aluminium, steel, etc) gave rise to a large range of research searching for inhibitors. One of the most popular alternatives was small heterocyclic molecules with attached and active ligands for atmospheric corrosion or (bio-)tensides or bulky . As the exact structure of such molecules is critical, there are tens of thousands of candidate molecules. Fast experimental or virtual methods or a combination are required to down select candidates from these candidates. During the last decades, RMIT and partners have applied various strategies aimed at “inverse design”. That is understanding the features that promote inhibitions and then using these features to down select from the candidate materials. Each strategy relied on developing molecular level descriptors of inhibitors and databases of the electrochemical performance and connecting these using either QPSR (quantitative property structure relationships) or various machine learning and

artificial intelligence methods. Successive methods have refined both the molecular descriptors and the size and quality of the experimental databases. The latest models are very effective in describing the connection between molecular descriptors and electrochemical data, but the prediction capability of the models still needs enhancement. Two strategies are being pursued to enhance this predictive capability, deepening the fundamental knowledge of inhibition and formation of inhibition layers, and developing refined learning approaches. Advanced molecular modelling that uses the hybrid quantum mechanics/molecular mechanics (QM/MM) method combined with non-equilibrium Green's functions (NEGF) formalism to include the electrode potential effects and accurately simulate inhibitor/surface interactions at a charged interface in a solution is providing a refined understanding of both inhibitor bonding to a surface and inhibitor layer formation. Experimental studies are refining our understanding of inhibitor layer stability. In the second approach, “evolutionary algorithms” are combined with robotic experimentation. In this approach, rather than construct large databases, one begins with a constrained selection of possible inhibitors that are tested via robotic electrochemistry, and then a refined set of molecules is derived by “mutating” the original selection based on this testing results and the mutated selection is then tested and the process continues until an optimum selection of inhibitors is obtained.

In the third application, the team is looking to replace the galvanic protection of steel via traditional zinc galvanising with the protection of an aluminium coating derived from waste. Use of fresh zinc has a high energy cost and is leading to depletion in the supply of zinc. Intrinsically this should be possible as aluminium is significantly more electro-negative than zinc and should offer stronger galvanic protection for steel. However, the formation of a dense oxide on aluminium passivates it and prevents galvanic protection. Nonetheless, if a coating can be developed that does not passivate, then the galvanic protection will be maintained. This is the aim of a major European project, Alcoat, and what is central to this project is combined atomic level and electrochemical modelling to select the optimum alloy compositions.

96. Corrosion behavior of monophasic and multiphasic Al₅₀Au₅₀ ribbons in AlCl₃ + HCl solution

Corrosion behavior of monophasic and multiphasic Al₅₀Au₅₀ ribbons
in AlCl₃ + HCl solution

Z.C. Yana, H. Zhanga, Q. Chena, G.H. Lib, L.C. Zhangc,* , X.F. Biana, W.M. Wang,*

¹*Key Laboratory for Liquid-Solid Structural Evolution and Processing of Materials,
Ministry of Education, Shandong University, Jinan 250061, China*

²*Shandong Institute of Metrology, Jinan 250014, China*

³*School of Engineering, Edith Cowan University, 270 Joondalup Drive, Joondalup,
Perth, WA6027, Australia*

Abstract Monophasic Al₅₀Au₅₀ ribbons (labelled as S2ann) were obtained by melt spinning and annealing. The corrosion properties of S2ann were investigated in AlCl₃ + HCl solution with as-spun multiphasic ribbons (labelled as S2sp) for comparison. S2ann is self-passivated and has a wide passivation region, while S2sp tends to undergo Al₂Au-induced selective dissolution under anodic polarization. Besides, S2ann has a fluctuant open-circuit potential and a passive film with p-type semiconductor feature, which are not found in S2sp. The passive film of S2ann is examined to be Au-contained Al₂O₃ with a double-layer structure.

Keywords AlAu alloy; Passive film; OCP fluctuation; Space-charge region; Au-contained Al₂O₃.

97. Effect of the impurities in LiF-NaF-KF molten salt on the corrosion behavior of GH3535 alloy

Effect of the impurities in LiF-NaF-KF molten salt on the corrosion behavior of
GH3535 alloy

孙华

Abstract The present work investigated the effect of the impurities in molten LiF-NaF-KF (FLiNaK) salt on the corrosion behavior of GH3535 alloy at 700°C in the time range of 50h to 400h by means of the immersion test combining with the microstructural analysis. It was found that the impurities in the molten FLiNaK salt had an obvious influence on the corrosion behavior of GH3535 alloy. In the 1# salt with the low content of the impurities such as metal ions and HF, GH3535 alloy exhibited the general corrosion. And the corrosion voids were formed in the near-surface region of GH3535 alloy. The alloy corrosion is mainly attributed to the selective dissolution of Cr. In the 2# salt with the high content of the impurities, GH3535 alloy exhibited the intergranular corrosion. The alloy corrosion is mainly attributed to the dissolution of the matrix element Ni with the exception of Cr and Mo. The weight loss and corrosion depth of the alloy in both molten salts increased with the increase of the immersion time, while the corrosion type was not changed.

98. Effects of temperature and acetic acid on electrochemical corrosion behavior of X80 steel

Effects of temperature and acetic acid on electrochemical corrosion behavior of X80 steel

Yadong Li¹, Wanpeng Yao¹, Siquan Wang¹, JianJun Pang², Yan Li^{1,*}

¹*School of Materials Science and Engineering, China University of Petroleum (East China), Qingdao 266580, China*

²*School of Mechanical and Automotive Engineering, Zhejiang University of Water Resources and Electric Power, Hangzhou 310018, China*

Abstract The effects of temperature and HAc on the corrosion behavior of X80 steel were investigated by electrochemical measurements, including electrochemical impedance spectroscopy and potentiodynamic polarization curves. Results showed that the corrosion current density of X80 steel increased with the increase of

temperature. The near-surface pH values of X80 steel revealed that due to the formation conditions of the corrosion film, differences existed between electrochemical measurements and weight loss method results. The changes of cathodic and anodic charge transfer resistance indicating that the mechanism of HAc that affects the cathodic reaction process was found to be the buffering effect, and HAc served as the source of H^+ .

Keywords Pipeline steel; Electrochemical impedance spectroscopy; Near-surface pH; CO_2 corrosion

Reference

- [1] S.X. Zhang, F.Q. Xie, X.M. Li, J.H. Luo, G.G. Su, L.X. Zhu, Q.G. Chen, Failure analysis of the leakage in girth weld of bimetal composite pipe. *Eng. Fail. Anal.*, 2023, 143, p 106917.
- [2] E. Basilico, S. Marcelin, R. Mingant, J. Kittel, M. Fregonese, F. Ropital, The effect of chemical species on the electrochemical reactions and corrosion product layer of carbon steel in CO_2 aqueous environment: A review. *Mater. Corros.*, 2021, 72, p 1-16.
- [3] T. das Chagas Almeida, M.C.E. Bandeira, Moreira R M, O.R. Mattos, New insights on the role of CO_2 in the mechanism of carbon steel corrosion. *Corros. Sci.*, 2017, 120, p 239-250.

99.Experimental study on dew point corrosion coupled with ash deposition in simulated MSW incineration environment

Experimental study on dew point corrosion coupled with ash deposition in simulated
MSW incineration environment

周巧燕 刘欢

华中科技大学

Abstract Incineration is the dominant technology for municipal solid waste (MSW) treatment, with the advantages of rapid volume reduction and potential electricity-heat

recovery. With the decrease of exhaust gas temperature, dew point corrosion of materials in the flue gas purification system occurs more and more frequently. The flue gas here contains a high content of water vapor and various acidic gases (HCl, SO_x, etc.), which upon condensing along with fly ash depositing can lead to corrosion. This paper investigated the dew point corrosion coupled with ash deposition in a complex environment in the flue gas purification system of MSW incineration. Using our innovative self-designed simulation experimental apparatus, the quantitative effects of ash particles, acidic gas, and temperature on electrolyte composition were first investigated. Further, the electrochemical corrosion behavior of Q235 and coatings was clarified by polarization tests and electrochemical impedance spectroscopy. The results showed that the electrolyte mainly consisted of highly corrosive salts such as CaCl₂, KCl, and NaCl. The Cl⁻ concentration of the electrolyte was increased as the HCl in the flue gas varied from 0 to 600 ppm, reaching a maximum of 2.23 mol/L at 600 ppm. However, Cl⁻ and Ca²⁺ in the electrolyte were significantly decreased by 33.0% and 47.3%, respectively, as SO₂ increased (0-300 ppm). In addition, higher Cl⁻ and Ca²⁺ contents in the solution also resulted from the temperature decreasing (110 °C-50 °C), with HCl and SO₂ beginning to condense and more ions dissolution of ash. High Cl⁻ concentration reduced the solution resistance and charge transfer resistance, which resulted in raised corrosion rate. Numerous corrosion products were found on the Q235, including FeCl₂, Fe₂O₃, FeOOH, etc, while the resin coatings exhibited high impedance and good corrosion resistance. This study can provide guidance for corrosion control and waste heat utilization in MSW incinerators.

Keywords MSW incineration; dew point corrosion; ash deposition; coatings

100. Corrosion behavior of mild steel in acid solutions with presence of triazole derivatives

Corrosion behavior of mild steel in acid solutions with presence of triazole derivatives

A.D. Shitoeva¹, M.D. Plotnikova¹, A. S. Sofronov¹, A.B. Shein

Perm State National Research University, st. Bukireva 15, 614068, Perm, Russian Federation

Abstract Corrosion is a widely studied field of science. In order to understand mechanisms of action of corrosion inhibitors, the reactions at the interfaces between the corrosive electrolyte and a steel surface. This work is aimed at confirming the assumption about the formation of a protective film and the chemical adsorption of some triazole derivatives on mild steel surface by physicochemical methods. 4,5-diphenyl-4H-1,2,4-triazole-3-thiol (4,5-PhTAT) and 3,4-diphenyl-5-(prop-2-yn-1-ylthio)-4H-1,2,4-triazole (3,4-PhPTTA) were researched as corrosion inhibitors in acid solution (1 N, 5 N HCl and 0.1 N H₂SO₄). The protonation/deprotonation equilibrium constants were computed using the Marvin pKa Plugin program, with due consideration given to tautomerization. According to the results of the calculations carried out, it has been shown that in acidic H₂SO₄ solutions, inhibitors 4,5-PhTAT and 3,4-PhPTTA exist in different forms: 3,4-PhPTTA molecules are predominantly protonated, while 4,5-PhTAT exists as neutral molecules. Protection efficiency of 4,5-PhTAT and 3,4-PhPTTA increased with increasing concentration of HCl solution from 1 N to 5 N [1,2]. More over inhibition efficiency in H₂SO₄ is higher for both substances. Polarization curves method noted that 4,5-PhTAT and 3,4-PhPTTA are mixed type inhibitors in H₂SO₄ and cathodic type in HCl solutions. There was redistribution in polar and dispersion components of the free surface energy with adding triazole derivatives in corrosion media. Redistribution in polar and dispersion components consist with different forms of molecular existence [3].

Keywords mild steel, acid corrosion, triazole, inhibitor, potentiodynamic polarization, activation energy, electrochemical impedance spectroscopy, adsorption.

Reference

[1] Plotnikova, M. D., Solovyev, A. D., Shein, A. B., Vasyanin, A. N., & Sofronov, A. S. (2021). Corrosion inhibition of mild steel by triazole and thiadiazole derivatives in

5 M hydrochloric acid medium. *International Journal of Corrosion and Scale Inhibition*, 10(3), 1336-1354.

[2] Plotnikova, M. D., Solovyev, A. D., Shein, A. B., Bakiev, A. N., & Sofronov, A. S. (2021). New inhibitors based on substituted 1, 2, 4-triazoles for mild steel in hydrochloric acid solutions. *International Journal of Corrosion and Scale Inhibition*, 10(3), 1230-1244.

[3] Kozbial, A., Li, Z., Conaway, C., McGinley, R., Dhingra, S., Vahdat, V., Zhou, F., D'Urso, B., Liu, H. & Li, L. (2014). Study on the Surface Energy of Graphene by Contact Angle Measurements. *Langmuir*. 30, 598-606.

101.Preparation of CeO₂/ZnO resistive thin film and its corrosion behavior in 3.5wt% NaCl solution

Preparation of CeO₂/ZnO resistive thin film and its corrosion behavior in 3.5wt% NaCl solution

Abstract ZnO thin films were prepared by spin-coating combined with hydrothermal method, CeO₂ thin films were prepared by electrodeposition, ZnO/CeO₂ thin films were prepared by spin-coating, hydrothermal method combined with electrodeposition, CeO₂/ZnO thin films were prepared by electrodeposition combined with hydrothermal method, and CeO₂/ZnO thin films were prepared by scanning electron microscopy (SEM), X-ray diffraction (XRD), Fourier transform infrared spectroscopy (FTIR). The surface morphology, cross-section morphology, composition, crystal structure, semiconductor type and oxygen vacancy concentration of different thin film samples were observed and analysed by scanning electron microscopy (SEM), X-ray diffraction (XRD), Fourier transform infrared spectroscopy (FTIR), Mott-Schottky curve (M-S), X-ray photoelectron spectroscopy (XPS) and electron paramagnetic resonance spectroscopy (ESR). The surface adsorption energies, oxygen vacancy formation energies, heterojunction binding energies and interfacial diffusion barriers of Cl⁻ and O₂ were calculated by density functional theory (DFT). The

corrosion resistance of the films was investigated by polarisation curves and electrochemical impedance spectroscopy (EIS), the variation rule of the corrosion resistance of ZnO/CeO₂ and CeO₂/ZnO films with the immersion time was investigated by immersion experiments, and the resistive properties of ZnO/CeO₂ and CeO₂/ZnO films were investigated by resistive change experiments. The results show that the prepared CeO₂/ZnO films belong to the n-n heterojunction type semiconductor with a uniform surface, and the films have excellent corrosion resistance. In the immersion process, ZnO/CeO₂ film corrosion resistance is poor, no obvious change rule; CeO₂/ZnO film corrosion resistance first enhanced, and then weakened with the increase of immersion time. Resistance experiment process, ZnO/CeO₂ film presents very weak resistance performance, and high resistance state corrosion protection efficiency is only 70%; CeO₂/ZnO film presents stable and excellent resistance performance, low resistance state protection efficiency can still reach 96%, this is due to the formation of CeO₂/ZnO heterojunction interface of the higher electronic potential barrier impedes the corrosive medium to the substrate of the diffusion. The oxygen vacancy concentration in the CeO₂/ZnO film can be adjusted through the rheostatic cycling experiment to achieve cyclic switching between high and low resistance states (HRS and LRS), which can greatly extend the service life of the film.

Keywords Resistance switching; corrosion resistance; heterojunction; oxygen vacancy; DFT

102.Remarkably Corrosion Resistant Graphene Coating on Steel Enabled Through Metallurgical Tailoring

Remarkably Corrosion Resistant Graphene Coating on Steel Enabled Through
Metallurgical Tailoring

Raman Singh Raman Singh

Monash University - Clayton Campus (Melbourne)

Abstract Graphene coatings developed by chemical vapor deposition (CVD) that possess extraordinary/unique characteristics as barrier against aggressive environment can improve the corrosion resistance of Ni and Cu by up to two orders of magnitude. However, because of some compelling technical reasons, it has thus far been a nontrivial challenge to develop graphene coatings on the most commonly used engineering alloy, mild steel (MS). To circumvent the challenge simply by first electroplating MS with a Ni layer is attempted, and then developing CVD graphene over the Ni layer. However, this approach proved too simplistic and does not work. This necessitated an innovative surface modification of MS (based on basic metallurgical principles) that enabled successful CVD of graphene coating on MS. The graphene coating thus developed is demonstrated to improve the corrosion resistance of mild steel by two orders of magnitude in an aggressive chloride solution, through electrochemical testing. This improvement was not only sustained for the entire test duration of >1000 h; but there is a clear trend for the resistance to be possibly everlasting. The optimized surface modification that enabled development of CVD graphene coating on mild steel is generic in nature, and it should enable graphene coating on other alloy systems, which would otherwise not be possible. Enabled Through Metallurgical Tailoring

103. Research on fatigue properties of Q690 high strength steel in marine corrosive environment

Research on fatigue properties of Q690 high strength steel in marine corrosive environment

魏欢欢

东南大学

Abstract In recent years, steel-based materials have been widely used in offshore

proposed projects, and the durability of steel structures has become increasingly prominent. So far, the research results on the fatigue properties of Q690 high strength steel in the marine splash zone are still relatively small. Therefore, the indoor accelerated corrosion test and high cycle fatigue test were carried out, the S-N curves of different corrosion specimens were fitted, the effect of corrosion damage on the fatigue life of Q690 high strength steel was discussed, and the fatigue crack growth law was revealed by scanning electron microscope. The results show that with the increase of the degree of corrosion damage, the steel surface loses its metallic luster and gradually forms reddish brown lamellar corrosion. After 100 days of corrosion, the corrosion rate and corrosion depth rate of the test piece are 7.21% and 1.342mm/a respectively. Under cyclic load, the fatigue limit value of Q690 high strength steel specimen corroded for 100 days decreased by 38.89%, and corrosion damage accelerated the degradation rate of fatigue performance. In addition, when the stress level increases, the number of fatigue bands decreases and the cumulative damage increases. The research results are of great significance for the application of domestic high strength steel in marine environment.

Keywords Q690 high strength steel;marine splash zone;accelerated corrosion;electron microscope scanning;fatigue performance;fatigue damage

104.Self-Healing Enhancement of Diphenylmethane Diisocyanate (MDI) Polyurea Coating via Polytetramethyleneoxide-di-p-Aminobenzoate for Corrosion Protection in Marine Structures

Self-Healing Enhancement of Diphenylmethane Diisocyanate (MDI) Polyurea Coating via Polytetramethyleneoxide-di-p-Aminobenzoate for Corrosion Protection in Marine Structures

Yuanzhe Li ^{1,2,*}, WanLuoh Choo ²

¹*Transportation Design Institution, China Academy of Art, Hangzhou, 310002*

²*School of Materials Science & Engineering, Nanyang Technological University,*

Singapore, 639798, Singapore yuanzhe001@e.ntu.edu.sg (Y.Z. Li) &
wchoo004@e.ntu.edu.sg (W.L. Choo)

* Correspondence information: Dr. Yuanzhe Li, Transportation Design Institution,
China Academy of Art, Hangzhou, 310002 & School of Materials Science &
Engineering, Nanyang Technological University, Singapore, 639798, Singapore,
yuanzhe001@e.ntu.edu.sg (Y.Z. Li)

Abstract Metal structures and polymers are prone to degradation and corrosion, which can compromise their mechanical properties and lead to material failure. Protective coatings have been widely employed to mitigate the effects of corrosion and degradation triggered by reactions in the presence of moisture and oxygen. However, conventional coating techniques have limitations when it comes to maintaining and recoating large underwater structures such as ships and pipelines. Therefore, there is a pressing need to explore alternative coating solutions that do not require manual maintenance. Self-healing polyurea coatings are a promising alternative that has gained significant attention due to their superior properties.

Organic coatings that incorporate microencapsulated drying oil as the healing agent have been extensively studied for their self-healing ability in air (atmospheric oxygen), but the study on their self-healing ability in water (dissolved oxygen) remains limited. This paper investigates the efficacy of microcapsules and the self-healing ability of polyurea coatings in marine structures. Our findings reveal that the fabrication method employed did not result in optimal microcapsule distribution, as evidenced by the SEM image of clustered microcapsules, despite FTIR analysis indicating successful encapsulation of the healing agent. Moreover, the ratio and type of components utilized in polyurea fabrication were not optimal, which negatively impacted the flexibility of the resulting polyurea (MDI with p-Phenylenediamine) (PUA-p-PDA) coating. Nonetheless, our experiments showed that polyurea coatings formulated using different components Polyurea (MDI with polytetramethyleneoxide-di-p-aminobenzoate) (PUA-P1000) exhibited a high

elasticity of 267.7 N and demonstrated promising self-healing ability when cut in half. The challenges and limitations encountered during this research can provide useful insights for future studies on fabrication methods and experimental design.

Keywords Self-Healing, Polyurea Coating, Corrosion Protection, Microcapsules, Mechanical Properties

105.Surface Morphology, Microstructure and Emissivity of Rhenium Electrodeposited from Molten Salts

Surface Morphology, Microstructure and Emissivity of Rhenium Electrodeposited
from Molten Salts

袁伟超

国防科技大学

Abstract The effects of the electrodeposition (ED) processing parameters in molten salts on the surface morphology, microstructure, and emissivity of Re coatings were investigated in this study. The results indicated that the emissivity of the ED Re coating was related to the micromorphology, oxygen content and preferred orientation of the Re coating, among which, the coating micromorphology has the most impact. The emissivity of the Re coatings increases with decreasing average radius or increasing surface density of the coating characteristic microstructures. With increasing cathodic overpotential, corresponding to a high CsCl content or a high current density or a low molten salt temperature, the Re coating tended to change from lateral growth mode to outward growth mode, with preferred growth plane of the coating changing from (200) to (110), and meanwhile the surface morphology of the Re coating changing from stout branch-like to spiked starfish-like, resulting in an increase in emissivity. The optimal deposition processing parameters for the high-emissivity black Re coatings were as follows: temperature ranging from 720°C to 780°C, cathode current density of 50 mA/cm² to 90 mA/cm², and the CsCl content

higher than 60wt.%. The obtained black Re coatings had an emissivity higher than 0.7, with a preferred growth crystal plane of (110), and a typical spiky starfish shaped micromorphology.

Keywords rhenium coating; molten salt electrodeposition; surface morphology; microstructure; emissivity

106. Bridge for the thermodynamics and kinetics of electrochemical corrosion: designing of the high corrosion-resistant copper-nickel alloy

Bridge for the thermodynamics and kinetics of electrochemical corrosion: designing
of the high corrosion-resistant copper-nickel alloy

Zinuo Wang, Peng Zhou, Tao Zhang*, Fuhui Wang

*Shenyang National Laboratory of Material Science, Northeastern University,
Shenyang*

Abstract Copper-nickel alloy has become an important marine engineering material due to its excellent erosion resistance and resistance to Cl⁻ corrosion, and is widely used in seawater pipeline systems. However, there are still serious corrosion issues such as perforation and leakage during use. So adding some micro-alloying elements to the copper-nickel alloy foundation, in other words, using alloying methods to develop new alloys, can better meet industrial needs. However, the current alloying design is still based on the trial-and-error method, and there is an urgent need for a guideline constructed based on the existing knowledge framework, which exposes the influence mechanism of alloying elements and guides the design of alloys. In this paper, we propose a design concept for highly corrosion-resistant copper-nickel alloys based on the “Dissolution-Ionization-Diffusion-Deposition (DIDD)” model previously proposed by Tao Zhang et al [1]. The DIDD model establishes a bridge between the thermodynamics and kinetics of electrochemical corrosion and quantitatively describes the corrosion process at the metal/solution (M/S) interface. Factors influencing the cation concentration, pH and deposition process at the M/S

interface are also presented. According to the model, the influence of micro/low alloy elements on the corrosion behavior can be obtained. The main element Cu in the copper-nickel alloy has a high electrode potential and good thermal stability, which leads to a slow dissolution rate and a long time for redeposition into dense corrosion products. And the seawater corrosion resistance of Cu-Ni alloy is due to the formation of a layer of highly adhesive, dense, and protective film, mainly composed of Cu₂O. The designed high corrosion resistant copper nickel alloy system is “Cu-30Ni-MA”, where MA is a micro-alloying element. From the perspective of electrochemical dissolution, the condition that MA needs to meet is $E_{M/M^{n+}}^{\theta} < E_{Cu/Cu^{+}}^{\theta}$, forming an asynchronous dissolution relationship with the matrix elements Cu and Ni, thereby promoting the enrichment of Cu element in a layer before dissolving into cation ions, resulting in the formation of higher concentrations of Cu ions at the metal/solution interface, laying the foundation for deposition. From a deposition perspective, select elements with deposition lines lower than Cu₂O to act as heterogeneous nucleation agents. The downward amplification effect of MA priority nucleation plays a crucial role in achieving accelerated passivation behavior. Alloy elements not only have a stepwise amplification effect on the nucleation rate, but appropriate composition can maximize this effect. So, select a few more alloy elements and see if it is feasible to significantly increase the nucleation rate of Cu₂O through stepwise amplification effect. Three alloying elements, Fe, Mn and Cr, were selected, and comparative calculations were carried out on the selected binary, ternary, quaternary and quintuple alloys using DIDD to determine whether it was feasible to utilize the step-by-step scaling-up effect to substantially increase the nucleation rate of Cu₂O. Experimental verification was then carried out using static immersion, corrosion weight loss, and electrochemical testing. The results show that the properties of the designed alloys are more consistent with the calculation results, proving that it is effective and feasible to utilize the DIDD model mechanism to guide the alloy design.

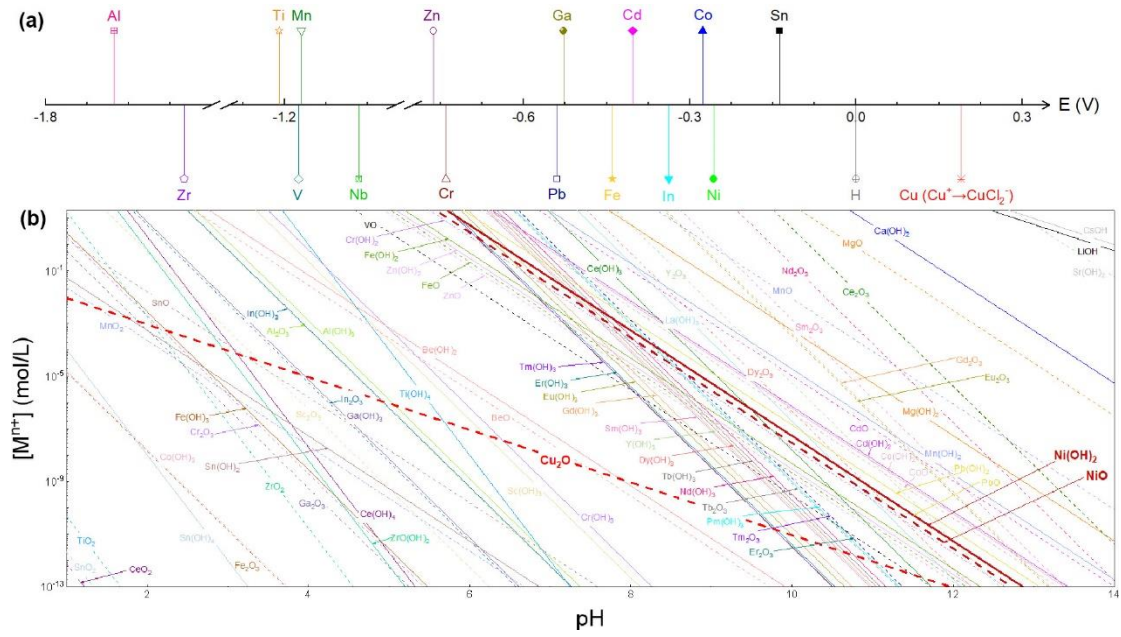


Fig. 1 (a) Electrode potential sequence; (b) critical line of deposition

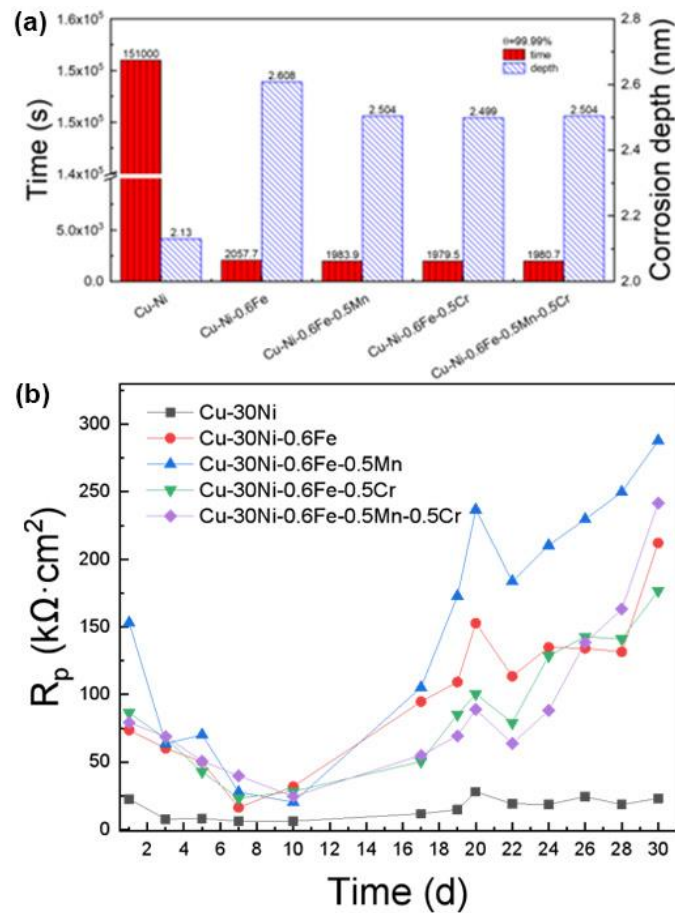


Fig. 2 (a) Calculated results; (b) EIS results

Keywords Copper-nickel alloy, corrosion resistance, alloy designing, DIDD model

References

[1] Y. Zhao, T. Zhang, H. Xiong, F. Wang, Bridge for the thermodynamics and kinetics of electrochemical corrosion: Modeling on dissolution, ionization, diffusion and deposition in metal/solution interface, *Corros. Sci.* 191 (2021) 109763.

107. 油气钻采装备工具耐蚀合金修复层腐蚀磨损行为及机制研究

摘要 激光增材制造(LAM)合金在制备过程中由于存在较高的温度梯度,容易产生残余应力,增加了材料的失效风险。一般来说,热处理是降低材料内应力的有效方法。本研究采用 67°旋转策略制备了 LAM 镍基合金,并对热处理后试样的磨损及腐蚀机理进行了深入研究。显微组织结果表明 LAM 镍基合金是由尺寸为 1 ~ 4 μm 的柱状结构和尺寸为 0.3 ~ 1 μm 的胞状结构组成。试样中 Cr23C6 和 MoSi2 含量随热处理温度的升高而增加。另外,高矿化度下温度的提升迅速恶化了 LAM 镍基合金的亚晶晶间腐蚀,呈现出熔池线及晶间与析出相协同作用的局部腐蚀,而其耐磨性则因热处理后完整性优越的氧化层和继续析出的 MoSi2 的支撑作用而增强。这个研究将有助于设计和优化高性能的 LAM 镍基合金。

108. 海洋菌藻共生对金属腐蚀与污损的影响机制

海洋菌藻共生对金属腐蚀与污损的影响机制

董雨侨¹, 宋光铃^{2, 3*}

¹ 山东大学海洋研究院, 青岛 266237

² 南方科技大学海洋科学与工程系, 深圳 518055

³ *School of mechanical and mining engineer, University of Queensland, Qld 4072*

Australia

*guangling.song@hotmail.com, songgl@sustech.edu.cn

Abstract 海洋中生物污损层组成复杂,底层优先附着的微生物吸引其他大型海洋生物像微藻、藤壶等附着,经过不断地竞争共同进化,最终稳定成膜。然而,迄今为止,污损层中各生物间的共生关系对金属腐蚀的影响鲜有研究。本文就海

洋环境中的三角褐指藻(*Phaeodactylum tricornutum*)及其共生细菌(*Bacillus altitudinis*)对 Q235 碳钢、304 不锈钢、Mg 合金三种海洋工程材料的影响展开研究,发现:在海藻-细菌-Q235 碳钢体系中,底层细菌导致碳钢腐蚀,上层海藻生物膜通过两者之间的“共生”进一步加速腐蚀作用;而腐蚀溶解所产生的铁离子作为生长因子刺激海藻生长,形成污损的恶性循环。在海藻-细菌-304 不锈钢体系中,304 不锈钢的腐蚀速率相比于单一细菌体系下降 97.7%;同时,在表面形成智能自修复的磷酸铁腐蚀产物层,协同保护 304 不锈钢。这种抑制腐蚀的机理,可作为不锈钢缓蚀的一种环保型新方法。海藻-细菌-Mg 体系的研究揭示了单一共生细菌可以有效地抑制 Mg 的自腐蚀,由于腐蚀过程中产生的 Mg^{2+} 促进了细菌的代谢,使其聚集形成保护性生物膜,进而分泌具有抗腐蚀性的代谢产物;同时活化的生物膜加速 Mg 表面形成结晶产物。这三者共同保护了 Mg 基体。这些研究结果表明:污损层对不同的材料间具有不同的腐蚀作用,生物膜可“正向”地影响金属的腐蚀,同时金属的腐蚀也能“逆向”地影响生物膜的生长,这两种“互逆”的作用在生物腐蚀的研究过程中均不可忽视。

关键词: 生物污损; 菌藻共生; 生物膜; 金属材料; 腐蚀防治

109. 油气钻采装备/工具耐蚀合金修复层腐蚀磨损行为及机制研究

油气钻采装备/工具耐蚀合金修复层腐蚀磨损行为及机制研究

王勤英

西南石油大学

摘要 激光增材制造(LAM)合金在制备过程中由于存在较高的温度梯度,容易产生残余应力,增加了材料的失效风险。一般来说,热处理是降低材料内应力的有效方法。本研究采用 67° 旋转策略制备了 LAM 镍基合金,并对热处理后试样的磨损及腐蚀机理进行了深入研究。显微组织结果表明 LAM 镍基合金是由尺寸为 1~4 μm 的柱状结构和尺寸为 0.3~1 μm 的胞状结构组成。试样中 $Cr_{23}C_6$ 和 $MoSi_2$ 含量随热处理温度的升高而增加。另外,高矿化度下温度的提升迅速恶化了 LAM 镍基合金的亚晶晶间腐蚀,呈现出熔池线及晶间与析出相协同作用的局部腐蚀,

而其耐磨性则因热处理后完整性优越的氧化层和继续析出的 MoSi_2 的支撑作用而增强。这个研究将有助于设计和优化高性能的 LAM 镍基合金。

110.氮化碳薄膜用于光阴极防腐蚀

氮化碳薄膜用于光阴极防腐蚀

司文平*

河北工业大学, 材料科学与工程学院, 先进轻合金团队, 天津

siwp@hebut.edu.cn

摘要 镁合金作为最轻的结构材料, 在航空航天、交通运输和生物医学领域有着广泛的应用, 但由于其标准电化学电位非常低, 在某些特定的工作条件下, 耐腐蚀性差是一个关键的限制因素[1, 2]。镁的有效防腐对于进一步延长其使用寿命、可靠性和扩大其应用场景具有重要意义。与其他防腐方法相比, 太阳能驱动的光电阴极保护 (PCP) 策略显示出一些吸引人的特点, 因为它既不涉及电能也不涉及牺牲阳极[3, 4]。PCP 机制基于光生电子从半导体光阳极的导带迁移到目标金属, 导致比其腐蚀电位更负的电位[5, 6]。当电子从较低电位流向较高电位时, 光阳极的导带电子应该比金属的腐蚀电位更负。氮化碳相比传统金属氧化物半导体, 具有较高的导带位置, 其光生电子还原能力较强, 与金属耦合后, 其光生电子可转移到金属用于防腐。与其他半导体材料相比具有更显著的优势。然而, 目前氮化碳薄膜光电极处于较初始水平, 薄膜附着力、光电化学性能都有待提高。基于小分子前驱体, 本论文设计了气相-熔融相共沉积方法, 气相沉积保证了氮化碳与 FTO 衬底较好的结合力, 而熔融相沉积提高了氮化碳负载量。本论文制备的氮化碳光电极与衬底结合力强, 具有较高稳定性。将此氮化碳光电极与表面处理过的镁合金相耦合, 镁合金的腐蚀电位明显负移, 起到了预期保护。

关键词: 氮化碳; 涂层; 金属防腐; 镁合金

参考文献:

[1] Li M-X, Wang C, Li Y-J, Wang D-W, Zha M, Gao Y, et al. Tailoring the microstructure and enhancing the corrosion resistance of extruded dilute

- Mg-0.6Al-0.5Mn-0.25Ca alloy by adding trace Ce. Corros Sci 2022;207:110605.
- [2] Wang XJ, Xu DK, Wu RZ, Chen XB, Peng QM, Jin L, et al. What is going on in magnesium alloys? J Mater Sci Technol 2018;34:245-7.
- [3] Liu Y, Yao H, Wu L, Xie Z-H, Zhong C-J. Temperature-controlled and shape-dependent ZnO/TiO₂ heterojunction for photocathodic protection of nickel-coated magnesium alloys. Appl Surf Sci 2023;614:156109.
- [4] Li Y, Ouyang Y, Fang R, Jiang X, Xie Z-H, Wu L, et al. A nickel-underlayer/LDH-midlayer/siloxane-toplayer composite coating for inhibiting galvanic corrosion between Ni layer and Mg alloy. Chem Eng J 2022;430:132776.
- [5] Liu J, Wang N, Zheng F, Wang C, Wang J, Hou B, et al. CuInS₂/TiO₂ heterojunction with elevated photo-electrochemical performance for cathodic protection. J Mater Sci Technol 2022;122:211-8.
- [6] Feng M, Liu Y, Zhang S, Liu Y, Luo N, Wang D. Carbon quantum dots (CQDs) modified TiO₂ nanorods photoelectrode for enhanced photocathodic protection of Q235 carbon steel. Corros Sci 2020;176:108919.

111.超临界二氧化碳中 AlCrFeNi 系高熵合金的腐蚀行为研究

超临界二氧化碳中 AlCrFeNi 系高熵合金的腐蚀行为研究

杨万欢^{1,+}, 赵雪丽^{1,+}, 李伸², 邹吉春^{1,2}, 徐驰³, 杨文¹, 钟巍华^{1,*}

¹ 中国原子能科学研究院, 北京, 102413;

² 南昌大学, 南昌, 330031;

³ 北京师范大学, 北京, 100091

zhongwh@ciae.ac.cn

摘要 超临界二氧化碳 (S-CO₂) 布雷顿循环因其高热电转换效率、部件尺寸小和循环布局简化, 在第四代快堆动力系统中变得愈加重要。鉴于较高的工作温度 (可达 750°C) 及较长的设计寿命, 材料在高温 S-CO₂ 环境下的腐蚀是 S-CO₂ 布雷顿循环系统应用的一大障碍。腐蚀可导致部件有效承载壁厚度的损失及, 叶轮机械部件因氧化颗粒碎片的产生而形成的三体磨损。此外, 在 S-CO₂ 布雷顿循环

中,材料在氧化的同时存在渗碳行为,进而导致结构合金脆化。高熵合金(HEAs)由于其独特的微观结构和优异的耐腐蚀性引起了人们的广泛关注。然而, HEAs 在超临界二氧化碳(S-CO₂)环境下的腐蚀行为与机理尚不明确。本文首先通过真空电弧熔炼法发展了一种新型双相 AlCrFeNiMn (AM-HEA) 和 AlCoCrFeNi_{2.1} (AN) 共晶高熵合金(EHEA), 随后将上述两种高熵合金在 500 °C、25 MPa 的 S-CO₂ 中分别腐蚀 400 h 和 800 h, 最后通过 SEM、TEM、XRD 以及 XPS 等宏微观方法研究其在 S-CO₂ 环境中的腐蚀行为及机理。AM-HEA 的实验结果表明, 等轴亚晶粒基体相和边界相的耐蚀性差异是由于其组织和合金成分的差异造成的, Mn 元素偏析在边界区氧化膜形成过程中有着重要作用, 致密 Al₂O₃ 膜阻碍了 S-CO₂ 对 AM-HEA 的进一步腐蚀。AN-EHEA 的实验结果表明, 在面心立方(FCC)相和体心立方(BCC) B2 相上形成了完全不同的钝化层, FCC 相表面腐蚀产物是外层为 Cr₂O₃、内层为 Al₂O₃ 的双层结构, 相表面腐蚀产物是 Al₂O₃ 的单层结构, Al₂O₃ 氧化膜总体上是致密且连续的。Al₂O₃ 氧化膜通过防止氧气进入基体来抑制进一步的氧化, 有利于提高抗腐蚀性。同时, 本研究中两种 HEAs 均未观察到渗碳现象的发生。

关键词: 高熵合金; S-CO₂ 腐蚀; AlCrFeNiMn; AlCoCrFeNi_{2.1}

112.二回路水化学条件下溶解氧对流动加速区 CRUD 的影响

二回路水化学条件下溶解氧对流动加速区 CRUD 的影响

单红梅^{1#}, 张桐^{1#}, 袁誉坤², 郭琦¹, 刘志远³, 刘非³, 徐健^{1,4*}, Tetsuo Shoji⁴

中山大学深圳校区材料学院, 深圳市

中广核研究院有限公司, 放废与放化研究所, 深圳

国家电力投资有限公司, 北京

Tohoku University, Japan

xujian3@mail.sysu.edu.cn

摘要 在本工作中, 使用微孔流通装置模拟 CRUD (corrosion-related unidentified deposit) 在传热管和支撑板之间的流动加速区域的趁机行为。利用 304 不锈钢微孔圆盘试样, 研究了溶解氧浓度对 CRUD 趁机特性的影响。通过 FIB-SEM, Raman,

三维超景深显微镜以及 TEM 等多种分析方法对试样的形貌、成分以及微观结构进行了表征。本实验中所有的试样都在微孔周围形成了 CRUD，例如溶解氧浓度为 2000 ppb 时 SEM 如图 1 (a) 所示。溶解氧浓度的变化导致 CRUD 相组成的变化。当溶解氧浓度为 5 ppb 和 2000 ppb 时，CRUD 的主要成分为 FeCr_2O_4 和 Fe_2O_3 ，而在溶解氧浓度为 200 ppb 时，二者共存^[1,2]。根据图 1 (b) 中的模拟结果所示，在微孔处形成了较大的流体速度。根据方程 (1)，更高的流速将以更高的速度剪切过量电荷，产生更大的流动电流，以促进氧化和 CRUD 的形成^[3,4]。因此 CRUD 将优先在流动加速区域产生。

$$I_{str} = 2\pi \int_0^a r \cdot u(r) \cdot \rho(r) dr \quad (1)$$

其中， I_{str} 是流动电流 (A)， a 是水力半径 (m)， r 是以管道中心轴为原点的径向距离 (m)， $u(r)$ 是流体速度分布 (m/s)

在保持其他实验条件不变，仅改变溶解氧浓度的情况下，流动加速区域上 CRUD 的宽度和厚度发生了变化。根据方程 (2)，在实验条件下，流动电流与离子浓度成反比。例如图 1 (c) 示意图所示，由于溶解氧浓度的增加促进了离子溶解，导致溶液中的离子浓度更高，进而导致 EDL 更薄，这意味着溶解氧浓度的增加会导致过量电荷的减少 (图 1 (d) 示意图所示)，从而影响 CRUD。沿着圆盘表面，从孔中心到圆盘边缘，作为 CRUD 沉积驱动力的流动电流逐渐降至零^[5]。然而只有当 CRUD 沉积的驱动力达到临界值时，才会发生沉积。综上，溶解氧浓度的增加导致离子浓度增加，最终通过电动作用机制影响导致流动加速区域的宽度逐渐减少。

$$\frac{1}{k} = \sqrt{\frac{\epsilon_0 \epsilon k T}{e_i^2 \sum c_i z_i^2}} \quad (2)$$

其中 ϵ 是水的相对介电常数， k 是玻尔兹曼常数 (k)， T 是温度 (K)， e_i 是电荷， c_i 和 z_i 分别是阳离子和阴离子的浓度和价态， $\frac{1}{k}$ 是 EDL 的厚度。

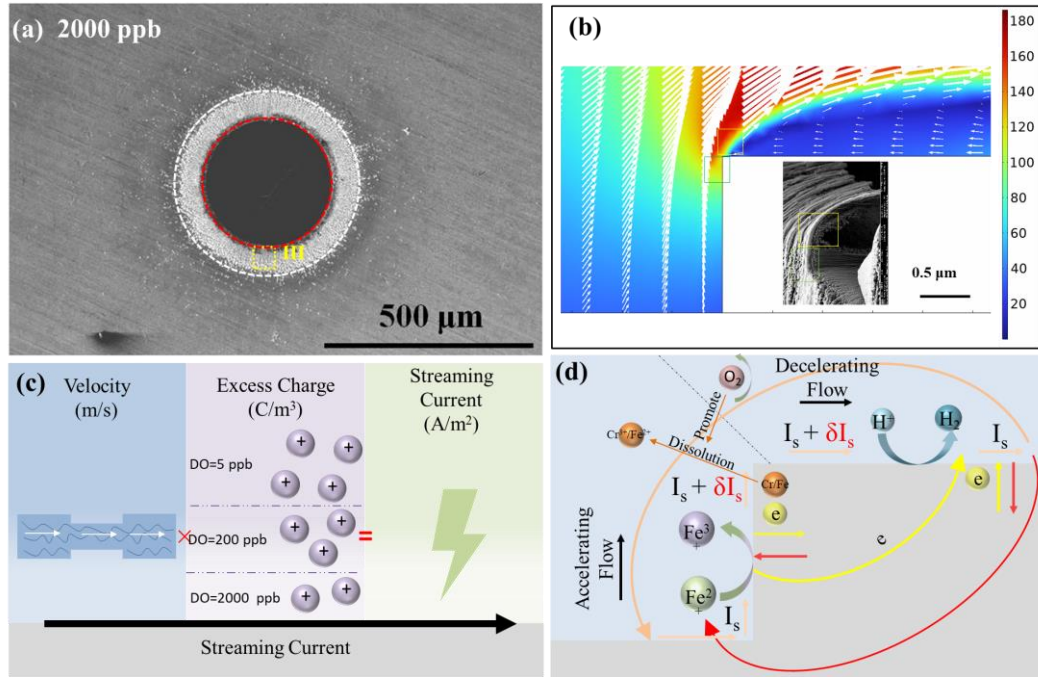


图 1 (a) 溶解氧浓度为 2000 ppb 时试样表面的 SEM 形貌, (b) 流体速度分布模拟, (c-d) 流动电流及电动作用机制示意图

关键词 微孔; CRUD; 电动机制; 高温水; 流动加速区域

参考文献

[1] PUIGDOMENECH B B I. Revised pourbaix diagrams for iron at 25–300°C [J]. Corrosion Science, 1996, 38(12): 2121-35.

[2] KUANG W, WU X, HAN E-H. Influence of dissolved oxygen concentration on the oxide film formed on 304 stainless steel in high temperature water [J]. Corrosion Science, 2012, 63: 259-66.

[3] MCGRADY J, SCENINI F, DUFF J, et al. Investigation into the effect of water chemistry on corrosion product formation in areas of accelerated flow [J]. Journal of Nuclear Materials, 2017, 493: 271-9.

[4] CIONCOLINI A, CASSINERI S, DUFF J, et al. Micro-orifice single-phase flow at very high Reynolds number [J]. Experimental Thermal and Fluid Science, 2018, 91: 35-40.

113. 钛基表面涂层的催化反应活性调控和结构相转变规律研究

钛基表面涂层的催化反应活性调控和结构相转变规律研究

陈思远^{1,*}, 王戈^{2,#}, 李伟华^{1,*}

¹ 河南省科学院化学研究所, 河南郑州

² 北京科技大学材料科学与工程学院, 北京

摘要 增强光生电子产生效率有利于提升光催化自清洁涂层的自清洁性能和耐久性。钛基涂层表面的催化反应受到固气反应界面化学成分及相结构的影响。催化剂表面活性位点的电子结构状态影响反应物分子的表面化学吸附和电子转移,从而影响到反应活性。光催化自清洁涂层的防水和防腐蚀性能要求材料具有强疏水能力和抗腐蚀介质粒子渗透能力,实现该目标的基础是从分子界面反应的角度分析水分子与表面官能团反应的活性状态及其对材料表面粒子渗透能力的影响。本摘要展示了基于反应温度和氧化性气氛条件控制 TiO₂ 相结构的方法。研究发现高温和氧化性气氛有利于实现 TiO₂ 从锐钛矿相转变为金红石相。结合理论计算结果和高倍透射显微镜观察,我们确定了 TiO₂ 从锐钛矿相向金红石相转变是从 (211) 面开始的。研究发现,锐钛矿与金红石相形成的异质结构可显著增强光激发电子-空穴对产生效率,从而有效改变催化剂表面的羟基自由基和超氧自由基浓度,通过前驱体设计有效控制杂质金属掺入量,进一步实现对 TiO₂ 基涂层的带边位置调节,有效提高其光能利用率和光电转化效率[1-4]。通过本摘要提供的手段调控 TiO₂ 异质相结构密度,增强表面涂层的内电场,将显著提升 TiO₂ 基自清洁涂层的自清洁效率和杀菌能力。

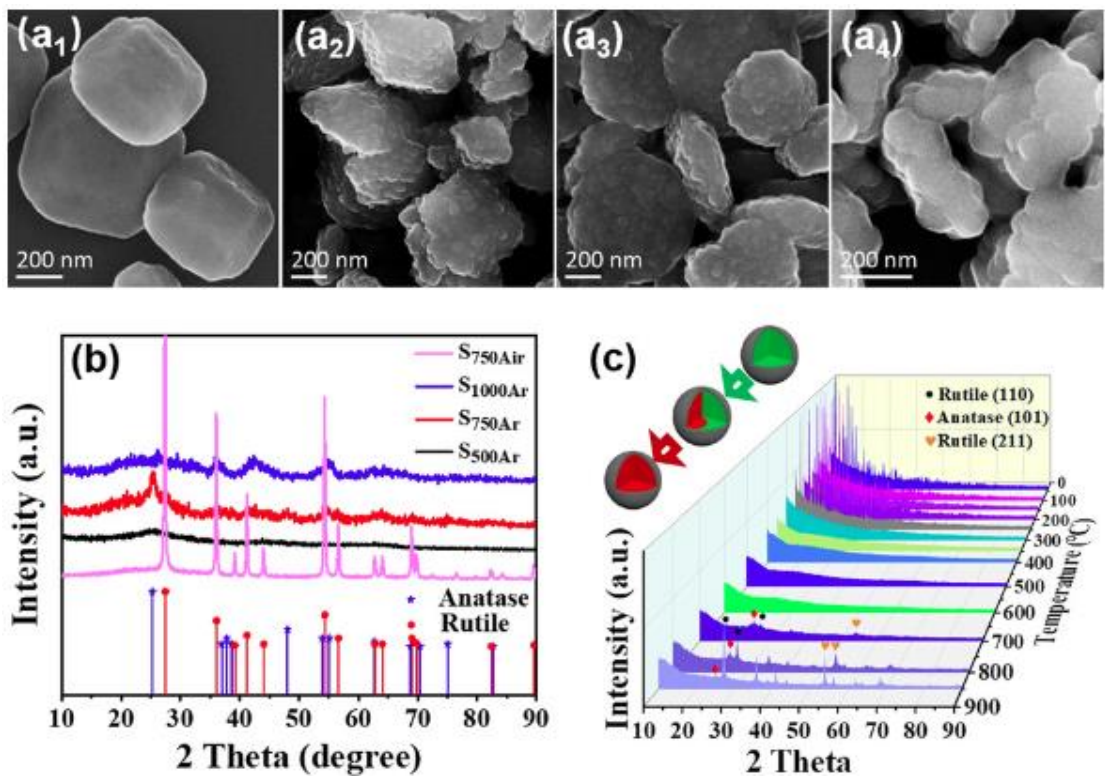


图 1a 不同温度煅烧样品的 SEM 图(a1.1500°C 氩气煅烧样品, a2.750°C 氩气煅烧样品, a3.1000°C 氩气煅烧样品, a4.750°C 空气煅烧样品); 图 1b 不同温度煅烧粉末样品的 XRD 图谱; 图 1c 不同温度氩气煅烧样品的原位 XRD 分析[5]

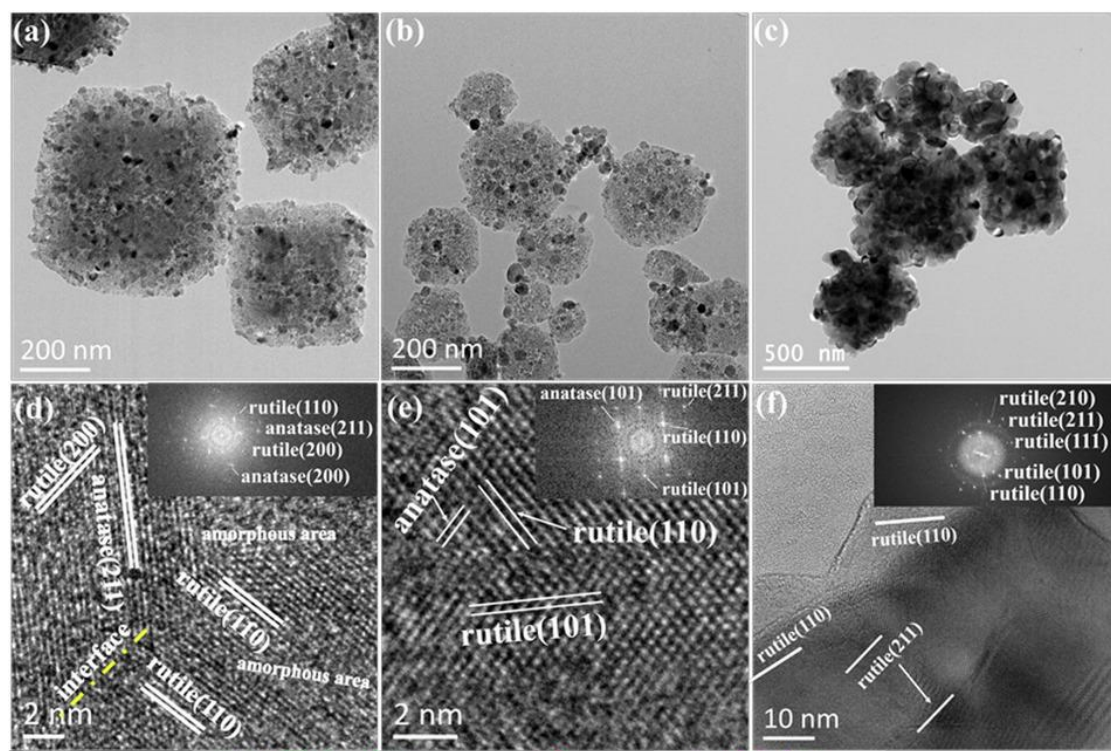


图 2a.750°C氩气煅烧样品的 TEM 图;图 2b.1000°C氩气煅烧样品的 TEM 图;图 2c.750°C空气煅烧样品的 TEM 图;图 2d.750°C氩气煅烧样品的 HRTEM 图;图 2e.1000°C氩气煅烧样品的 HRTEM 图;图 2f.750°C空气煅烧样品的 HRTEM 图;HRTEM 图中右上角嵌入图为选区电子衍射。[5]

关键词 光催化自清洁涂层; TiO₂ 相结构; 相结构调控方法

参考文献

- [1]S. Chen, G. Hai, H. Gao, X. Chen, A. Li, X. Zhang, W. Dong, Modulation of the charge transfer behavior of Ni(II)-doped NH₂-MIL-125(Ti): Regulation of Ni ions content and enhanced photocatalytic CO₂ reduction performance[J]. Chemical Engineering Journal, 2021, 406:126886.
- [2]S. Chen, F. Yang, H. Gao, J. Wang, X. Chen, X. Zhang, J. Li, A. Li, Construction of dual ligand Ti-based MOFs with enhanced photocatalytic CO₂ reduction performance[J]. Journal of CO₂ Utilization, 2021, 48:101528.
- [3]A. Li, S. Chen, F. Yang, H. Gao, C. Dong, G. Wang, Metalloporphyrin-Decorated Titanium Dioxide Nanosheets for Efficient Photocatalytic Carbon Dioxide Reduction[J]. Inorganic Chemistry, 2021, 60(23):18337-18346.
- [4]S. Chen, X. Xu, H. Gao, J. Wang, A. Li, X. Zhang, Fine-Tuning the Metal Oxo Cluster Composition and Phase Structure of Ni/Ti Bimetallic MOFs for Efficient CO₂ Reduction[J]. Journal of Physical Chemistry C, 2021, 125(17):9200-9209.
- [5] S. Chen, H. Gao, M. Han, X. Chen, X. Zhang, W. Dong, G. Wang, In-situ Self-transformation Synthesis of N-doped Carbon Coating Paragenetic Anatase/Rutile Heterostructure with Enhanced Photocatalytic CO₂ Reduction Activity [J]. ChemCatChem, 2020, 12:3274.

114.表面组织调制对降低 AlMg 变形铝合金板晶间腐蚀速率的关键作用

表面组织调制对降低 AlMg 变形铝合金板晶间腐蚀速率的
关键作用

薛菲*, 曹高辉#, 曹零勇, 张文, 杨兵

宝山钢铁股份有限公司中央研究院宝武铝业技术中心，上海
上海运输工具轻量化金属材料应用工程技术研究中心，上海
中国宝武三门峡铝基新材料研发中心，河南三门峡
汽车用钢开发与应用技术国家重点实验室(宝钢)，上海

摘要 5xxx 系 AlMg 铝合金具有高强度、高延伸率、可焊接性及高耐蚀性，广泛服役于苛刻的海洋环境及大气腐蚀环境中的覆盖件和结构件。汽车轻量化趋势要求材料设计必须考虑在不断减重的基础上兼具更高强度等力学性能。5xxx 系铝合金主要通过合金元素 Mg 的固溶强化来实现高强度。高含量的 Mg 元素在长时间的中低温服役时有逐步析出的趋势，以 β 相的形式分布在晶界位置，导致材料耐晶间腐蚀和应力腐蚀的敏感性增高。 β 相相对于 α -Al 基体是阳极，在腐蚀环境下优先发生电化学腐蚀，成为 AlMg 铝合金在特定环境下本征溶解源。绿色环保趋势下，再生材料的使用导致各种“脏”合金在生产工序上不断累积，打破了已有的电位体系，对未来 AlMg 铝合金耐蚀性机理和研发提出了新的考验，也拓展了新的设计维度。目前，国际头部铝企已生产出再生材占比 100% 的“零碳”铝材、暂应用于较为简单的服役环境。对提升传统 AlMg 铝合金耐蚀性的研发主要集中在成分体系的微合金改良、热处理工艺的优化以及新型涂层的开发等，对晶界的调控鲜少报道。以上改良措施或引入新的元素种类对回收提出新的考验，或未改善析出总量、仅延缓老化初始点未缩短老化进程，或对晶间腐蚀速率的控制及其有限。

本研究在传统商业 AlMg 合金材料(样品 A)基础上，基于晶界工程理念、对材料表面组织结构进行最小调制(样品 B)，对 Mg 元素老化析出网络进行类型优化，极大提升高 Mg 变形 AlMg 合金板材耐晶间腐蚀性能，为高占比再生材的未来 AlMg 材料研发提供了低成本的解决方案。

如表 1 所示：与传统商业材料相比，经表面组织调制后的 AlMg 变形铝合金晶间腐蚀速率显著降低，宏观腐蚀与电化学数据具有良好的一致性，腐蚀电流密度可用来预测 G67 腐蚀速率。图 1 显示了调制前后的 AlMg 合金板材 β 相的分布特征：传统 AlMg 铝合金材料老化后， β 相大量连续分布在晶界位置，形成网状阳极。调制后的新材料经同等老化处理后， β 相在表面呈现弥散分布的特征。

表1 调制前后腐蚀速率及电化学腐蚀性能对比

样品序号	腐蚀速率 (mg/cm ²)	自腐蚀电位 (V)	自腐蚀电流密度 (A · cm ⁻²)	点蚀电位 (V)
样品A	30.24	-0.75	1.123 × 10 ⁻⁶	-0.73
样品B	5.59	-0.96	2.618 × 10 ⁻⁸	-0.66

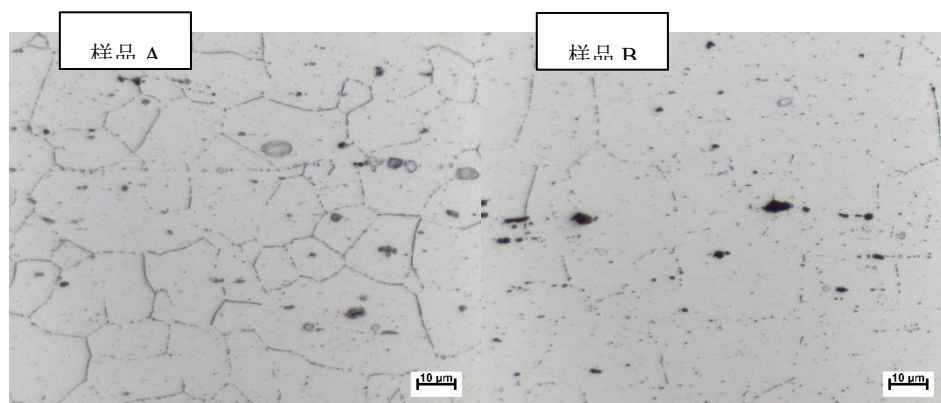


图1 调制前后加速老化后板材β相分布对比（1000倍）

关键词 晶间腐蚀；AlMg合金；老化；晶界设计；β相

115.Er的添加对锌铝镁镀层组织和腐蚀性能的影响

Er的添加对锌铝镁镀层组织和腐蚀性能的影响

刘广会*, 徐呈亮*, 蒋光锐

首钢集团有限公司技术研究院, 北京, 100043

摘要 热镀锌产品以其良好的耐腐蚀性被应用于生产和生活的各个方面。一些研究已经在锌铝镁涂层中添加了第四种微量合金元素以形成四元合金以获得更好的性能。本文通过感应熔炼制备了四种不同成分的微量Er添加的Zn-Al-Mg合金铸锭，成分分别为1#：Zn-1.7%Al-1.1%Mg-0.1%Er、2#：Zn-1.7%Al-1.1%Mg-0.5%Er、3#：Zn-7%Al-2%Mg-0.1%Er、4#：Zn-7%Al-2%Mg-0.5%Er四种成分合金，并在带有氩气保护气氛的加热炉中进行熔炼并开展了水冷条件下的凝固试验，得到凝固组织。通过微观组织表征和电化学测试，研究了添加Er的Zn-Al-Mg合金的凝固组织和腐蚀行为。通过相图计算预测了Er的化合物的析出的类型。利用扫描电子显微镜（SEM）和电子探针（EPMA）

以及场发射扫描电镜（JSM-7001F）分析了合金的显微组织和相类型。随着 Er 的添加，合金的凝固组织有一定的细化，且从能谱分析来看，析出的化合物系 $\text{Er}_2\text{Zn}_{17}$ ，其密度大于锌液，可能在实际热浸镀工艺中生成底渣，需综合考量。最后，运用电化学方法对各合金样品进行了电化学测试。其中 Tafel 极化曲线测试结果和交流阻抗图谱测试结果可以看出，添加 Er 后低铝低镁合金的耐蚀性仍普遍低于中铝中镁产品。对于同类样品而言，Er 的添加有利于耐蚀性能的提升。结合实际产品可能出现的表面质量问题及锌渣的生成，Er 的添加效果有待进一步评估。目前，对含 Er 的四元合金的组织 and 性能的研究很少，因此，研究 Er 含量对合金组织和性能的影响具有重要意义。

关键词 含 Er 锌铝镁合金；凝固组织；耐腐蚀性； $\text{Er}_2\text{Zn}_{17}$

19th APCCG

